CHEMICAL APPLICATIONS OF MAGNETIC RESONANCE.

A thesis submitted in partial fulfilment of the requirements of the Board of the Faculty of Physical Sciences for the degree of Doctor of Philosophy, at the University of Oxford.

by

Raymond A. Dwek

Lincoln College,
Oxford.

Physical Chemistry Laboratory,
Oxford.

May, 1966.

A B S T R A C T

The electron-nuclear Overhauser effect on s_{in} $\frac{1}{2}$ nuclei in solutions containing free radicals has been calculated from a method based on the treatment used by Solomon. The magnitude and sign of the enhancement of the nuclear signal, which may be represented by a factor ρ depends on the nature and time dependence of the electron-nuclear coupling, which is assumed to be either dipolar or scalar. The time dependence for the dipole-dipole interactions is assumed to arise from the translational diffusion of the free radicals and the molecules containing the nuclei. Three models are employed for the scalar interactions. In the first of these, termed the Sticking Model, the scalar interaction is assumed to be finite only while a molecule and free radical are "stuck" together. This sticking time is assumed to be short in comparison with the diffusional correlation time. However, an alternative model in which this assumption is not made has been postulated to explain certain experimental results. This is termed the Modified Sticking Model. In the third model, called the Diffusion Model, the hypothesis is made that the scalar interaction is a very short range interaction with magnitude

$$\propto B(d/R) \exp.\left[-\lambda(R-d) \right],$$

where $\lambda d \gg 1$, B and λ are constants, R is the distance between a nucleus and an electron, and d is the distance of closest approach, inside of which the interaction is zero. In this model the time dependence of the scalar interaction, as in the case of the dipolar interactions, arises from the relative diffusion of the molecules and free radicals in the solution.

For all the models of the scalar interaction, ρ may be plotted as a function of $\omega_s \tau_c$ where ω_s is the electron Larmor frequency and τ_c the correlation time and it is found that the sign of ρ may change. The product $\omega_s \tau_c$ may be altered by working at different magnetic fields or changing ρ_c. From measurements, at two different magnetic fields, of the nuclear spin-lattice relaxation times, the concentration of free radical in the solution and ρ, the theories allow the calculation of the mean diffusion coefficient of the radicals and molecules in solution, the correlation times and the measure of the relative importance of scalar and dipolar interactions.

Experiments on fluorinated and protonic solvents containing the radical tri-tert-butyl phenoxyl (T.T.B.P.) have been carried out at two different magnetic fields. The proton-free radical interactions may be explained in terms of dipole-dipole interactions. On the other hand with

fluorine nuclei scalar coupling does seem to be important. The Sticking Model does not succesfully describe the effect of this coupling. The other models give reasonable values for the calculable parameters, but it is difficult to decide unambiguously between them.

If scalar coupling does occur, a scalar shift of the nuclear resonance is expected. This has been observed for hexafluorobenzene solutions containing T.T.B.P. The theoretical and experimental results are compared, and while either theory might explain the observed shift, less assumptions have to be made in using the Diffusion Model.

The correlation time dependence of the Overhauser effect has also been studied for two systems, hexafluorobenzene and 1-1-1-trichloro-2-2-2-trifluoro-ethane, at two magnetic fields. The correlation times were altered by addition of carbon disulphide or a chlorinated hydrocarbon or by changing the temperature of the sample. Qualitatively the Diffusion Model was in best agreement with the experimental results, but quantitiatively, neither model was satisfactory.

In the Diffusion Model, the assumption $\lambda d \gg 1$ is made and in an attempt to obtain better agreement with the experimental results ρ has been calculated using different values of λd in the scalar interaction function. The best agreement between experiment and theory was for values of $\lambda d \geq 1000$.

Measurements of the proton electron Overhauser effect can usually be interpreted in terms of dipolar interactions (positive ρ) between the electrons and the protons. However for the resonances of the tert-butyl groups of tri-tert-butyl phenol in solutions of T.T.B.P. ρ is negative. This has been shown to be associated with the proton exchange between the radical and phenol molecules. It is postulated that in the radical molecule the scalar coupling between the electron and the tert-butyl protons, occurs at least in part by a hyperconjugative mechanism. The random rotation of these tert-butyl groups could modulate this scalar coupling. This would lead to a positive polarisation of the tert-butyl protons, which persists when the radical accepts a proton and becomes a tri-tert-butyl phenol molecule.

A C K N O W L E D G E M E N T S.

I am deeply indebted to Professor R.E. Richards, F.R.S., for his help, encouragement and supervision during this work.

My grateful thanks are also due to my colleagues in the Physical Chemistry Laboratory, especially to my co-members of the double resonance group, notably Dr. J.A. Ladd, Mr. D.J. Shields and Dr. J.G. Kenworthy. I have benefitted greatly from discussions with Dr. Kenworthy and from his help in experimental technique.

I would like to thank Dr. L. Lyons for his help in computing and Dr. P.W. Atkins for several helpful discussions.

I should also like to express my appreciation to the technicians and staff of the department and to the Science Research Council for the award of a Research Studentship.

Finally, I would like to thank my wife for her help in the preparation of this thesis and especially with the diagrams.

* * * *

C O N T E N T S

Page

C H A P T E R I

Rate Equations for a Two Spin System (1)

Consider a system containing n_S particles of spin interacting with n_I ($> n_S$) particles of spin I. If a magnetic field, H_o, is applied along the z direction the Hamiltonian for this interaction is:-

$$H = H_M - \hbar \gamma_I H_o I_z - \hbar \gamma_s H_o S_z + H' \qquad \ldots\ldots (1.1)$$

where H_M is the Hamiltonian of the motion of the particles and commutes with the spin operators I_z and S_z. The next two terms are the Zeeman energies of the two types of spin in the magnetic field H_o, while H' is the spin-spin interaction term which is considered as a perturbation. It will be assumed that all S spins are always coupled to an I spin, but that there is a rapid exchange between coupled and uncoupled I spins, so that the magnetisation of the I spins is homogeneous throughtout the sample. If both types of spin have a quantum number $I_z = {}^1/2$, then the four eigenstates of the spins will be defined by the relations:

$$I_z \mid + \rangle = +\tfrac{1}{2} \mid + \rangle$$
$$I_z \mid - \rangle = -\tfrac{1}{2} \mid - \rangle$$
$$S_z \mid +) = +\tfrac{1}{2} \mid +)$$
$$S_z \mid -) = -\tfrac{1}{2} \mid -)$$

so that the four unperturbed eigenstates of the n_s interacting pairs are $|+>|+)$, $|+>|-)$, $|->|+)$ and $|->|-)$ with the respective occupation numbers N_{++}, N_{+-}, N_{-+} and N_{--}. The eigenstates, $|+>$ and $|->$, of the uncoupled I spins have occupation numbers N_+ and N_-.

Figure 1.1 gives a pictorial representation of the system at any instant. The W's are transition probabilities and defined as follows:

W_1 is the probability of an I transition caused by interaction with an S spin.

W_1' is the probability of an S transition caused by interaction with an I spin.

W_L is the probability of an I transition caused by interaction with other I spins or any other magnetic species other than an S spin.

W_0 is the probability of simultaneous I and S transitions in the opposite sense (flip-flop process).

W_2 is the probability of simultaneous I and S transitions in the same sense (flip-flip process).

W_L' is the probability of an S transition caused by interaction with other S or any magnetic species other than an I spin.

Hence W_L and W_L' will occur in conjunction with W_1 and W_1' respectively.

Figure 1.1

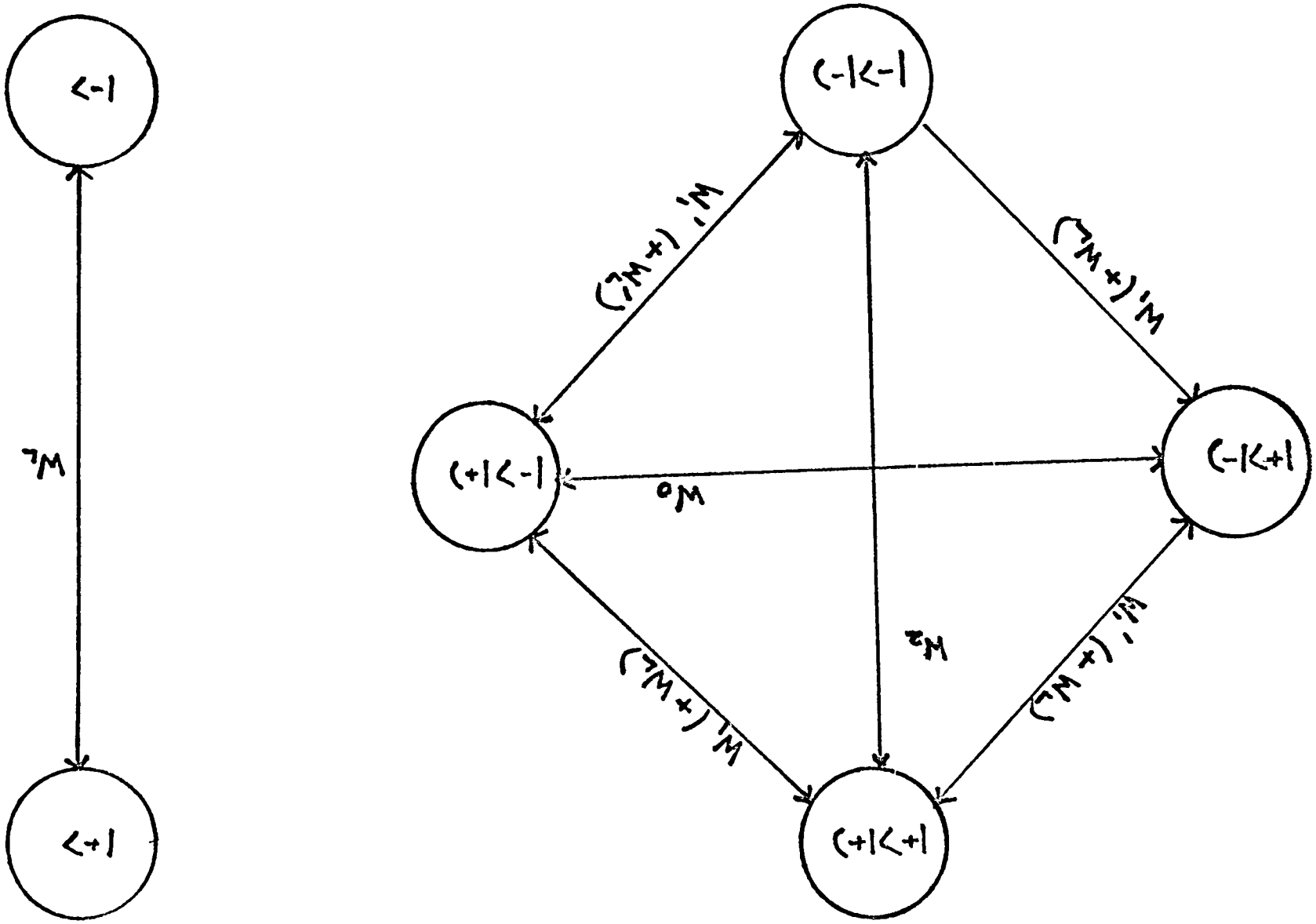

From the definition of the W's it follows that

$$\frac{dN_{++}}{dt} = -(W_1 + W_2 + W_1' + W_2)N_{++} + (W_L' + W_1')N_{+-} + (W_1 + W_L)N_{-+} + W_2 N_{--} + \text{constant},$$

$$\frac{dN_{+-}}{dt} = -(W_1 + W_2 + W_1' + W_0)N_{+-} + (W_L' + W_1')N_{++} + (W_1 + W_L)N_{--} + W_0 N_{-+} + \text{constant},$$

$$\frac{dN_{-+}}{dt} = -(W_1 + W_2 + W_1' + W_0)N_{-+} + (W_L' + W_1')N_{--} + (W_1 + W_L)N_{++} + W_0 N_{+-} + \text{constant},$$

.....(1.2)

$$\frac{dN_{--}}{dt} = -(W_1 + W_2 + W_1' + W_2)N_{--} + (W_L' + W_1')N_{-+} + (W_1 + W_L)N_{+-} + W_2 N_{++} + \text{constant},$$

$$\frac{dN_{+}}{dt} = -W_L N_{+} + W_L N_{-} + \text{constant},$$

$$\frac{dN_{-}}{dt} = -W_L N_{-} + W_L N_{+} + \text{constant}.$$

The effect of exchange between coupled and uncoupled $\underline{I}$ spins on the populations can be ignored, since such processes do not involve spin flips and thus do not contribute to $\underline{I}_z$.

The constants in equation (1.2) are obtained by considering the system at temperature equilibrium and inserting the proper Boltzmann factors.

The experimentally observable quantitites are the macroscopic magnetic moments proportional to I_z and S_z. Thus:-

$$\frac{KI_z}{\gamma_I} = (N_{++} + N_{+-} + N_{+}) - (N_{-+} + N_{--} + N_{-}) \quad \ldots\ldots (1.3)$$

and $$\frac{KS_z}{\gamma_s} = (N_{++} + N_{-+}) - (N_{+-} + N_{--}) \quad \ldots\ldots\ldots (1.4)$$

Hence using (1.3)

$$\frac{K}{\gamma_I}\frac{dI_z}{dt} = -(W_0 + 2W_1 + W_2)(N_{++} + N_{+-} - N_{-+} - N_{--})$$
$$-(W_2 - W_0)(N_{++} + N_{-+} - N_{+-} - N_{--})$$
$$-2W_L(N_{++} + N_{+-} - N_{+} - N_{-} - N_{--} - N_{-})$$
$$+ \text{constant.} \quad \ldots\ldots\ldots(1.5)$$

and a similar expression for $\frac{K}{\gamma_s}\frac{dS_z}{dt}$ can be derived by using (1.4).

Since the magnetisation of the I spins is homogeneous, then using (1.3), the polarization of the coupled spins (n_s in number) is given by

$$(N_{++} + N_{+-} - N_{-+} + N_{--}) = \frac{n_s}{n_I}\frac{K I_z}{\gamma_I} \quad \ldots\ldots (1.6)$$

Thus:

$$\frac{K}{\gamma_I}\frac{dI_z}{dt} = -\left[(W_0+2W_1+W_2)\frac{n_s}{n_I}+2W_L\right]I_z-(W_2-W_0)S_z + \text{constant} \qquad \ldots\ldots (1.7)$$

and similarly for $\frac{K}{\gamma_s}\frac{dS_z}{dt}$. Where γ_I and γ_s are the gyromagnetic ratios for spins $\underline{I}$ and $\underline{S}$.

Setting I_z and S_z equal to I_0 and S_0 at equilibrium ($dI_z/dt = 0$) we obtain:-

$$\frac{dI_z}{dt} = -\left[(W_0+2W_1+W_2)\frac{n_s}{n_I}+2W_L\right](I_z - I_0)-(W_2-W_0)(S_z - S_0) \qquad \ldots\ldots\ldots (1.8)$$

Nuclear Relaxation in Paramagnetic Solutions.

If $\underline{S}$ represents an electronic spin and $\underline{I}$ a nuclear spin, then the electronic longitudinal relaxation time, will in general be much less than that for the nucleus. Thus in the time scale of observation of the nuclear relaxation, the electronic magnetisation may be regarded as decaying instantly and thus

$$S_z = S_0 \qquad \ldots\ldots\ldots (1.9)$$

Equation (1.8) then becomes:-

$$\frac{dI_z}{dt} = -\left[(W_0+2W_1+W_2)\frac{n_s}{n_I}+2W_L\right](I_z - I_0) \qquad \ldots\ldots\ldots (1.10)$$

showing that the nuclear spins $\underline{I}$ have a simple decay, with a relaxation time given by:-

$$\frac{1}{T_1} = \frac{n_s}{n_I} (W_0 + 2W_1 + W_2) + 2W_L \qquad \ldots\ldots (1.11)$$

If there are no $\underline{S}$ spins present, then the relaxation time for the nuclear spins $T_{1,0}$ will be given by:

$$\frac{1}{T_{1,0}} = 2W_L \qquad \ldots\ldots (1.12)$$

Thus:-

$$\frac{n_s}{n_I} (W_0 + 2W_1 + W_2) = \frac{1}{T_1} - \frac{1}{T_{1,0}} \qquad \ldots\ldots (1.13)$$

From equation (8), at equilibrium $\frac{dI_z}{dt} = 0$ and

$$\underline{I_z} - I_0 = \frac{-(W_2 - W_0)}{\left[\frac{n_s}{n_I} (W_0 + 2W_1 + W_2) + 2W_L\right]} \frac{\gamma_I}{\gamma_S} (\underline{S_z} - S_0) \ldots (1.14)$$

$$= - \frac{\frac{n_s}{n_I} (W_0 + 2W_1 + W_2)}{\left[\frac{n_s}{n_I}(W_0 + 2W_1 + W_2) + 2W_L\right]} \cdot \frac{n_I}{n_s} \frac{(W_2 - W_0)}{(W_0 + 2W_1 + W_2)} \cdot \frac{I}{S} \cdot (\underline{S_z} - S_0)$$

$\ldots\ldots (1.15)$

$$= - \frac{1/T_1 - 1/T_{1,0}}{1/T_1} \cdot \frac{n_I}{n_s} \cdot \rho \cdot \frac{\gamma_I}{\gamma_s} \cdot (\underline{S_z} - S_0) \ldots (1.16)$$

where $\rho = (W_2 - W_0)/(W_0 + 2W_1 + W_2)$. The magnitude of ρ thus depends on the coupling between the different spins $\underline{I}$ and $\underline{S}$. A leakage factor f, which measures the proportion of the relaxation of the nuclear spins which occurs by coupling with the electron spins may be defined as

$$f = 1 - T_{1}/T_{1,0}$$

Thus:-

$$\underline{I_z} - I_0 = -f.\rho. \frac{n_I}{n_s} \frac{\gamma_I}{\gamma_s} (\underline{S_z} - S_0) \qquad \ldots\ldots\ 1.17$$

The Overhauser Effect.

If the spins $\underline{S}$ are subjected to a fluctuating field H_2, at the appropriate resonance frequency then $\underline{S_z}$ in equation (1.16), will be given by (2)

$$\underline{S_z} = S_0 \cdot \left(\frac{1}{1 + \gamma_s^2 H_2^2 T_1^S T_2^S} \right) \qquad \ldots\ldots\ (1.18)$$

where T_1^S, and T_2^S are the spin-lattice and spin-spin relaxation times for spin $\underline{S}$.

Thus from equation (1.17)

$$I_z - I_0 = -f.\rho \frac{n_s}{n_I} S_0 \left(\frac{1}{\gamma_s^2 H_2^2 T_1^S T_2^S + 1} - 1 \right) \frac{\gamma_I}{\gamma_S} \ldots(1.19)$$

From the Curie Law (3) the net magnetisation M of a sample containing N spins in an applied field H_o, is given by

$$\underline{M} = \frac{N \gamma_n^2 \hbar^2 I(I+1) H_o}{3kT} \qquad \ldots\ldots\ldots (1.20)$$

Thus for the two types of spin $\underline{I}$ and $\underline{S}$, both of the same quantum number, in the magnetic field H_o,

$$\frac{\underline{S_o}}{I_o} = \frac{n_s}{n_I}\left(\frac{\gamma_s}{\gamma_I}\right)^2 \qquad \ldots\ldots\ldots (1.21)$$

Substitution of (1.21) into (1.19) yields

$$\frac{\underline{I_z} - I_o}{I_o} = f.\rho \frac{\gamma_s}{\gamma_I}\left(1 - \frac{1}{1+\gamma_s^2 H_2^2 T_1^s T_2^s}\right) \ldots(1.22)$$

Thus the polarization of the spins $\underline{I}$ depend on the power being used in the irradiation of spins $\underline{S}$. This was first predicted by Overhauser in 1953 (4) for metals, but is of general application.

An enhancement factor, A, for the nuclear resonance may be defined as

$$A = (\underline{I_z} - I_o)/I_o$$

then equation (1.22) may be rewritten

$$A = f \cdot \rho \frac{\gamma_n}{\gamma_I} \left(1 - \frac{1}{1 + \gamma_s^2 H_2^2 T_1^S T_2^S} \right) \quad \ldots\ldots\ldots (1.23)$$

If P is the power of the S irradiation, then

$$P = \text{a const. } (\beta) \times H_2^2$$

which on substitution in (1.23) yields

$$A = + f \cdot \rho \frac{\gamma_n}{\gamma_I} \left(1 - \frac{1}{1 + a P} \right) \quad \ldots\ldots\ldots (1.24)$$

where a = a constant = $\dfrac{1}{\gamma_S^2 T_1^S T_2^S \rho^{-1}}$

Hence:-

$$A^{-1} = + \frac{\gamma_I}{\gamma_S} \frac{1}{f \cdot \rho} \left(1 + a^{-1} P^{-1} \right) \quad \ldots\ldots\ldots (1.25)$$

Thus a plot of A^{-1} against P^{-1} would be a straight line with the intercept (when $P = \infty$) given by

$$A_{max}^{-1} = + \frac{\gamma_I}{\gamma_S} \frac{1}{f \cdot \rho} (1) \quad \ldots\ldots\ldots (1.26)$$

If it is assumed that $1/T_1$, (the measured relaxation time of spins I when both spin types are present) is linearly related to radical concentration, such that

$$\frac{1}{T_1} = \frac{1}{T_{1,0}} + Kc \quad \ldots\ldots\ldots (1.27)$$

where K is a constant, then it follows from the definition of f $(= 1 - T_1/T_{1,0})$

$$\frac{1}{f} = 1 + (Kc\, T_{1,0})^{-1} \qquad \ldots\ldots\ldots (1.28)$$

which on substitution in equation (1.26) gives

$$A_{max}^{-1} = + \frac{\gamma_I}{\gamma_S} \frac{1}{\rho} \left[1 + (T_{1,0}K)^{-1} c^{-1}\right] \ldots\ldots\ldots (1.29)$$

Thus a plot of A_{max}^{-1} against c^{-1} should also be a straight line, which (for $C = \infty$) extrapolates to a value of A^{-1}, which is the value of the reciprocal enhancement of the nuclear resonance of a solution that would be obtained when infinite microwave power is applied to the electron spin and assuming that there is perfect coupling between the spins.

Hence:-

$$A_{\infty}^{-1} = + \frac{\gamma_I}{\gamma_S} \frac{1}{\rho}$$

and since γ_I γ_S and A_{∞}^{-1} are known ρ can be determined experimentally. In order to calculate ρ theoretically, it is necessary to calculate the transition probabilities W_0, W_1 and W_2. This can be carried out using first order perturbation theory, if the spin-spin interaction considered as the perturbation in equation (1.1) is made explicit.

In the present instance, for the two spins with quantum number $F_2 = {}^1/2$, dipole - dipole and scalar ($A\underline{I} \cdot \underline{S}$ type) interactions will be considered. It may be shown (5) that in the case of dipolar coupling P is positive, but that for scalar coupling p may be either positive or negative. Experimentally (6,7,8,9) it has been found that the enhancements of proton resonances are negative while those of fluorine nuclei, may be either positive or negative depending on the system. These positive enhancements might arise either from scalar coupling or, from a "three spin effect". These are discussed in later sections.

Spectral Density Function

If $|m_i\rangle$ and $|m_j\rangle$ are two eigenstates of the unperturbed Hamiltonian with corresponding energies E_i and E_j, the transition probability per unit time between these two states, using first order perturbation theory, is

$$W_{ij} = \frac{1}{t'} \frac{1}{\hbar^2} \left| \int_0^t \langle m_j | H'(t) | m_i \rangle \, e^{-i\omega_{ij}t} \, dt \right|^2 \qquad (1.30)$$

with $\omega_{ij} = (E_j - E_i)$

In the cases to be considered here the Hamiltonian H^1 will be time dependent and thus $\hbar$ will be a random function and maybe represented by $\langle f(t) \rangle$. In order to set a time scale

to the random motion a correlation time τ_c is introduced. A correlation function $g(\tau)$ may then be defined as

$$g(\tau) = \overline{\langle f(t)\, f(t+\tau) \rangle} \quad \ldots\ldots\ldots \quad (1.31)$$

and the correlation time τ_c is the shortest interval of time within which $f(t+\tau)$ becomes unrelated to $f(t)$.

The motion of the neighbouring magnetic moments of a particular nucleus will produce at this nucleus a randomly oscillating magnetic field which may be resolved by Fourier analysis, into many components, some of which have the correct frequency to induce relaxation transitions. The matrix element in (1.30) corresponding to a particular transition will depend upon the intensity of the component with this frequency corresponding to this transition energy. This intensity is given the symbol $J(\omega)$ and is often called the spectral density at a particular frequency ω and $J(\omega)$ is the Fourier transform of the correlation function

i.e. $$J(\omega) = \int_{-\infty}^{+\infty} g(\tau)\, e^{-i\omega\tau} \quad \ldots\ldots\ldots \quad (1.32)$$

Thus from a knowledge of $J(\omega)$ the transition probabilities W, may be evaluated. In equation (1.15) the transition probabilities which occur in describing the relaxation of the nuclei in a solution containing a paramagnetic substance are W_0, $(W_1 + W_2)$ and W_2. From the definition of the W's

the calculation of each of these will involve a knowledge of $J(\omega_I + \omega_S)$, $J(\omega_I)$ and $J(\omega_I - \omega_S)$ respectively.

In order to calculate these spectral density functions, the nature of the time dependence of the Hamiltonian and hence the form of the correlation function must be known. In the case of intra-molecular dipole-dipole interactions, an exponential correlation function has been shown to describe the time dependence accurately. However, in the case of inter-molecular dipole-dipole interactions this is not generally true.

Dipole-Dipole Interaction.

Hubbard (10,11) has considered a model of spins fixed off the centre of spheres whose translational and rotational motion are described by a diffusion equation. He has shown that the contribution of the rotational motion is very much less than that of the translational motion, and that to a first approximation, it is equally valid to treat the spins as being at the centre of hard spheres, and to consider only the translation of the spheres. This is similar to the treatment considered by Abragam (12) and Pfeifer (13).

The usual dipole-dipole Hamiltonian H_{DD} is:-

$$H_{DD} = \gamma_S^2 \gamma_I^2 \left[\frac{3(\underline{S}.\underline{r})(\underline{I}.\underline{r}) - \underline{I}.\underline{S}}{r^5} \quad \frac{}{r^3} \right] \qquad \ldots\ldots\ldots(1.33)$$

where $\underline{I}$ and $\underline{S}$ are the vector operators for the spins and $\underline{r}$ is the interspin vector. The time dependence of the Hamiltonian arises because r is time dependent, because the spins are executing random motion with respect to each other.

This model for the time dependence of r has enabled the calculation of the reduced dipolar spectral density function $j_d(\omega)$, where $j_d(\omega)$ is defined as:-

$$j_d(\omega) = \frac{jd(\omega)}{jd(0)} = \frac{15}{2} \cdot I(u) \qquad \ldots\ldots\ (1.35)$$

where $u = |\omega\tau_D|^{\frac{1}{2}}$ and τ_D is the dipolar correlation time, and I(u) is given by:-

$$I(u) = u^{-5}\left\{u^2 - 2 + e^{-u}\left[(u^2-2)\sin u + (u^2+4u+2)\cos u\right]\right\} \qquad (1.36)$$

When the correlation function is exponential in form $j_d(\omega)$ is of the form

$$j_d(\omega) = \frac{1}{1+\omega^2\tau_D^2} \qquad \ldots\ldots\ (1.37)$$

For comparison graphs of $j_d(\omega)$ versus $\omega\tau_D$ for each of these models for the time dependence of the coupling, are shown in Fig. 1.2.

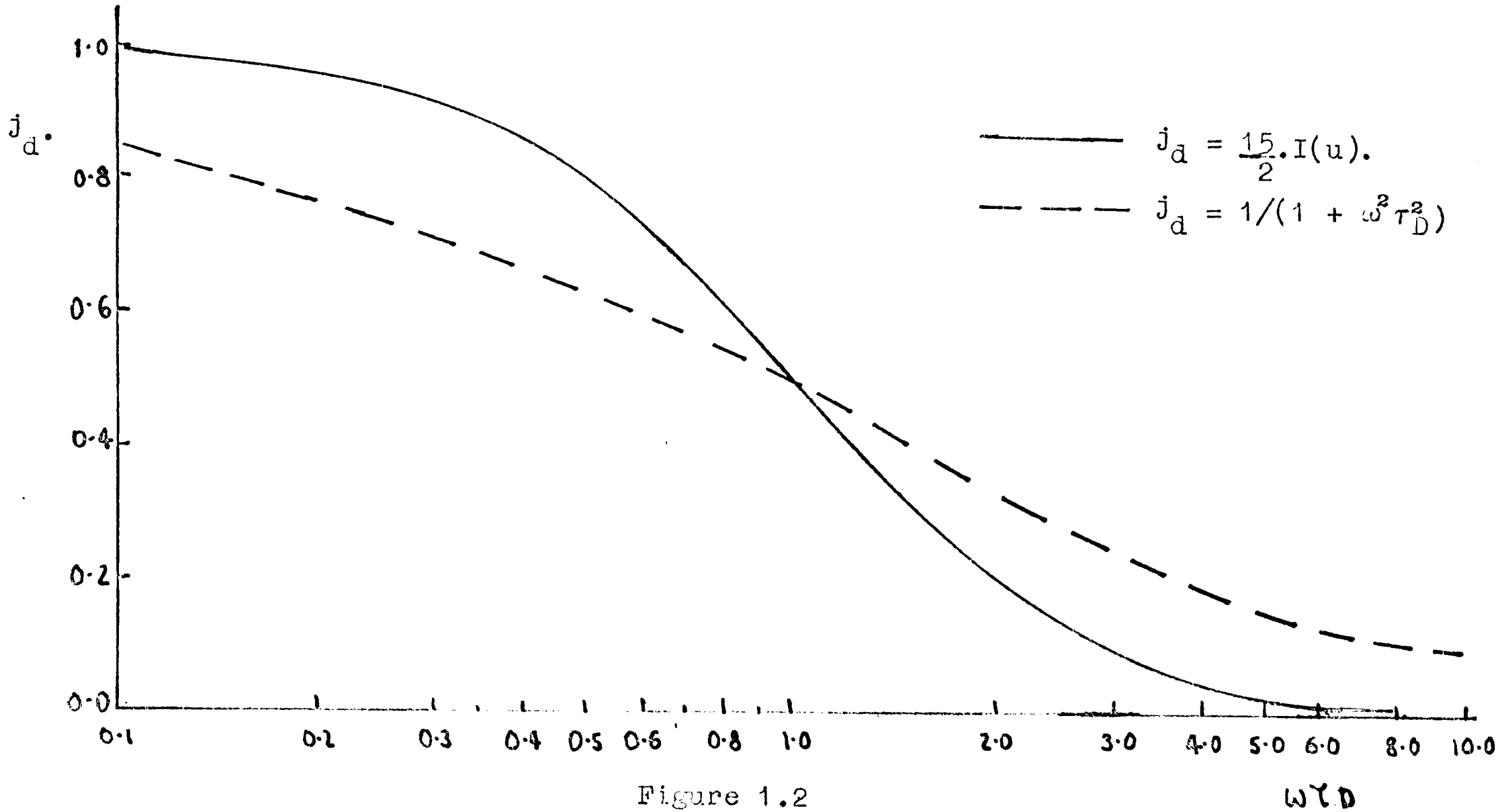
j_d.
1·0
0·8
0·6
0·4
0·2
0·0
0·1
0·2
0·3
0·4
0·5
0·6
0·8
1·0
2·0
3·0
4·0
5·0
6·0
8·0
10·0
ωτD
$j_d = \frac{15}{2}.I(u).$
$j_d = 1/(1 + \omega^2\tau_D^2)$

Figure 1.2

Scalar Coupling.

The scalar interaction between the i^{th} nucleus and the j^{th} electron can be written

$$\hbar B_{ij}\, \underline{I}_i \cdot \underline{S}_j$$

where $\underline{I}_i$ is the spin operator for the nucleus and $\underline{S}_j$ is the spin operator for the electron. This interaction if time dependent would be a relaxation mechanism. The time dependence could arise from either the time dependence of B_{ij} or $\underline{S}_j$. The former is referred to as scalar coupling of the first kind and the latter as of the second kind (14).

An example of scalar coupling of the second kind has been given by Bloembergen (15). He has shown that in aqueous solutions of manganous ion, each ion is surrounded by a co-ordination sphere of water molecules, and that there exists a scalar coupling between the electron spin of the paramagnetic Mn^{++} ion and the water protons of the solvation sphere. This electron-nucleus interaction is then randomly modulated by the short relaxation time of the electronic spin i.e. by several flips of the electronic spin whilst a water molecule is coupled to a particular ion.

In the case of scalar coupling of the first kind, the time dependence of the scalar interaction, arises from the time dependence of the coupling constant. An obvious example

of this is chemical exchange such that at one instant, spins I and S were on the same molecule and therefore coupled, and at a later time they are on different molecules and therefore not coupled. The value of the coupling constant is thus J, when I and S are coupled and zero when they are not and the scalar interaction can then be represented by a step function. An example of this is the case of the HF molecule (1,17) in which the scalar coupling between the nuclei is modulated by chemical exchange which is catalysed by small amounts of water. The value of the scalar coupling constant was found to be 615 ± 50 c.p.s. This is several orders of magnitude smaller than the dipolar coupling, and the scalar coupling is the dominant relaxation mechanism, because of its greater efficiency, resulting from a more favourable correlation time (18) This illustrates the point that the efficiency of a coupling as a relaxation mechanism depends not only on its magnitude but also upon its time dependence.

Experiments on various fluorinated organic solvents containing free radicals, carried out in this laboratory at 3,300 and 12,500 gauss, have indicated that scalar coupling exists between the unpaired electron on the radical and the fluorine nucleus. Since the time dependence for the modulation of this scalar coupling, if it is to be a significant

relaxation mechanism, is of the order of the inverse of the electron Larmor frequency i.e. $\sim 10^{-10}$ sec. in this case, and the relaxation time of the electron spin is known to be $\sim 10^{-6}$ sec., then this latter time dependence will not be of the correct order of magnitude to modulate the scalar coupling. Thus scalar coupling of the second kind seems unlikely, and it would appear that scalar coupling of the first kind may be involved in interpreting the results. It is chemically unlikely that for the systems studied there is sticking between a nucleus and a radical. Thus an exchange mechanism such as for HF can be ruled out. The scalar interaction, however, is probably short range and reaches a maximum on collision. Hubbard (5) has suggested that this may be approximated by a step function. The calculation of the scalar spectral density function is then similar to that for HF. Hubbard has evaluated the spectral density function for this model, which is termed the Sticking Model. An alternative model for the time dependence of the scalar coupling constant is a steep exponential function and Hubbard has also evaluated the spectral density function for this case termed the Diffusion Model. These are discussed below.

The Diffusion Model.(5)

In this model the scalar interaction is assumed to be a very short range interaction of magnitude:

$$B_{ij} = K\,(d/R_{ij})\exp\left[-\lambda(R_{ij} - d)\right] \qquad \ldots\ldots\ldots (1.3)$$

where K and λ are constants, R_{ij} is the distance between the nucleus and the electron, and d is the distance of closest approach. Since the interaction is short range, it must follow that $\lambda d \gg 1$. When this is so, the factor (d/R_{ij}) in the scalar interaction has little effect on its functional dependence but the presence of this factor greatly increases the ease of calculation of the scalar spectral density function $J_e(\omega)$. The time dependence of B_{ij} arises because R_{ij} changes as the molecule and free radical diffuse about in the liquid.

The Sticking Model. (5)

This model has been previously used by Abragam (18). Here, B_{ij} is zero unless the molecules containing the electron and the nucleus are stuck together, in which case B_{ij} is a constant K. The time dependence arises because the time of sticking τ_e is assumed to be a random variable. However, in order to apply this model to the scalar coupling (first treating dipolar coupling by the diffusion model, it is assumed that the time of sticking is short compared with the

diffusional correlation time, for otherwise the finite sticking time would have to be taken into account in the calculation of the dipolar spectral density function.

The modified sticking model.

Muller Warmuth has postulated that a better fit to the experimental results might be obtained (19) if the sticking time is increased until it becomes comparable with the diffusional correlation time. It is however, difficult to envisage a chemical mechanism for the sticking which is sufficiently versatile to cover every case. It is possible to justify the use of random diffusion to treat the dipolar coupling, if it is assumed that only a small fraction of the I spins are "stuck" to a free radical. The majority of I spins would then diffuse up to and away from the radical, undergoing collision but not sticking (perhaps because of incorrect orientation). Alternatively, if there is no chemical sticking, it must be that an extended step function is a good approximation to the variation of the scalar coupling constant with internuclear distance in a collision. If this is the case the scalar spectral density function will be similar to that in a true sticking model, without, necessarily implying any sticking on this model. Thus the treatment of the dipolar coupling would be similar in each case.

The Three Spin Effect.

To explain the positive enhancements (negative ρ) observed with fluorine nuclei in solutions containing free radicals, it has been assumed that scalar coupling of the electron to the fluorine nucleus occurs. However, these positive enhancements might arise through a three spin interaction with other nuclei (e.g. H) which may be present in the solution, by assuming that the interactions are dipolar. Thus coupling to the electrons will produce a negative polarization of the fluorine nuclei, but the polarization of the protons is also negative and, since the gyromagnetic ratios of hydrogen and fluorine nuclei are positive, the fluorine nuclei will tend to be positively polarized by coupling to the protons (equation (1.26)). If the proton polarisation and the proton-fluorine coupling are of the correct magnitude, the positive tendency produced by the three spin interaction may outweigh the negative polarization produced by direct fluorine-electron coupling.

This effect can be investigated by strongly irradiating the sample at the proton frequency, whilst simultaneously applying microwave power to excite the electron resonance and observing the fluorine nuclei. If the polarisation of the fluorine nuclei occurs via the protons, there should be a change in the fluorine enhancement when the protons are

irradiated. The results of triple irradiation experiments are described in detail elsewhere (20), and it has been shown that for the systems discussed in this thesis, the three spin effect is generally only significant in solutions far more dilute than have been used in the present investigation. Furthermore, positive fluorine enhancements have been observed in systems where no third spin is present (e.g. C_6F_6) and some compounds give negative fluorine enhancements at low magnetic fields but positive enhancements at high fields. Neither observation is explicable in terms of a three spin effect.

Applications of the Overhauser Effect.

The applications of the Overhauser effect fall into two main categories:

(a) Information about electron-nuclear coupling.

(b) The enhancement of nuclear resonances too weak to be detected by other means.

An example of (b) is the detection of C^{13} nuclear resonance spectra. C^{13} is only 1% abundant in natural carbon and under normal conditions its resonance signal is not easily observable. Work in this laboratory (20) has demonstrated the feasibility of enhancing C^{13} signals and both positive and negative enhancements have been observed.

The work presented in this thesis is mainly concerned with testing quantitatively the models postulated for the modulation of intermolecular electron-nuclear scalar coupling.

Interpretation of Data for the Diffusion and Sticking Model. (5)

The relative effect of scalar and dipolar interactions may be described by a quantity

$$\zeta = J_e(0)/J_d(0) \qquad \ldots\ldots \quad (1.39)$$

where $J_e(0)$ and $J_d(0)$ are the spectral density functions for scalar and dipolar coupling at zero frequency. If $\zeta = 0$, the interaction is only dipolar, if $\zeta \gg 1$ the scalar interaction is dominant.

When dipolar and scalar interactions are important ρ can be calculated as a function of ζ. Because ρ depends also on the spectral density near the electron Larmor frequency, ρ can be plotted as a function of frequency for various values of ζ. In practice it proves to be convenient (5) to present ρ as a function of $(\omega_s \tau_c)^{1/2}$ where τ_c is the diffusional correlation time defined as

$$\tau_c = \frac{d^2}{\frac{1}{2}(D_I + D_s)} \qquad \ldots\ldots\ldots \quad (1.40)$$

where d is the distance of closest approach of an electron and a nucleus, D_I and D_S are the self diffusion coefficients of the solvent molecules and of the radicals respectively.

In order to obtain plots for ρ it is necessary to calculate the spectral density functions for each model, and values of the reduced functions

$$j_d(\omega_s) = Jd(\omega_s)/Jd(0).$$

$$je(\omega_s) = Je(\omega_s)/Je(0)$$

are tabulated by Hubbard as a function of $(\omega_s\tau_c)^{\frac{1}{2}}$. The expression for ρ is then:-

$$\rho = \frac{40\, j_d(\omega_s\tau_c) - 3\zeta\, j_e(\omega_s\tau_c)}{56\, j_d(\omega_s\tau_c) + 24 + 3\zeta\, j_e(\omega_s\tau_c)} \qquad \ldots\ldots\ (1.41)$$

Plots of $(\omega_s\tau_c)^{\frac{1}{2}}$ for different values of ρ are shown in figures 1.3 and 1.4.

From measured values of ρ at the two magnetic field strengths 3,300 gauss and 12,500 gauss, the possible values of $(\omega_s'\tau_c)^{\frac{1}{2}}$ and $(\omega_s''\tau_c)^{\frac{1}{2}}$ can be obtained as well as the values of ζ. The single prime refers to measurements at 3,300 gauss and the double prime to those at 12,500 gauss.

From the possible values of $(\omega_s\tau_c)^{\frac{1}{2}}$, the values of $j_d(\omega_s)$ and $j_e(\omega_s)$ for the two models can be obtained.

Further, since

$$\frac{1}{T_1} - \frac{1}{T_{1,o}} = n_e Jd(0)\left[\frac{28}{3}\, j_d(\omega_s\tau_c) + 4 + \tfrac{1}{2}\zeta\, j_e(\omega_s\tau_c)\right] \ldots (1.42)$$

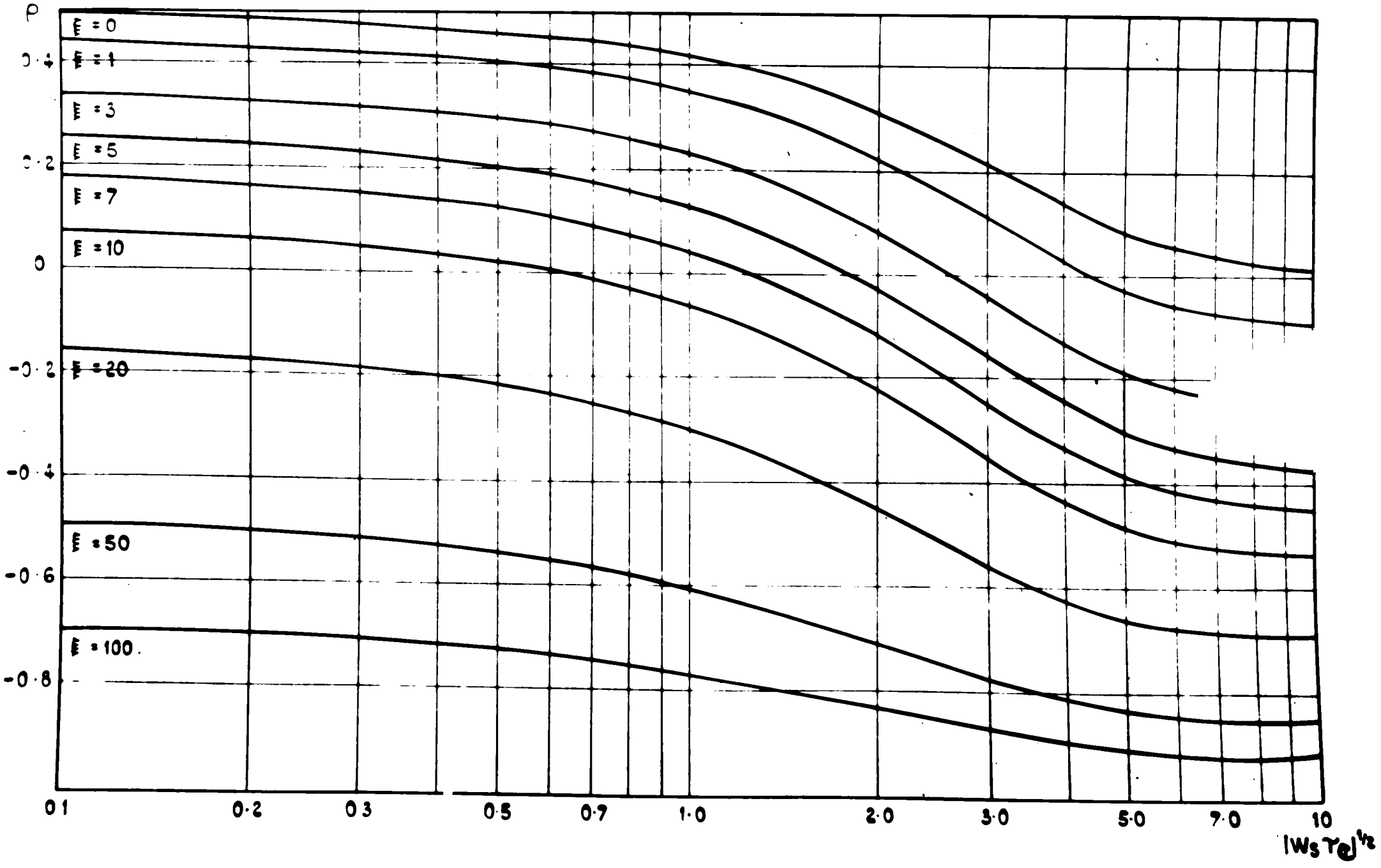

Figure 1.3 Plots of ρ vs. $(\omega_s \tau_c)^{1/2}$ for the Sticking Model for different values of ξ

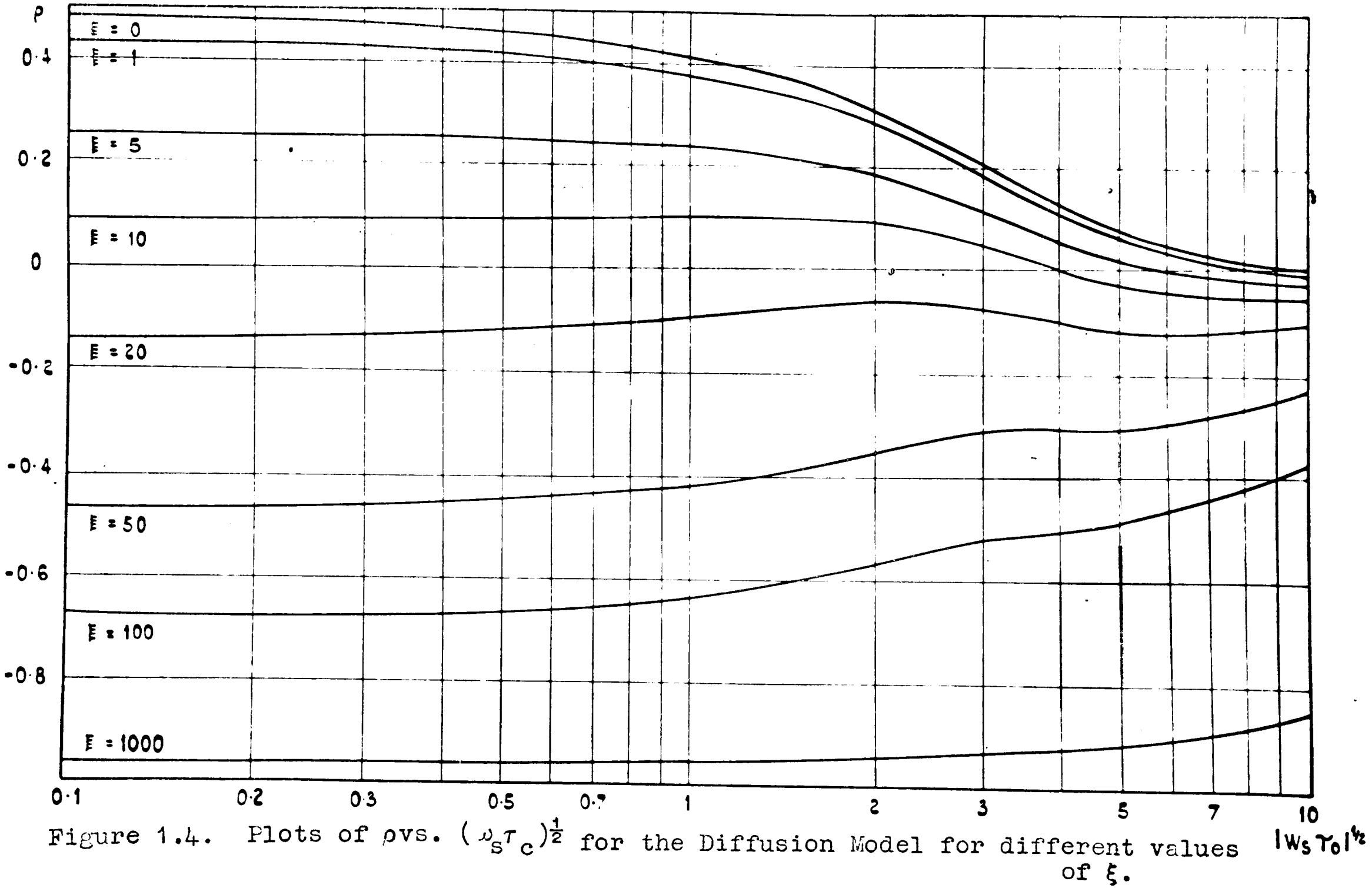

Figure 1.4. Plots of ρ vs. $(\omega_s \tau_c)^{\frac{1}{2}}$ for the Diffusion Model for different values of ξ.

where n_e is the number of unpaired electron spins/c.c. of liquid, then the ratio

$$\left\{ \frac{1}{T_1} - \frac{1}{T_{1,o}} \right\} \Big/ \left\{ \frac{1}{T_1''} - \frac{1}{T_1'} \right\}$$

can be calculated and compared with the measured values of T_1', T_1'' and $T_{1,o}$, for agreement between calculated and experimental values will support the model chosen. In concentrated radical solutions, T_1 is very short compared with $T_{1,o}$ and it is sufficient to measure the ratio $(1/T_1')/(1/T_1'')$.

Furthermore, since

$$Dd = \frac{\gamma_1^2 \gamma_2^2 \hbar^2}{90 \; Jd(0)} \qquad \ldots\ldots\ldots (1.43)$$

where $b = \frac{1}{2}(b_s + b_1)$, values of J and of the distance of closest approach d can be obtained.

Interpretation of Data for the Modified Stickiness Model.

Muller Warmuth uses a different notation (19) for this model, from that previously used by Hubbard for the diffusion and Stickiness models. In order to compare experimental data, on all models, it is more convenient to transpose Muller Warmuth's equations into the Hubbard notation. Thus ρ is given by:-

$$\rho = \frac{5\,j_d(\omega_s\tau_c) - 5K\delta\left(\frac{1}{(1+\delta\omega_s^2\tau_c^2)}\right)}{j_d(\omega_s\tau_c) + \left(\frac{1}{(1+\delta\omega_s^2\tau_c^2)}\right)} \qquad \ldots\ldots\ldots (1.44)$$

and

$$\frac{1}{T_1} - \frac{1}{T_{1,0}} = n_e I_d(0)\left[\frac{28}{3} j_d(\omega_s\tau_c) + 4 + \frac{20}{3}\delta\left(\frac{1}{1+\delta\omega_s^2\tau_c^2}\right)\right]$$

$$\ldots\ldots\ldots (1.45)$$

where

$$\delta = \tau_e/\tau_c$$

$$K = \frac{5\,b^2 I^2(B)^2}{\omega_s^2\, n_e\, \gamma_I^2\, \gamma_S^2} \qquad \ldots\ldots\ldots (1.46)$$

τ_e is the correlation time for the scalar interaction (i.e. the time of sticking). n_b is the probability that one nucleus is stuck to any electron at any time.

I is the coupling constant in cycles/sec.

Thus ρ can be plotted as a function of $(\omega_s\tau_c)$ for various values of K and δ. As before, the measured values of ρ at 3,500 gauss and 12,500 gauss yield possible values of $(\omega'_s\tau_c)$ and $(\omega''_s\tau_c)$ in addition to values of K and δ. The calculation of the relaxation time ratio, T''_1/T'_1, d and D can then be carried out in an analagous manner to that used for the Li fusion and sticking models.

C H A P T E R I I

The Overhauser Experiment.

The Overhauser experiment involves pulsing a sample containing unpaired electrons and suitable nuclei in a magnetic field, irradiating at the electron resonance and noting any effect on the nuclear resonance. The enhancement of the nuclear resonance can be measured as a function of the applied microwave power used to excite the electron resonance, the concentration of the unpaired electron spins, and the strength of the magnetic field. If the nuclear spin-lattice relaxation times are also measured, then all the parameters mentioned at the end of chapter I, may be calculated.

The Spectrometers.

(i) The X-band spectrometer

This has a magnetic field of 12,500 gauss (electron frequency 35,00 Mc/s) and details have been published (21). However, Mr. J.G. Kenworthy has modified the probe by reducing the diameter of the nuclear resonance coil to 3mm, and providing a means of air cooling the sample.

(ii) The L-band Spectrometer.

This has a magnetic field of 3,300 gauss (electron frequency 9,200 Mc/s) and details have been published (22).

To enable the temperature dependence of the Overhauser effect to be studied at 3,300 gauss, Dr. J.C. Kenworthy and Dr. J.A. Ladd have constructed a variable temperature cavity. This cavity is rectangular and operates in the H_{012} mode. The incident microwave power is introduced through a co-axial coupler and tuning is effected by means of a plunger. A glass tube passing through the region of maximum microwave magnetic field serves to support the n.m.r. receiving coil in the cavity and to centre the sample in the field. The bottom end of the tube is connected by lewar sleeved tubing either to a source of heated compressed air, or to a supply of liquid nitrogen whose rate of evaporation into the system is controlled by an electrical heater. For insulation, the major portion of the wave guide cavity is filled with polystyrene foam. The cavity is similarly insulated on the outside to prevent radiation affecting the pole pieces of the magnet. In this way the temperature of the sample can be varied from -20°C to 100°C and maintained within ± 1.0° of a particular temperature (ignoring microwave heating effects) for the duration of an experiment. The sample temperature is measured at the beginning and end of each experiment by the substitution of a dummy sample containing liquid paraffin and one junction of a copper-constantin thermocouple.

(iii) The Low Field e.s.r. Spectrometer.

In order to measure the concentration of radical solutions used in the Overhauser experiments, a low field e.s.r. spectrometer was built. This has a magnetic field of 130 gauss (electron frequency 350 Mc/s). A full description of the apparatus has been published (23).

For the sake of completion, the published details of the above spectrometers are included in the Appendix.

Choice and Preparation of Radical Solutions.

The choice of a radical for the Overhauser experiments is governed by the following considerations:-

(i) Ease of preparation

(ii) Stability in the absence of oxygen

(iii) The spin lattice relaxation time of the electron, which should be sufficiently long to allow an appreciable saturation of the electron resonance - using the power available.

(iv) Magnitude of enhancements of the various resonances which should be large thus permitting accurate measurements on the systems studied.

(v) Solubility in the solvents to be investigated, which in the present work are non-polar.

The radicals commercially available were 1.1- Diphenyl -2-Picrylhydrazyl, (D.P.P.H.), which could be obtained from Koch Light Laboratories Limited, and 2-6-di-tert-butyl-α-(3,5,di-tert-butyl-4-oxo-2,5 cyclohexadien-1-ylidene)-p-tolyloxy, (Galvinoxyl), which could be obtained from Aldrich Chemical Company. In addition, α, γ -bis-diphenylene-β-(p-iso-propylphenol) allyl, (B.P.I.P.A.), was provided as a gift from Dr. S.L. Foley, and perchloro-diphenyl methane, (P.P.M.), was a gift from Professor M. Ballester.

Samples containing the above radicals, (which were all solids) were made up by adding the radical to the deoxygenated solvent under an atmosphere of nitrogen. Deoxygenation of solvents was carried out either by a "freeze-thaw" pump technique, or by purging with nitrogen.

A radical which could be prepared easily in the laboratory and was soluble in non polar solvents was 2-4-6 tri-tertiary butyl phenoxy (T.T.B.P.). The preparation of this was based on that used by Muller, Ley and Riedlinch (24), and was carried out as described below.

A known amount of 2-4-6 tri-tert butyl phenol was dissolved in the appropriate solvent, which must be immiscible with water in this particular preparation. An alkaline solution of potassium ferricyanide (which had previously been boiled to remove oxygen and then allowed to cool under an

atmosphere of nitrogen) was then added and the sample was shaken by using an electric shaker. During this process, a positive pressure of nitrogen over the solution was maintained to exclude any oxygen, since the radical, when formed, reacts with oxygen forming a peroxide (25). The ferricyanide solution oxidizes the phenol to the radical the presence of which can be detected by a deep blue colour in the organic layer, which is then separated from the aqueous layer, using an hypodermic syringe, and placed in a tube (which had been flushed out with nitrogen) containing molecular sieve, Linde Type 4A, which removed any water. This radical solution was maintained under a positive pressure of nitrogen and was stable for several weeks. When required for an experiment, the correct amount could be extracted by using a syringe and placed in the sample tube and then sealed off. The sample tube carried a Bunsen valve through which nitrogen was passed. This method has the advantage that it can be carried out in a series of test tubes, unlike that on which it is based where complicated apparatus is required. The percentage yield of the radical (based on the precursor concentration) varies between 50 - 100%, if the concentrations of the radical as determined on the low field e.s.r. spectrometer are correct.

If the solvent is miscible with water, some other oxidising agent such as lead dioxide is then used. In this case the procedure was to dissolve the precursor in the solvent and oxidize, in situ, with excess lead dioxide. After several hours the solution was centrifuged and the supernatant liquid was transferred to the sample tube. The percent conversion to radical was extremely small.

In both these preparations a large excess of the unchanged phenol in the final solution must be avoided, since this will alter the viscosity of the solution and affect the magnitude of the enhancement. (see Chapter 5). In practice, solutions up to 0.2M in the phenol were used in the above preparations.

Of all the radicals considered, T.T.B.P. gave the largest enhancement with fluorine and proton nuclei. The electron resonance of B.D.I.P.A. and P.D.V., unlike the other radicals and in particular contrast to D.P.P.H., could be very nearly saturated at both magnetic fields. However, both P.D.V. and B.D.I.P.A. were only slightly soluble ($< 10^{-2}$M) in fluorinated solvents, while D.P.P.H. was not very soluble in either protonic or fluorinated solvents. Hence T.T.B.P. was found to be the most suitable radical for the present set of experiments.

Since it was desirable to carry out a complete set of measurements for the same sample on the different spectrometers, special sample tubes had to be made since the diameters of the nuclear resonance coils at X and Q band are 5mm and 3mm, respectively. This tube was made by heating and drawing down (to 3mm) a portion of 5mm tubing and then heating the tube so that it bent into a V-shape with each arm a different diameter. The 3mm arm was then sealed off and the solution introduced via a Bunson valve on the other arm, as mentioned previously.

Experimental Procedures.

(a) Setting up the Spectrometers.

(i) Adjustements to the nuclear resonance detection system.

Phasing of the Signal.

The nuclear resonance signal is observed on the oscilloscope after passing through the phase sensitive detector and the r.f. phase is adjusted to select the absorption mode. The audio-phase detector is then connected into the circuit and the centre band phased out by adjusting the audio phase. The field is then adjusted to bring the first sideband to the centre of the scan.

Saturation check for the resonance.

The nuclear resonance signal is recorded and the intensity

of the r.f. field at the sample is altered by changing the r.f. field attenuator setting. This change is then compensated for by altering the signal attenuator. The nuclear resonance signal is again recorded and the process repeated for different settings of the r.f. field attenuator until the signal is a maximum.

(ii) Adjusting the magnetic field to the centre of the electron resonance.

The enhancement of the nuclear resonance is observed and the field adjusted until the enhancement is a maximum. This is achieved by moving the nuclear resonance frequency in steps of 1 Kc/s and altering the field until the resonance appears.

Experiments have been performed in which the magnetic field has deliberately not been at the centre of the magnetic field and the ρ value obtained from the measurements was at X-band within experimental error of the ρ value obtained when the above procedure was carried out. At Q-band however, quite different ρ values were obtained.

(iii) Adjustements to the microwave cavity.

Both cavities operate in the $H_{01,n}$ mode where n = 1 at X-band and about 5 at Q-band. The cavities have to be adjusted for minimum reflection of the microwaves. This indicates a maximum of microwave fields

within the cavity for a particular mode, for the larger are those fields the greater will be the saturation of the electron resonance. This adjustement is carried out with maximum microwave power applied to the sample and not altered throughout an experiment. Since both cavities can operate in several different modes, the mode in which the largest enhancement of the nuclear resonance occurs, is the one chosen for the experiment.

Considerable heating may occur when the microwave power is applied to the sample, particularly if the sample is polar. This heating may be minimized as follows:-

(i) The cooling air is allowed to flow as fast as is practicable.

(ii) The microwave power is applied for the smallest interval of time, before recording the signal. In practice this was assumed to be $5T_1$, where T_1 is the nuclear spin-lattice relaxation time. Thus, in general, concentrated samples with $T_1 \leqslant 0.1$ sec. were used in all experiments.

(iii) The cavities are designed to operate in the $H_{01,n}$ modes, with the samples at the position of the minimum electric vector. This is the vector that causes the heating, which can be

minimized by using narrow sample tubes. At X-band, where microwave heating was particularly noticeable, very narrow sample tubes were used and occasionally, with polar samples, this becomes necessary at K-band as well. The reduction in size of the sample improves the quality factor of the cavity but has a detrimental effect on the signal-to-noise ratio of the nuclear resonance. At X-band, the quality factor was also found to increase (even in narrow tubes) as the amount of sample in the cavity decreased.

Since heating tends to occur, a sufficient period of time between readings must be allowed so that the sample may cool.

(b) Measurement of the microwave power dependence.

The nuclear enhancement at several different microwave powers was measured by noting the height of the enhanced and unenhanced signals. It was assumed that the signal height ratios were the same as the signal area ratios. This is valid as long as the resolution of the magnet remains constant throughout an experiment. A plot of the reciprocal enhancement factor, A^{-1}, versus the reciprocal microwave power applied, P^{-1}, was then made. From equation (1.25) this ought to be a straight line plot. Fig. 2.1 shows a typical

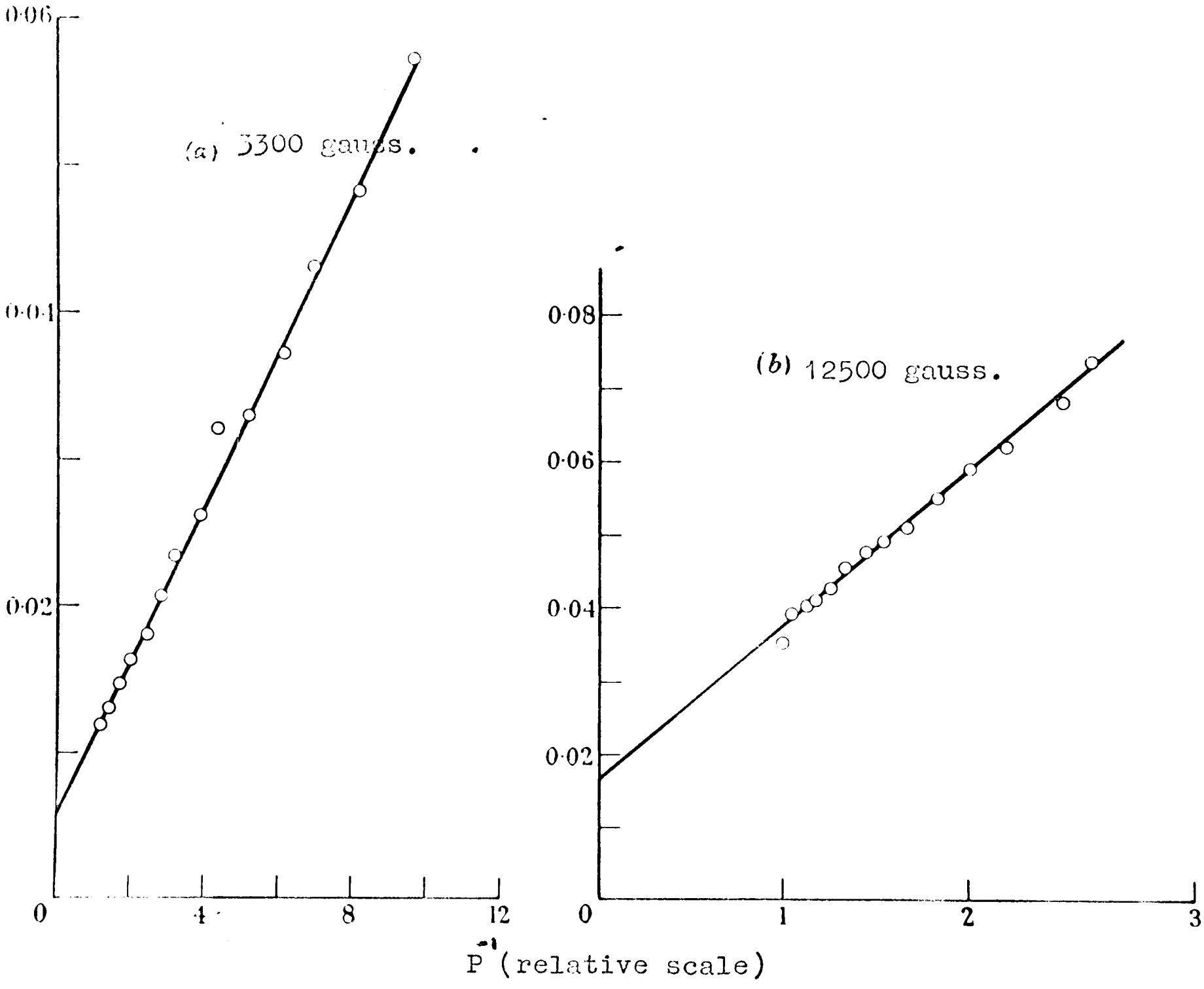
0·06
0·04
0·02
A
(a) 3300 gauss.
0
4
8
12
0·08
0·06
0·04
0·02
(b) 12500 gauss.
0
1
2
3
P⁻¹ (relative scale)

Figure 2.1

A^{-1}/P^{-1} curve for T.T.B.P. in benzene at 3,300 and 12,700 gauss. If the plots were not straight lines, then the results had to be rejected. These deviations might arise from:

(i) Heating of the sample by the microwaves (see particularly chapter 5, for the effect of temperature on the enhancement). At each different power the heating effect will be different.

(ii) Changes in the Klystron frequency during the experiment, which will result in the magnetic field no longer being at the centre of the electron resonance. This is checked by comparing the enhancement of a particular power at the beginning and end of an experiment.

(iii) Changes in the height of the unenhanced signal, (which is recorded at the beginning, and end of the experiment). If the difference is more than $\pm$ 10% the run has to be rejected.

(c) Measurement of the concentration dependence.

The above experiment was carried out for several different concentrations (c) of the radical. A plot of A_{max}^{-1} (obtained from the above measurements) versus c^{-1} was made. This is shown in fig. 2.2 for solutions of T.T.B.P. (prepared by the two different methods) in benzene at X-band fig. 2.3 shows a typical plot also for T.T.B.P./benzene

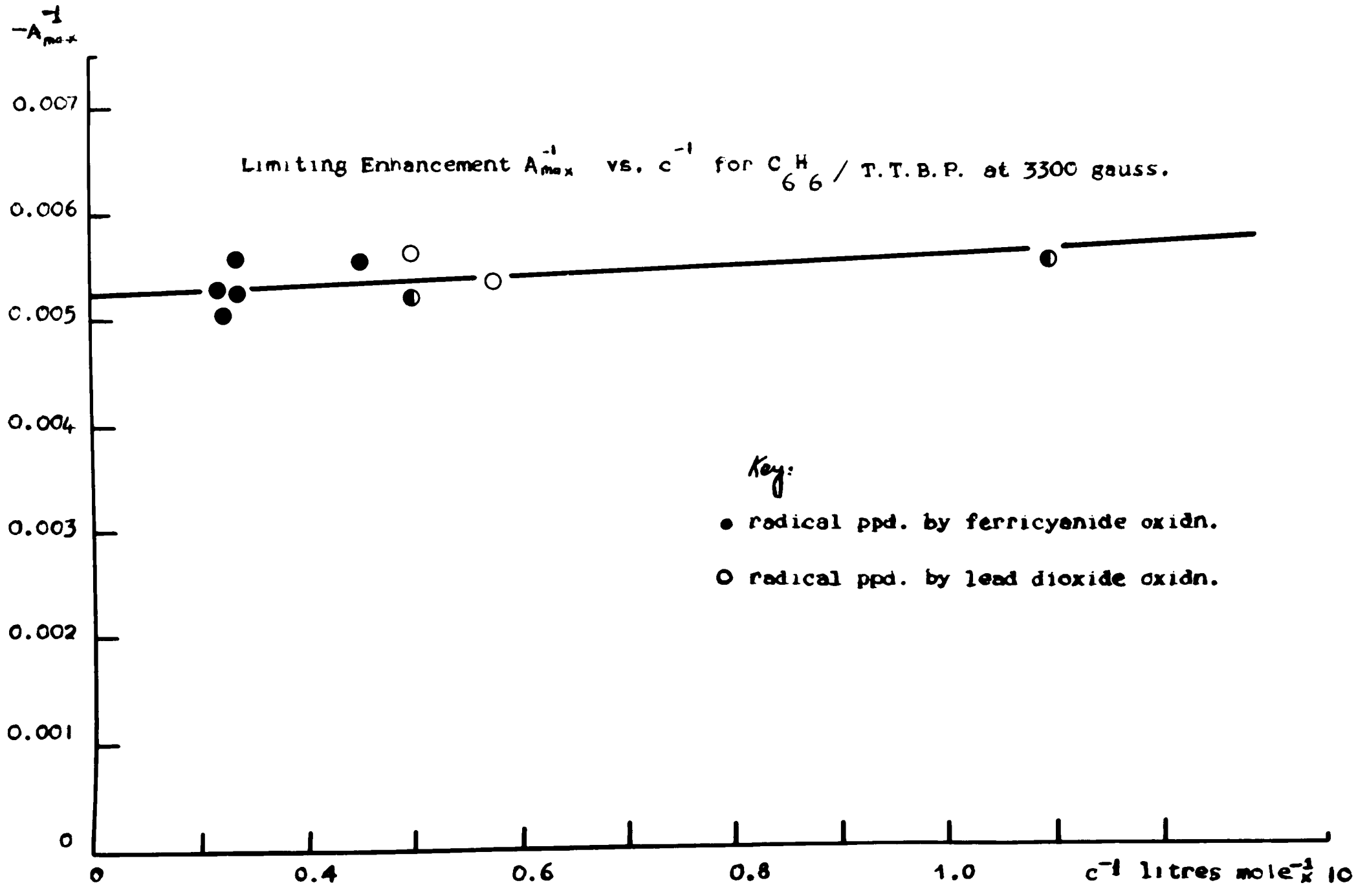
$-A_{max}^{-1}$
0.007
0.006
0.005
0.004
0.003
0.002
0.001
0
Limiting Enhancement A_{max}^{-1} vs. c^{-1} for C_6H_6 / T.T.B.P. at 3300 gauss.
Key:
● radical ppd. by ferricyanide oxidn.
○ radical ppd. by lead dioxide oxidn.
0
0.4
0.6
0.8
1.0
c^{-1} litres $mole^{-1}$ x 10

Figure 2.2

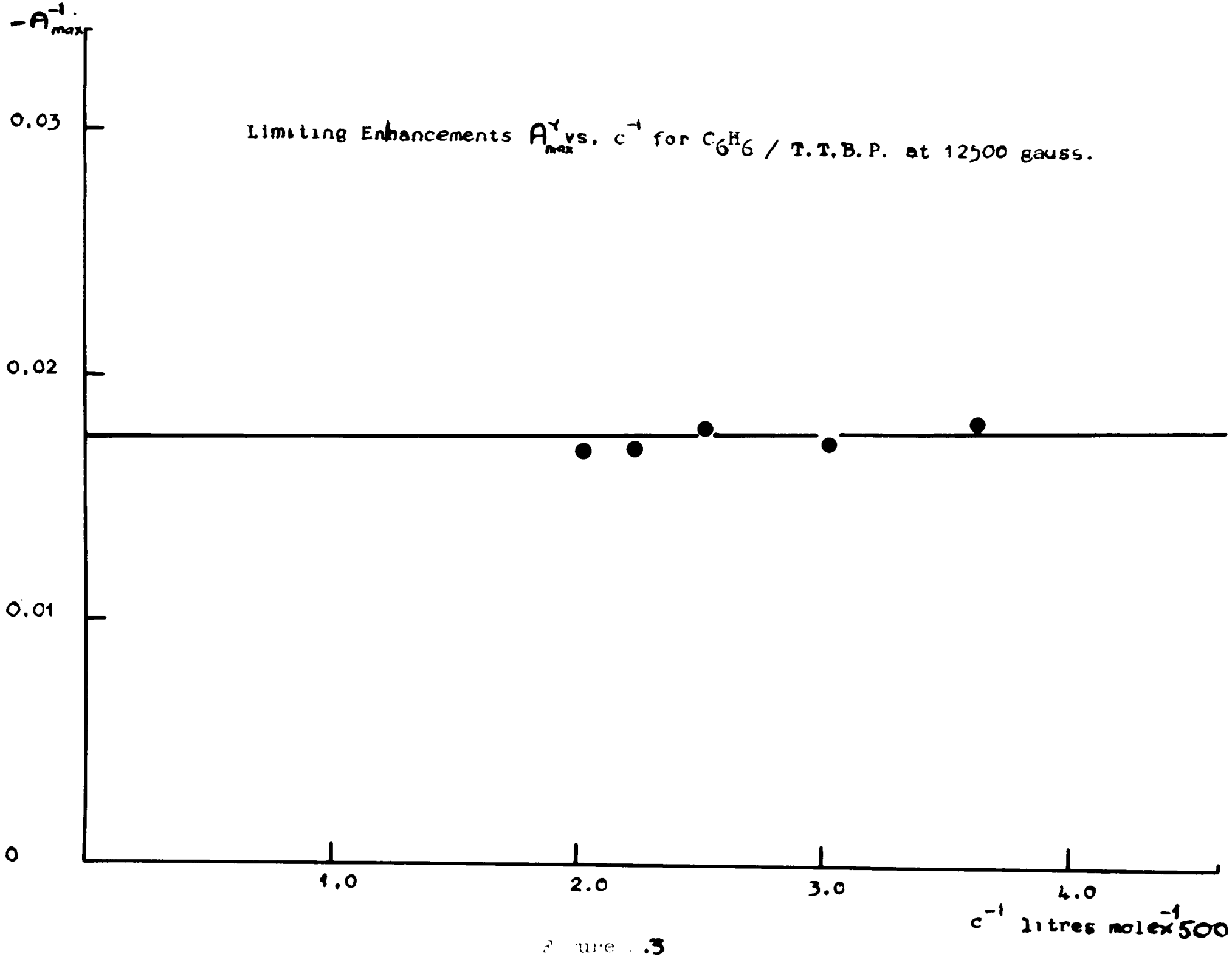
$-A^{-1}_{max}$
0.03
0.02
0.01
0
Limiting Enhancements A^{γ}_{max} vs. c^{-1} for C_6H_6 / T.T.B.P. at 12500 gauss.
1.0
2.0
3.0
4.0
c^{-1} litres mole^{-1} 500

Figure 3

solutions at Q-band.

The radical concentrations were estimated by measurement of the area of the e.s.r. signal, which making allowance for the volume of the solution, could then be compared with the area of the e.s.r. signal from a standard (potassium nitrosyl chromicyanide) of known spin concentration.

(d) Measurements of the nuclear spin lattice relaxation time.

These were measured by adjusting the field to 'sit' on top of the nuclear resonance signal and observing, on an oscilloscope or fast writing recorder, the rate of growth or decay of this signal, when the microwave power was turned on or off respectively. However, the r.f. field must be sufficiently small not to cause saturation of the nuclear resonance and experiment has shown (26) that this must be attenuated by at least 30 db from the normal setting if a true T_1 is to be obtained.

If the decay (or build up) curves are longer than one second, then they are recorded on a pen recorder, and the time axis is calibrated by rewinding the paper and running out the chart again with a 1 c.p.s. square wave fed to the pen. Faster T_1's are photographed on an oscilloscope using a known time base. On the X-band machine there is a Z-modulation facility and thus the brilliance can be modulated at a known frequency. The modulation is provided by a Venner counter

which produces a 100 c.p.s. or 10 c.p.s. square wave. Thus the trace may be made to blip every hundredth or tenth of a second.

From a knowledge of $T_{1,o}$ and T_1 the f-factor in equation (1.26) can be computed for each solution and thus the gradient of the A_{max}^{-1} vs. c^{-1} curve can be calculated, knowing A_{∞}^{-1}. This has been done for the benzene/C.T.B.P. solutions A_{max}^{-1}/c^{-1} plots shown in figures 2.2 and 2.3 when the calculated and theoretical lines were found to coincide.

C H A P T E R I I I

Field Dependence of the Overhauser effect.(44)

Introduction.

In order to distinguish between the three possible models for modulation of the scalar coupling, discussed in Chapter I, measurements have been carried out for some selected systems at 3,300 and 12,500 gauss. The results have then been fitted to each model in an attempt to find out which model was in best agreement with these experimental results. Clearly to provide a unique fit, results at several different fields are required, and where other data are available this has been taken into account. It is possible to calculate the theoretical ratio of the relaxation times at the two fields and comparison with the experimentally determined ratio, provides an extra criterion in fitting the results to a model.

Experimental.

Solutions of T.E.M.P.O. in the appropriate solvent were prepared as described in the previous chapter and the values at 3,300 gauss (ρ_1) and 12,500 gauss (ρ_2) obtained. The values quoted in Table 3.1, are the results of at least twenty five determinations for each sample. The spin lattice relaxation times of the solvent nuclei and the radical

concentrations of the solutions were also measured. Concentrated radical solutions were used in all cases and the measured spin lattice relaxation times of the nuclei were of the order of 0.1 secs. Since in all cases $T_{1'o'}$ the spin lattice relaxation time of the nuclei in the absence of radical, is long compared to that measured in the presence of radical, T_1, the leakage factor, was very nearly equal to unity, so that the limiting enhancement A_{∞}^{-1}, was equal to A_{max}^{-1} (equation 1.26 when f = 1) and could be obtained with only one extrapolation.

Results and Discussion.

Table 3.1. shows the ρ values at 3,500 gauss (ρ_x) and at 12,500 gauss (ρ_a).

The results for the proton resonances with the possible exception of those for $C_6F_5CH_3$ may be fitted to the curve calculated for pur dipolar coupling. On Hubbard's notation this is when $\xi = 0$. This curve is common to all models, when scalar coupling is absent. The parameters calculated for the systems studied are shown in Table 3.2, together with those calculated for other nuclei, using the "Diffusion Model". (In the case of $C_6F_5CH_3$, the enhancements were extremely small at 12,500 gauss and thus the error in ρ_a is ± 50%.

This interpretation for protons in terms of pure dipolar coupling, modulated by translational diffusion of the molecules,

is in good agreement with the work of Muller Warnath et al (8) and Poindexter (27) who have investigated a large number of protonic systems at low fields.

2. Scalar Coupling.

All the fluorine enhancements are positive at 12,500 gauss. Since, as has been pointed out, this is unlikely to arise from a "3-spin effect", an attempt was made to fit the results to each model.

The Sticking Model.

The results did not fit at all satisfactorily to this model even allowing for gross errors in the experimental values of ρ. However, if a very approximate fit was made then the correlation times calculated are of the order of 10^{-12}secs., which are an order of magnitude less than the values obtained for benzene - where the Sticking and Diffusion Models were identical.

The Diffusion Model.

Several fits for the experimental results are possible. Table 3.2 shows the parameters calculated using the "best" fits, and in the cases of $C_6H_5CF_3$, C_6F_6 and CF_3CCl_3, the low field results have been taken into account. From the high field data alone, a possible fit for C_6F_6 was on $\zeta = 20$, with $\tau_c = 3.9 \times 10^{-}$ secs., and the calculated and

TABLE 3.1

Solvent	* ρ' at 3,300 gauss	** ρ'' at 12,500 gauss
$C_6H_6^+$	+ 0.287	+ 0.09
$C_6H_5^+CH_3$	+ 0.264	+ 0.094
$C_6H_5CH_3^+$	+ 0.230	+ 0.080
$C_6H_4^+F_2$	+ 0.281	+ 0.101
$C_6H_4F_2^+$	+ 0.056	- 0.027
$C_6H_5^+CF_3$	+ 0.250	+ 0.057
$C_6H_5CF_3^+$	+ 0.087	- 0.004
$C_6F_5^+CH_3$	0.182	0.026
$Cl_3^+CCl_3$	+ 0.066	- 0.023
$C_6F_6^+$	- 0.079	- 0.070

* The error in the ρ' values is $\pm 10\%$

** The error in the ρ'' values is $\pm 15\%$

TABLE 3.2 (Diffusion Model)

Solvent	T_1''/T_1' calculated	$T_1''T_1'$ measured	τ_c $\times 10^{-12}$ s	d Å	$cm^2 s^{-1} 10^6$	Z
$C_6H^+_6$	1.4	1.3 ± 0.1	10	3.55	13.2	0
$C_6H^+_5CH_3$	1.4	1.3 ± 0.1	10.9	3.36	10.3	0
$C_6H_5CH_3$	1.35	1.3 ± 0.1	13.7	3.54	9.1	0
$C_6H_4^+F_2$	1.44	1.37 ± 0.05	9.3	3.29	10.8	0
$C_6H_4F^+_2$	1.27	1.24 ± 0.10	23.9	4.67	9.6	7
$C_6H^+_5CF_3$	1.4	1.4 ± 0.2	12.5	3.93	12.4	0
$C_6H_5CF^+_3$	1.24	—	25.3	5.25	10.9	4
$C_6F_5-CH^+_3$	1.3	1.1 ± 0.1	20.2	3.37	5.6	0
$CF^+_3CCl_3$	1.1	1.25 ± 0.015	48	6.6	9.1	3
$C_6F^+_6$	1.1	1.6 ± 0.1	51	5.4	5.7	9

* The fluorine resonance enhancements were too temperature sensitive to obtain accurate quantitive results.

experimental T_1''/T_1' ratio equal. This curve predicts that the enhancement is always positive, independent of field. Such a fit, however, is inconsistent with the low field data of Muller-Warmuth (8) and Poindexter (26) who observed a negative enhancement at low fields. Accordingly, the fit on $\zeta = 9$, which is not a good fit at high fields, has been chosen taking all results into account.

Systems containing both proton and fluorine nuclei provide a good test of the theory, for two sets of independent measurements can then be carried out. If the proton enhancements are interpreted in terms of pure dipolar coupling ($\zeta = 0$), then a diffusion coefficient can be calculated for the protons. This can then be compared with that obtained from fitting the fluorine data to the appropriate curve. The results should be identical as both nuclei are on the same molecule. For the systems studied, this agreement is good and probably within experimental error.

Modified Stickin Model.

Because of the extra variable here, it is very laborious to attempt to fit the experimental data to this model, particularly so, since sufficient low field data are not available. However, for C_6F_6, CF_3CCl_3, and $C_6H_5CF_3$ low field data are available and the curves which are the best fits to the experimental data are shown. The values of K and δ chosen

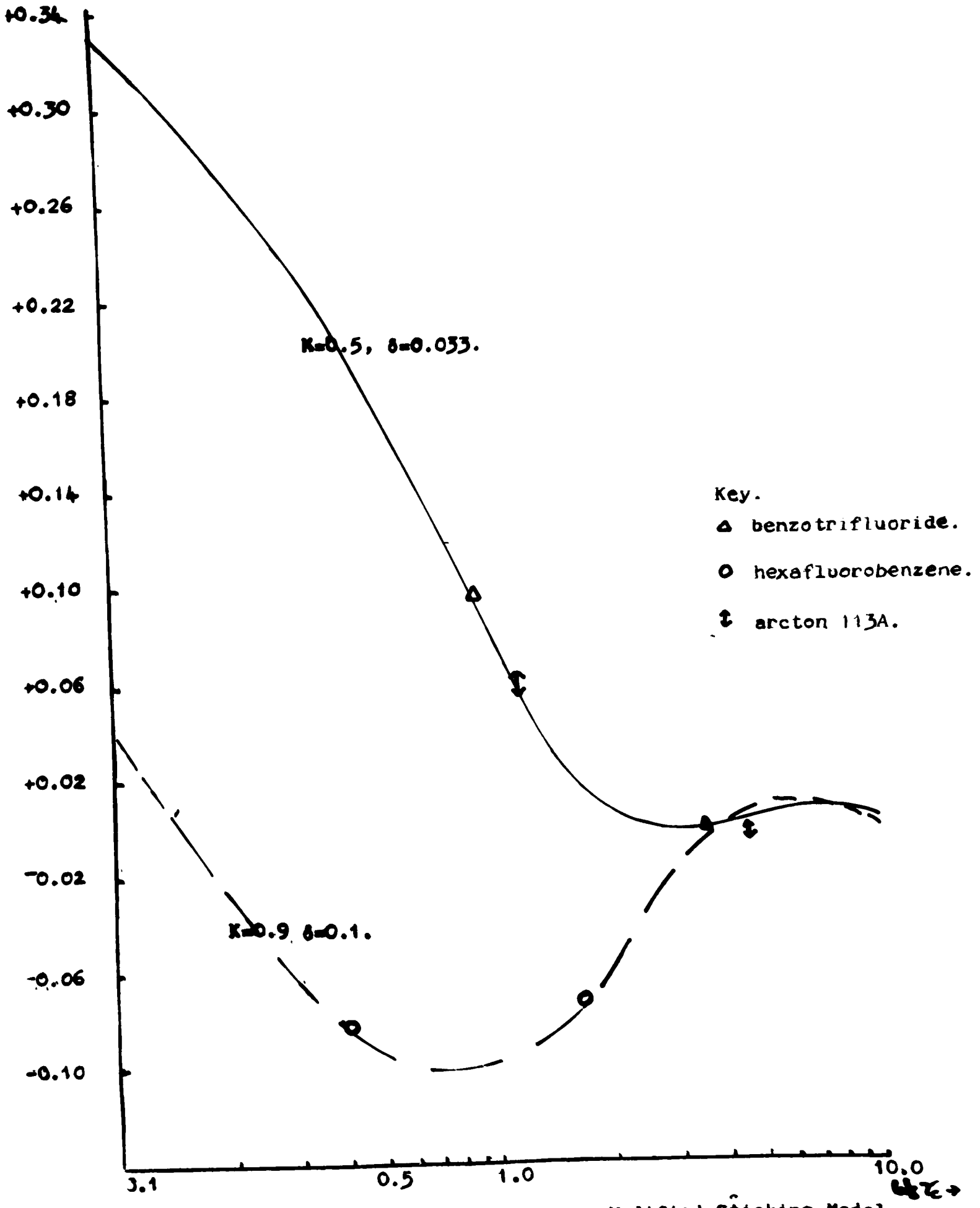

Figure 3.1 Plots of ρ vs. $\omega\tau$ for the Modified Sticking Model

for these fits were calculated by using a computer programme to plot families of curves for these different variables. The parameters calculated using this model are shown in Table 3.3, together, for the sake of comparison, with those calculated for the same systems using the Diffusion Model. Again, as on the latter model, the diffusion coefficients calculated for benzotrifluoride, from the proton and fluorine data are in reasonable agreement.

Comparison with experiment.

The Sticking Model is unsatisfactory in explaining the experimental results. On the other hand it is difficult to decide between the Modified Sticking and Diffusion Models. From the parameters calculated in Table 3.3, it can be seen that the agreement between these two theories for the arcton and benzotrifluoride is very good. On the other hand, the two theories do not yield the same parameters for C_6F_6. Both the values of the correlation time and diffusion coefficients differ considerably here.

One might expect that the correlation time in solutions of hexafluorobenzene would be greater than that for benzene ($\tau_c = 1 \times 10^{-10}$ sec) because of the increase in viscosity. On this basis the value of 5.1×10^{-10} sec. calculated on the Diffusion Model is more reasonable than 0.8×10^{-10} sec. obtained from the other. However, the relaxation time ratio

Table 3.3

Solvent	Diffusion Model						Modified Sticking Model					
	T_1''/T_1' measured	T_1''/T_1' calc.	$\tau_c \times 10^{10}$ s	d A°	$D_{cm}{}^2 s^{-1} \times 10^6$	β	T_1''/T_1' calc.	$\tau_c \times 10^{10}$ s	d A°	$D_{cm}{}^2 s^{-1} \times 10^6$	K	σ
C_6F_6	1.6	1.13	5.1	5.4	5.7	9	1.7	0.8	3.3	12.9	0.9	0.1
CF_3CCl_3	1.25±0.015	1.1	4.8	6.6	9.1	3	1.3	2.4	5.6	10.3	0.5	0.03
$C_6H_5CF_3$												
(E)	1.40	1.4	1.25	3.93	12.4	0	1.4	1.25	3.93	12.4	0	0
(F)	-	1.24	2.53	5.25	10.5	3.4	1.4	1.32	4.6	15.9	0.5	0.03

is in good agreement with experiment for the Modified Sticking Model and not for the Diffusion Model.

Conclusion.

While the Sticking Model is a poor fit to the experimental results, it is difficult to decide unambiguously between the other two models. Clearly, more results are required to test the Modified Sticking Model for a wider range of compounds. This would necessitate more work at low fields.

It may seem surprising that scalar coupling is observed with fluorine nuclei and not protons. However all that this scalar interaction implies is an overlap of the free radical electronic wave function with the wave function of the protons or fluorine atoms of the solvent at the moment of impact. The free radical electron must then reach the nucleus possibly through a polarization mechanism, by means of a contact interaction which will be much greater for fluorine than for a proton because of the increased value of the ns wave function at the nucleus. Thus scalar coupling to protons might occur, but it may be too small to be observed. Other indications of scalar coupling to fluorine nuclei have been found from measurements of the ratio of the spin-lattice and spin-spin relaxation lines of the fluorine resonances in solutions of free radicals in fluorinated benzenes (32).

Furthermore, evidence for "through space" scalar coupling between fluorine atoms, has been obtained from a study of solvent effects on nuclear spin coupling constants (33.).

Thus, since scalar coupling of the electron to the fluorine atom does seem likely, a scalar shift of the fluorine resonances in radical solutions would be expected. If the theoretical shifts for the two theories are calculated and compared with the experimental ones, then this would provide some additional information towards a choice of models. This is discussed in the following chapter.

C H A P T E R I V

Scalar Shifts.

Introduction.

The results of the previous chapter indicate that the positive fluorine enhancements observed can be explained, if it is assumed that scalar coupling of the electron to the fluorine occurs. If this is the case, a scalar shift of the fluorine resonance in radical solutions would be expected. Further, this shift should collapse when the electron resonance is saturated. In this chapter, this shift is calculated for hexafluorabenzene for the Modified Sticking Model and the Diffusion Model and this is compared with that observed experimentally.

Theory.

The scalar shift $\Delta\omega_I$ of the nuclear frequency ω_I is given by. (20)

$$\Delta\omega_I = -\bar{B}ij \langle \omega_o \rangle \qquad \ldots\ldots(1.1)$$

where $\bar{B}ij$ is the average value of the coupling constant for the i^{th} nucleus and j^{th} electron.

$\langle M_o \rangle$ is the expectation value of the total S magnetisation at equilibrium which from the Curie Law (3) may be written.

$$\langle So \rangle = N_s \cdot \gamma_s \cdot \hbar \cdot \frac{S(S+1)}{3\,KT} \cdot \quad Ho \qquad \ldots\ldots (4.2)$$

where N_s is the number of unpaired electron spins hence:

$$\Delta\omega_I = - \bar{B}ij \;\; N_s \cdot \hbar \left(\frac{\gamma_s}{\gamma_I}\right) \frac{S(S+1)}{3\,KT} \;\; (\gamma_I Ho) \qquad ..(4.3)$$

$$\therefore \qquad \frac{\Delta\omega_I}{\omega_I} = - \bar{B}ij \;\; N_s \cdot \hbar \left(\frac{\gamma_s}{\gamma_I}\right) \frac{S(S+1)}{3\,KT} \qquad \ldots\ldots (4.4)$$

In order to evaluate $\Delta\omega_I/\omega_I$, $\bar{B}ij$ must be known and the calculation of this depends on the model for the time dependence of the scalar interaction.

(A) Modified Sticking Model.

Let w_B be the probability that a particular nucleus is interacting with an electron at any given time. Then

$$\bar{B}ij = w_B \cdot B \qquad \ldots\ldots\ldots (4.5)$$

If n_o be the average number of nuclei interacting with one electron at any time and N_I be the total number of nuclei, then assuming the time each electron is unstuck is negligible then,

$$w_B = \frac{n_o}{N_I} \cdot N_s \qquad \ldots\ldots\ldots (4.6)$$

Thus equation (4.5) becomes:

$$\frac{\Delta\omega_I}{\omega_I} = - \frac{n_o}{N_I} \cdot B \cdot \left(\frac{\gamma_s}{\gamma_I}\right) \;\; N_s^2 \; \frac{\hbar \;\; S(S+1)}{3\,KT} \qquad \ldots\ldots (4.7)$$

which is similar to the expression derived by Bloembergen (29). B, the coupling constant which is finite when a radical and molecule are "stuck" together and zero otherwise is given by: (19)

$$K = \frac{5\omega_B \cdot d^3}{8\pi \gamma_s^2 \gamma_I^2 \hbar^2 N_s} \quad (D/\hbar^2) \qquad \ldots\ldots (4.8)$$

(B) Diffusion Model

The coupling of an electron to a nucleus is assumed to vary according to the equation (5)

$$Bij = B \cdot \frac{d}{R} \; e^{-\lambda(R-d)} \qquad \ldots\ldots(4.9)$$

so that $\bar{B}ij$ will be the average value of Bij over all values of Rij from d.

$$\therefore \quad \bar{B}ij = \frac{1}{V} \int_v Bij\,(R)\, d^3R$$

$$= \frac{1}{V} 4\pi \int_d^{Rm} dR\, R^2 Bij(R) \qquad \ldots\ldots (4.10)$$

where Rm is the maximum value of R governed by the dimensions of the sample, and V is the total volume of the solution. Integrating equation (4.10) by parts and assuming that $\lambda d \gg 1$ then:

$$\bar{B}ij = \frac{1}{V} \cdot 4\pi \cdot \frac{B\, d^2}{\lambda} \qquad \ldots\ldots (4.11)$$

Thus from equation (4) :-

$$\frac{\Delta\omega_I}{\omega_I} = -\frac{4\pi}{V} \cdot d^3 \cdot \frac{\gamma_s}{\gamma_I} N_s \cdot \kappa \frac{S(S+1)}{3kT} \left(\frac{B}{\lambda d}\right) \quad \ldots\ldots (4.12)$$

From the definition of ζ (5)

$$\zeta = \frac{Je(0)}{Jd(0)} = 100 \left(\frac{B}{\lambda d}\right)^2 \frac{d^3}{\gamma_I^2 \cdot \gamma_s^2 \cdot \kappa^2}$$

$$\therefore \left|\frac{B}{\lambda d}\right| = \frac{\zeta^{\frac{1}{2}} \cdot \gamma_I \cdot \gamma_s \cdot \kappa}{100\, d^3} \quad \ldots\ldots\ldots (4.13)$$

Thus by substituting for $B/\lambda d$ in equation (12) $\Delta\omega_I/\omega_I$ can be evaluated.

Experimental.

The shifts of the fluorine resonances in several solutions of the radical T.T.D.P. in hexafluorobenzene were measured using tetra-methyl silane as an internal standard. The experiments were performed on the 12,500 gauss spectrometer. With this instrument it is possible to change from proton to fluorine resonances quickly and easily, and the resonance frequencies can be measured exactly using the Schomandl ND5 and NDF 1 frequency synthesisers. The procedure involved changing from the proton to the fluorine resonance and vice versa, several times for each solution. This enabled the elimination of errors in the shifts arising from any drift

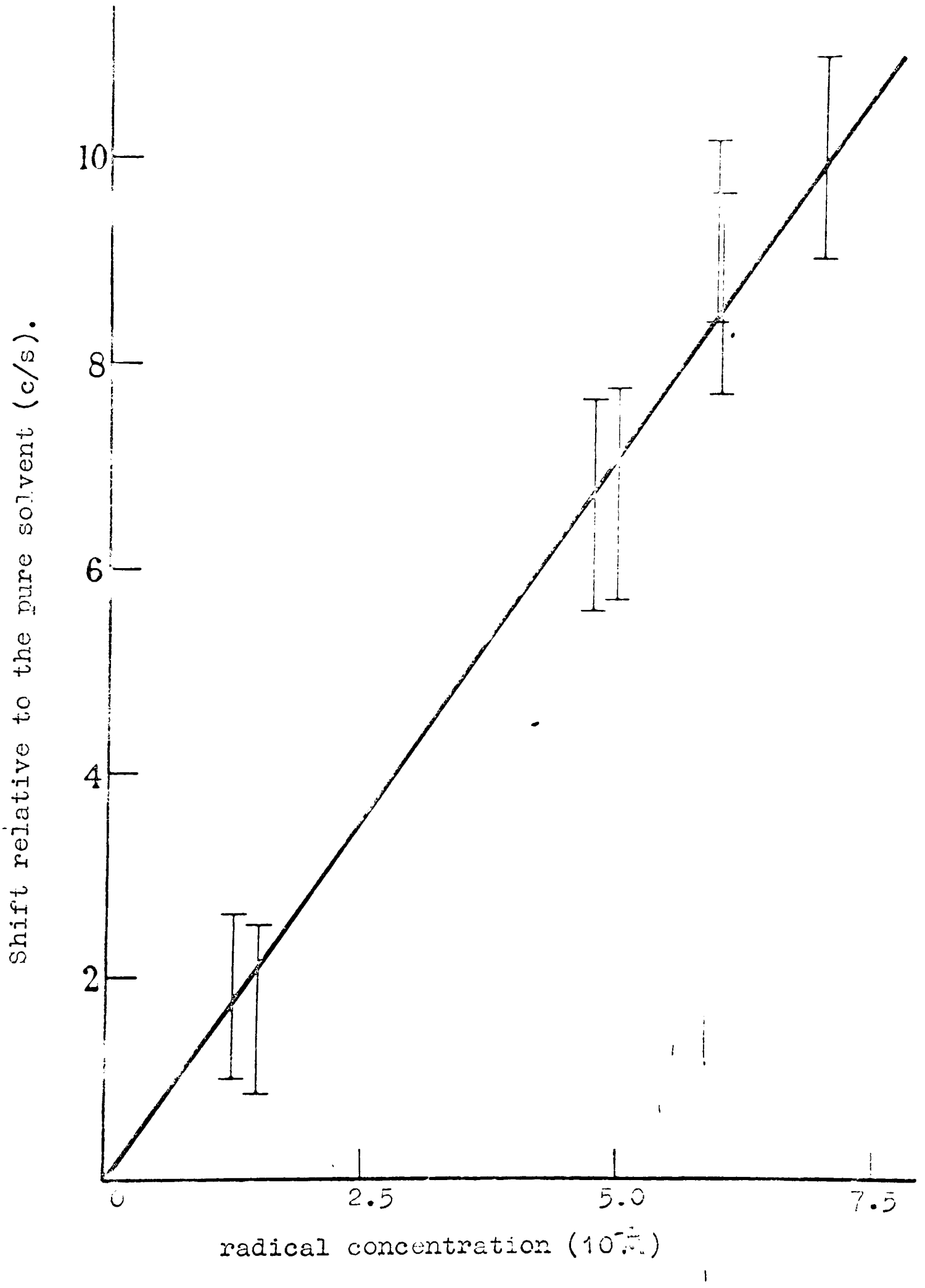
Shift relative to the pure solvent (c/s).
10
8
6
4
2
0
2.5
5.0
7.5
radical concentration (10⁻⁷M.)

Figure 4.1

(which was assumed to be linear) in the magnetic field. The error in the shifts is ± 1 c.p.s.

Results and Discussion.

Figure 4.1 shows the measured shifts plotted against radical concentration. The fluorine resonance shifts down field and although the shifts are of the same order as the line widths, there is no doubt about the sign.

If the shift of the fluorine resonance is caused by scalar coupling to the radical, the shift should collapse when the electron resonance is saturated. When microwave power was applied to a 10^{-2}M solution of the radical, the fluorine resonance shifts approximately 1.5 c.p.s. up field, but the proton resonance shows a very small downfield shift. This latter shift probably results from the change in paramagnetic susceptibility when the electron resonance is saturated, whereas the up field shift of the fluorine resonance is the net result of the partial collapse of the downfield scalar shift and the susceptibility shift. These shifts are shown in Fig. 4.2. In order to calculate the shifts for the Modified Sticking Model it is necessary to decide on a value for n_0 in equation (6). i.e. it is necessary to decide how many nuclei are coupled to <u>each</u> electron at any one time. If it is assumed that some form of chemical association is implied in the "sticking" process, and if a 1:1 complex is

(a).

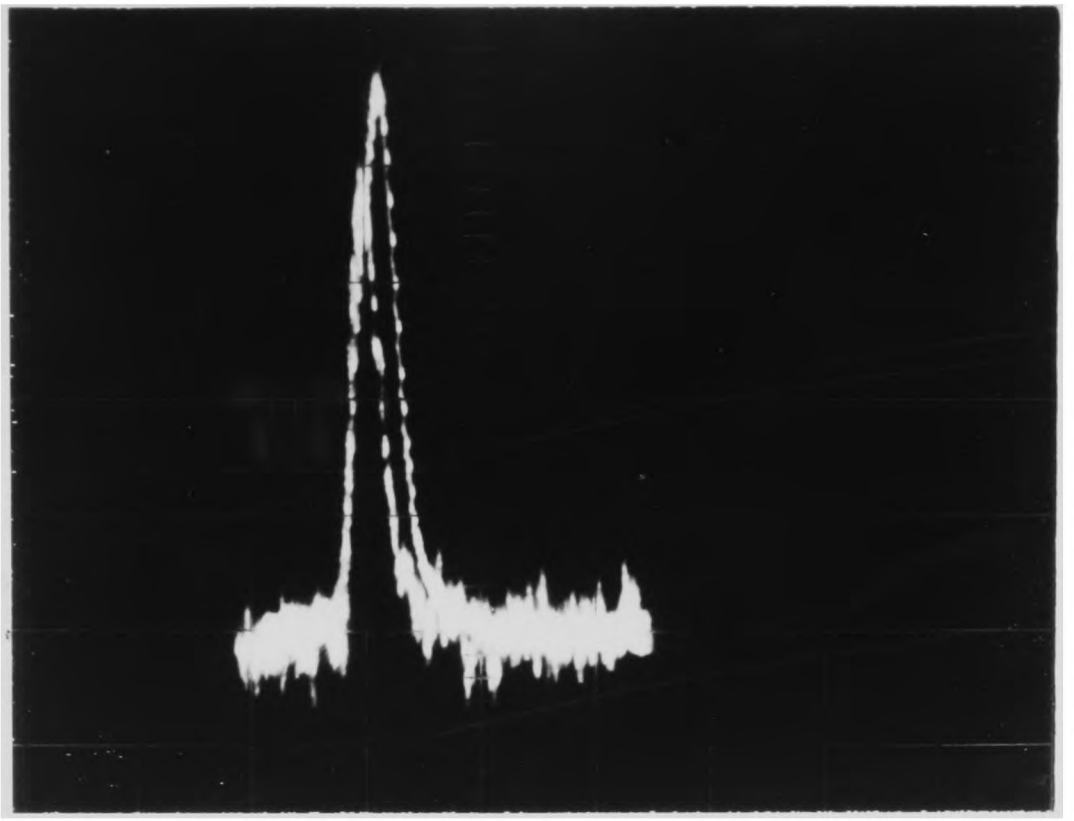

Figure 4.2. (a). C_6F_6 + T... .^{19}F resonanc..Large peak has gain reduced ten times. (b). C_6T_6 + T.M.S. ^{1}H resonance. Large peak has gain reduce ten times. Scale = 23c.p.s./cm. Scan is from high to low field, which is from left to right.

(b).

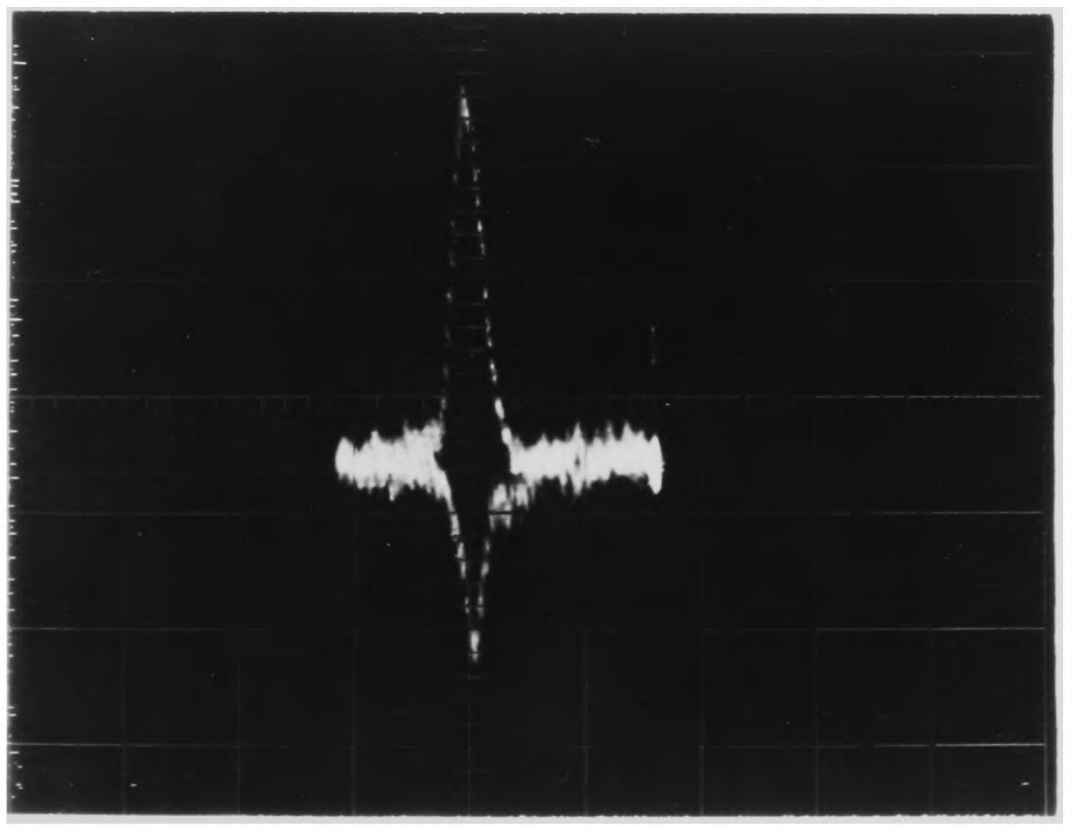

produced, then each electron will interact with all six fluorine nuclei in the solvent molecule to which the radical is stuck. The calculated shift for a 10^{-2} M solution of the radical in hexafluorobenzene is then 0.78 c.p.s. If each radical molecule "associates" with two solvent molecules then $n_o = 12$, and the calculated shift is doubled. Higher values of n_o can be ruled out from steric considerations, since molecular models indicate that it is difficult for more than two solvent molecules to be "associated" with one radical molecule. However, it has been assumed that the amount of time that an electron is not coupled to the n_o nuclei, is negligible but if this is not the case the calculated shift(s) will be less, and the coupling constant greater.

The modulus of the coupling constant $|B|$ can be evaluated directly on the Modified Sticking Model, and making the same assumptions as in the calculation of the shifts, the corresponding value is 0.53 Mc/s (or half this). The Diffusion Model, yields only values of $|B/\lambda d|$ where λ is a constant such that $\lambda d \gg 1$. In a later chapter, it is shown that $\lambda d = 1000$ is the minimum value of λd if the approximations made by Hubbard in evaluating the scalar spectral densities for this model are to be valid. Thus in this case only a minimum value for $|B|$ can be estimated by assuming $\lambda d = 1000$.

The results are summarized below for a 10^{-2} solution of the radical in hexafluorobenzene.

Modified Sticking Model.		Observed Shift at 50 Mc/s.	Diffusion Model	
Coupling Constant B	Shift at 50 Mc/s.		Coupling Constant B	Shift at 50 Mc/s
0.53×10^6 Mc/s	0.78 c/s	1.9 ± 0.3	410×10^6 Mc/s	1.5 c/s

On the Modified Sticking Model B corresponds to the constant value of the coupling constant between the electron and the nucleus when a radical and solvent molecule are "stuck" together. On the Diffusion Model, B, corresponds to the instantaneous value of the coupling constant at the distance of closest approach of the radical and solvent molecule.

It is difficult to know what fraction of the electron being transferred, the coupling constants correspond to. Symons (30) has calculated that for an electron in an isolated 2s orbital of a ^{19}F atom, the coupling constant to the nucleus is approximately 50,000 Mc/s. Thus if a comparison is possible a value of B of 410 Mc/s corresponds to the transfer of only a small percentage of the electron density to the fluorine nucleus.

The observed shift is in rather better agreement with that calculated for the Diffusion Model, but this may be fortuitous considering the poor fit of the ρ values for hexafluorobenzene to $\bar{3} = 9$. On the other hand, by taking $n_o = 12$, on the Modified Sticking Model, agreement is again obtained between experiment and theory. Thus either theory could explain the observed shift. Finally, as the shift is to low field, the coupling constant will be positive.

Conclusion.

Many more assumptions have to be made in the calculation of the scalar shifts for the Modified Sticking Model than for the Diffusion Model, if the theoretical and experimentally observed shifts are to agree. On this basis it follows that the Diffusion Model is probably the more favourable of the two. However, if the order of magnitude of the coupling constant predicted by the Diffusion Model is correct, then the maximum value of the coupling constant becomes comparable with the H_0 field, and when this is so, it is not valid to treat the coupling as a small perturbation. In this event the generally accepted relaxation theory may not be applicable, particularly at low fields. It may then be necessary to formulate two theories for the scalar interactions one at high magnetic fields where the scalar coupling is a small perturbation of the Zeeman levels and a further one at low fields where this is not the case.

C H A P T E R V

Correlation Time Dependence of the Overhauser effect.(45,46)

Introduction

In chapter 3, it was concluded that the results of the radical T.T.B.P. in benzene could be interpreted in terms of pure dipolar coupling which is modulated by the translational diffusion of the molecules. If however, a solution of the radical in benzene is prepared by oxidation of a saturated solution of tri-tert-butyl phenol, then the measured ρ values were less than those quoted in chapter 3.

At 3,300 gauss the fluorine resonance spectra of methyl pentafluorotoluene consists of a low field peak, arising from the p-fluorine and an unresolved high field multiplet. If a solution of this and the radical T.T.B.P. is allowed to warm up in the microwave cavity, then the initial enhancement of the low field peak, which is positive becomes negative. If then cooling air is applied to the sample, the enhancement becomes once again positive. This is illustrated in Fig. 5.1.

The results of the above experiments can be interpreted if it is assumed that a change in the translational correlation time τ_c had occurred. In the first case τ_c was increased by increasing the viscosity of the sample, with the excess of unchanged phenol in solution. In the second case τ_c was

Figure 5.1

Repeated scan of low field peak of Fluorine spectrum of $C_6F_5CH_3$.

a --power on.

b --cooling air on.

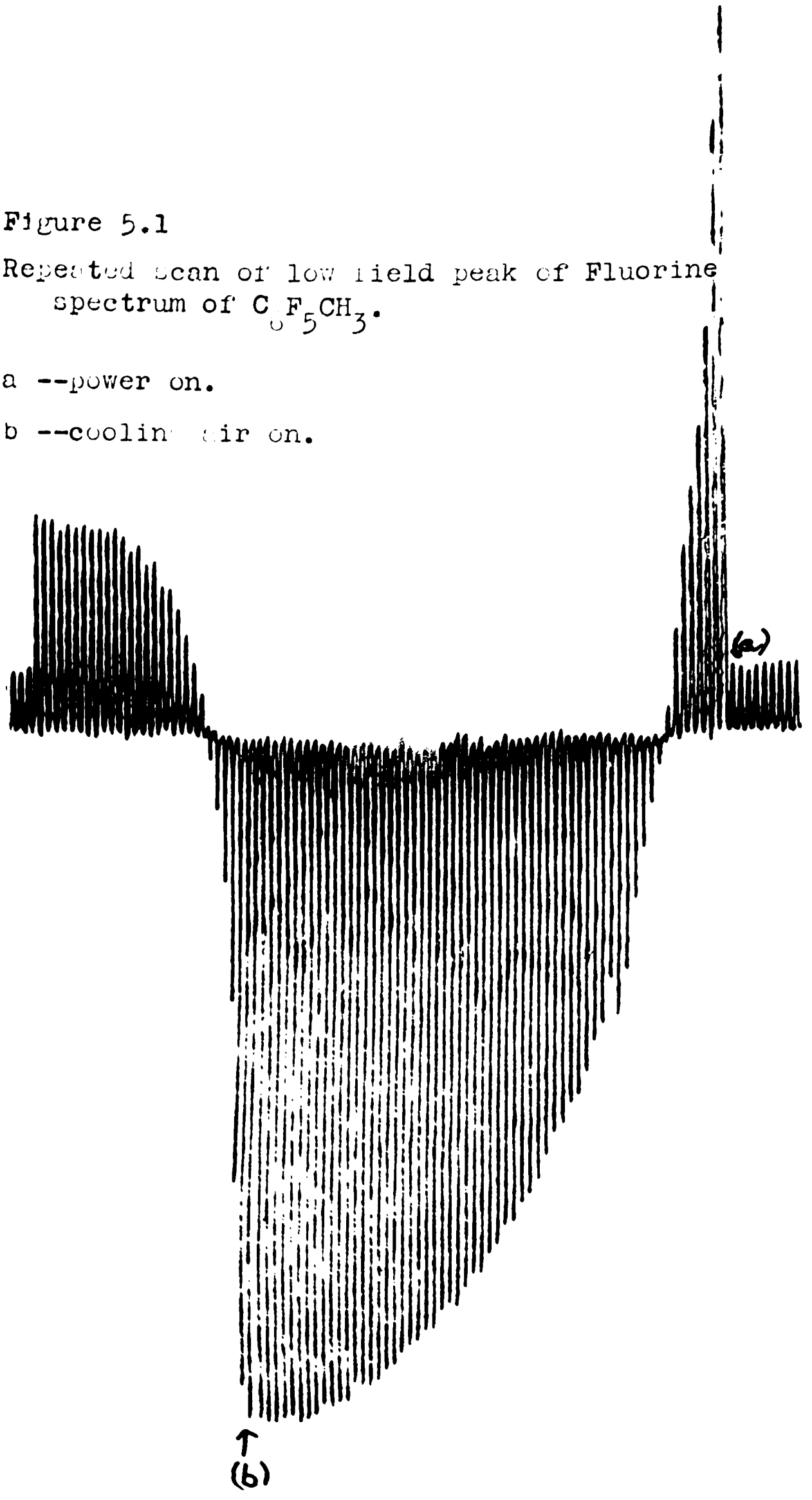

decreased, by increasing the temperature, which results in a decrease in viscosity. It was these experiments which initiated the work described in this chapter.

For both the Modified Sticking Model and the Diffusion Model ρ has been evaluated as a function of $\omega_s\tau_c$ (Chap. I) (where ω_s is the electron angular resonance frequency). The product $\omega_s\tau_c$ can be altered either by working at different magnetic fields, or by varying τ_c. This latter possibility is accomplished either by changing the temperature of the sample or by addition of some inert, miscible solvent which has a much higher (or lower) viscosity than that of the material under test. This change in τ_c at fixed ω_s, could result in a change in sign of the enhancement if the ρ versus $\omega_s\tau_c$ curve crosses the $\rho = 0$ axis.

The fluorine resonances of solutions of T.F.B.P. in p-difluorobenzene, of monofluorobenzene, of arcton 113A and benzotrifluoride are negatively polarised at 3,300 gauss and positively polarised at 12,500 gauss. These results can be fitted to the Diffusion Model, and in the case of benzotrifluoride to the Modified Sticking Model as well, which for particular values of ξ or K and δ, predict a change in sign of ρ as $\omega_s\tau_c$ increases. If it is assumed that ξ, K and δ remain constant, then this result could be checked by changing τ_c at fixed ω_s. When τ_c is increased by addition

of liquid paraffin the the polarisation at 3,300 gauss changes from negative to positive. An increase in temperature can then shorten τ_c enough to change the nuclear polarisation back once again, to a negative value.

The results for hexafluorobenzene, may be fitted to curves on either the Modified Sticking or Diffusion Models, both of which predict a change in the sign of ρ as $\omega_s\tau_c$ decreases. Thus if the viscosity of a solution of the radical in hexafluorobenzene is lowered, by addition of carbon disulphide, the polarisation which is positive at 3,300 gauss, becomes negative.

Similar changes in the sign of fluorine nuclear polarisations have been described by Imbaud & Bertlet (31), which occur when the temperature is changed, or on dilution with other materials. In these cases the authors have suggested that a three spin effect may be responsible, but it seems more probable that the change of correlation time is the important factor. In any event triple irradiation experiments (20) on the systems described above gave no indication of any three spin effect.

In this chapter, it has been attempted to determine experimentally the form of the ρ versus $\omega_s\tau_c$ curve, by variation of τ_c at fixed ω_s, for two systems, hexafluorobenzene and arcton 113A. The results have then been compared with

those predicted from the Modified Sticking and Diffusion Models.

Experimental

The ρ values for solutions of T.I.E.P. in either the arcton or hexafluorobenzene were measured as a function of temperature at 3,300 gauss, by using the variable temperature cavity described in chapter II. The ρ values were also measured as a function of the viscosity at 3,300 gauss and 12,500 gauss. In order to reduce the viscosities of the solutions under study, the following procedure was adopted. A solution of the T.T.B.P. radical in one of the fluorinated solvents was prepared as described in chapter II, and a solution of the radical in carbon disulphide was made up in a similar manner. The concentrations of the two solutions were compared by examining their E.S.R. spectra and the most concentrated was diluted with the appropriate solvent until the concentrations was equal. Mixtures of the two solutions were then made up containing various volume percentages of carbon disulphide. In this way the radical concentration was kept constant. In order to increase the viscosities of the solutions, the same procedure was followed but using a 45% chlorinated hydrocarbon, Cereclor S45, C_{14}-C_{19}, instead of carbon disulphide. As in chapter III, the leakage factor

was very nearly equal to unity, so that the limiting enhancement could again be obtained with only one extrapolation.

The viscosities of mixtures similar to the samples were measured at 25°C using several Ostwald viscometers. It was assumed that the addition of the radical to the sample did not affect the viscosity significantly.

Results and Discussion

The self diffusion coefficient of a nucleus X with radius a in a medium of viscosity η is given by the Stokes-Einstein equation:

$$D_X = \frac{kT}{6\pi\eta a} \qquad \ldots\ldots\ldots (5.1)$$

The mean diffusion coefficient D, of two components I and S in solution is thus

$$D = \tfrac{1}{2}(D_I + D_S)$$

$$= \frac{1}{12}\,\frac{kT(a_I + a_S)}{\pi\eta \cdot a_I \cdot a_S} \qquad \ldots\ldots\ldots (5.2)$$

where a_I and a_S are the radii of the I and S molecules. Since the diffusional correlation time τ_c is defined as

$$\tau_c = \frac{d^2}{D}$$

then

$$\tau_c = \frac{12\pi d^2}{kT}\,\frac{a_I\, a_S}{(a_I + a_S)}\cdot\eta \qquad \ldots\ldots (5.3)$$

thus τ_c is directly proportional to viscosity η . This direct dependence has been found to be in good agreement with experiments in many cases (34, 35) and it will be assumed for this work even for the diffusion of a small molecule in a solution made more viscous by addition of a long chain hydrocarbon.

In order to interpret the effect of varying the temperature the assumption will be made that the temperature dependence of η is given by

$$\eta = \eta_0 . e^{\Delta E/RT} \qquad \ldots\ldots (5.4)$$

where η_0 is a constant and ΔE is an activation energy for the process. Thus from equation (5.3),

$$\tau_c = \tau_0 e^{\Delta E/RT} \qquad \ldots\ldots (5.5)$$

where $$\tau_0 = \frac{12\pi d^2 (a_I a_S)}{K (a_I + a_S)} . \eta_0$$

In order to calculate the variation of τ_c with temperature it is then necessary to decide on a value for ΔE. For mobile organic liquids it has been found that ΔE lies in the range 1 - 3 k cal/mole (36, 37).

For the diffusion model, it has been shown that ρ is a function of $\omega_s \tau_c$. Thus a change in the electron resonance frequency will have an identical effect on ρ , to a similar

change in τ_c. However, for the Modified Sticking Model, this dependence upon $\omega_s\tau_c$ will only be true if it is assumed that f ($= \tau_e/\tau_c$) remains a constant for a given solution as the viscosity is varied.

(1) Hexafluorobenzene.

The results of varying the viscosity of solutions of T.T.E.P. radical in hexafluorobenzene by addition of either Aroclor 545, or carbon disulphide are shown in Table 5.1. The values obtained at 3,300 gauss are plotted as ρ versus τ_c/τ_{25} in figure 5.2. τ_{25} is the diffusional correlation time for hexafluorobenzene at 25°C (the magnet temperature) which is used as a reference point. Results obtained at 12,500 gauss are plotted on the same graph by multiplying each ordinate by the ratio of the two resonance frequencies. (3.8 in this case). This assumes that increasing the resonance frequency by 3.8 times is equivalent to increasing τ_c by 3.8 times.

The ρ values for 3,300 gauss are usually the result of only one measurement. It is difficult to estimate the probable random error but the ± 12% shown in the figure seems reasonable by comparison with repeated measurements on other systems. Measurements at 12,500 gauss are more difficult and the results quoted for C_6F_6/CS_2 mixtures are averages of at least five determinations. The errors shown

Figure 5.2 Plot of ρ vs. τ/τ_{25} for C_6F_6.

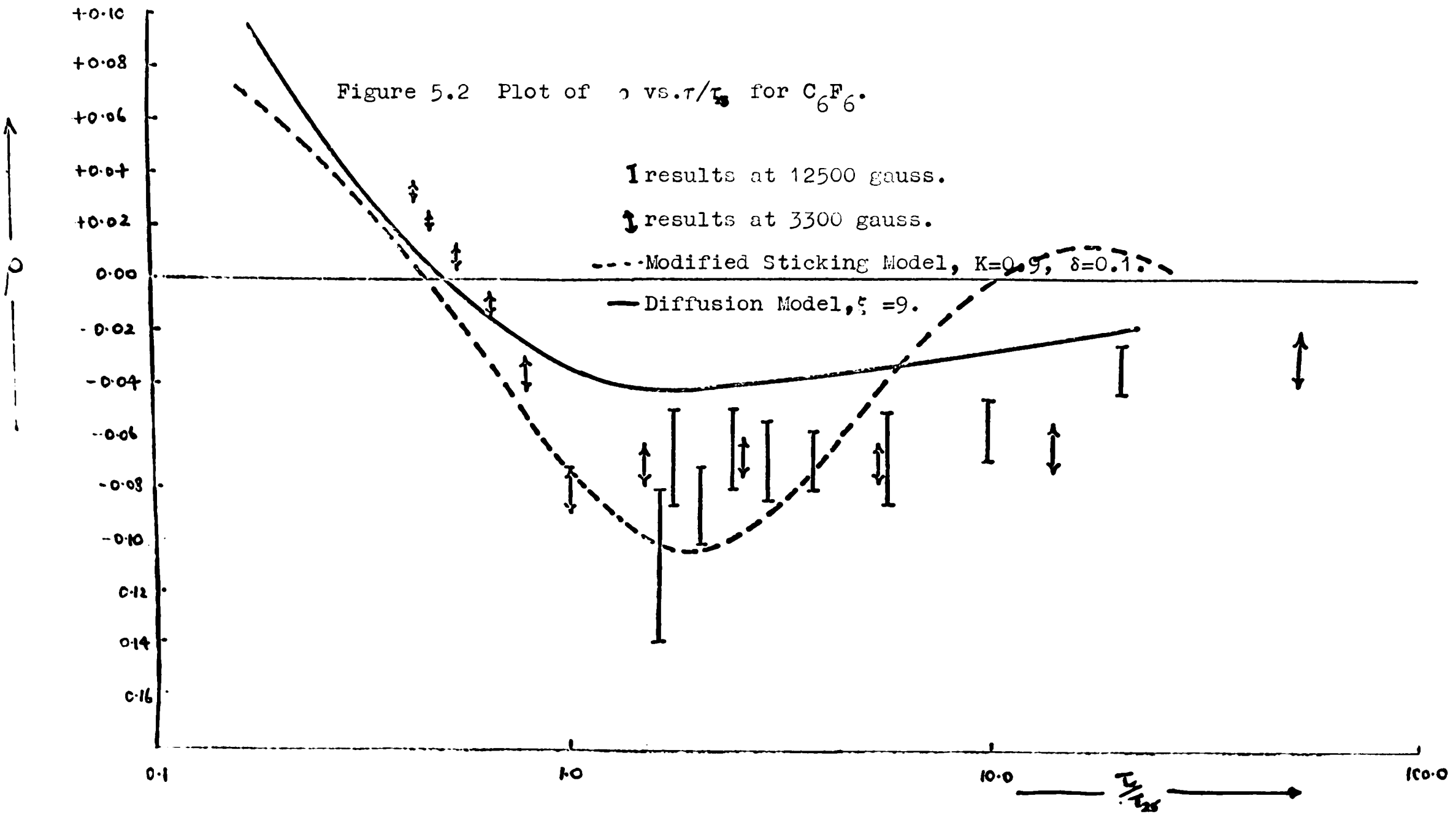

are ± 25%.

Decreasing the viscosity at 3,300 gauss caused the positive enhancement observed with pure hexafluorobenzene solutions to decrease and become negative in solutions containing more than 50% carbon disulphide. Increasing the viscosity at 3,300 gauss or varying the viscosity either way at 12,500 gauss produced no striking change in the magnitude of the enhancements. No serious discontinuity seems to result from the assumption that ρ is a function of the product $\omega_s \tau_c$. Comparison of the variable temperature results (Table 5.2) with the carbon disulphide dilution results enables a choice of a value for the activation energy ΔE. With ΔE = 1.5 Kcals/Mole, then the two sets of results are found to lie on the same curve. (Figure 5.2). The range of temperature over which studies could be made was limited by the freezing point of the solution on the one hand and by decomposition of the T.T.B.P. radical at approximately 100°C on the other. If however, ΔE = 2.5 Kcal/Mole then the variable temperature results fit precisely on the curve for the Modified sticking Model, but the correlation with the carbon disulphide dilution results is lost.

Figure 5.1 also shows the best fits of the experimental data to the Diffusion Model ($\zeta = 9$) and to the Modified Stickling Model ($\Sigma = 0.9$ and $\zeta = 0.1$). Neither theory gives

TABLE 5.1

C_6F_6	% CS_2 (VOL)	η op.	ρ(3300 gauss)	ρ(12500 gauss)
	0	0.93	- 0.080	- 0.069
	16.7	0.73	- 0.036	- 0.068
	33.3	0.60	- 0.009	- 0.064
	50.0	0.50	+ 0.009	- 0.086
	66.7	0.43	+ 0.023	- 0.064
	83.3	0.40	+ 0.034	- 0.110
	% Cereclor S45 (VOL)			
	0	0.93	- 0.080	- 0.070
	16.7	1.40	- 0.070	- 0.064
	33.3	2.45	- 0.067	- 0.056
	50.0	5.05	-.0.070	- 0.034
	66.7	13.10	- 0.064	- 0.029

TABLE 5.2

T °C	ρ value at 3,300 gauss	
	C_6F_6	CF_3COCl_3
3	+ 0.110	-
10.5	+ 0.092	-
25	+ 0.082	+ .054
40.5	+.0.057	-
48.5	-	+ 0.091
50	+ 0.043	-
62	+ 0.021	-
65.5	-	+ 0.11
74	-	+ 0.13
76	+ 0.006	-
84	+ 0.006	-
97	+ 0.017	-

an entirely satisfactory description of the results for hexafluorobenzene. Qualitatively the Diffusion curve is the better. The other predicts that the sign of ρ should change at least twice whereas only one such change has been observed. The parameters calculated from each theory are given in chapter III.

(2) Arcton 113A. (1,1,1,-trichloro- 2,2,2 trifluoro-ethane)

Table 5.3 shows the results of similar experiments on solutions of Arcton 113A. These are plotted as ρ versus τ_t/τ_{25} in figure 5.4. The key explains which points refer to 3,300 gauss and which to 12,500 gauss. The results of variable temperature experiments at 3,300 gauss, shown in Table 5.3 are also plotted in figure 5.3 with ΔE = 3.5 Kcal/mole. They are then in good agreement with the variable viscosity results.

The general shape of the curve is similar to that obtained for hexafluorobenzene solutions, but is shifted upwards towards more positive ρ values. The fit on the Diffusion Model to $\bar{3}$ = 3, takes into account the low field data. On the Modified Sticking Model several curves were found which gave approximate fits to the data. The best is probably K = 0.5 and δ = 0.03 The curves for both these models are also shown in figure 5.3. (The parameters

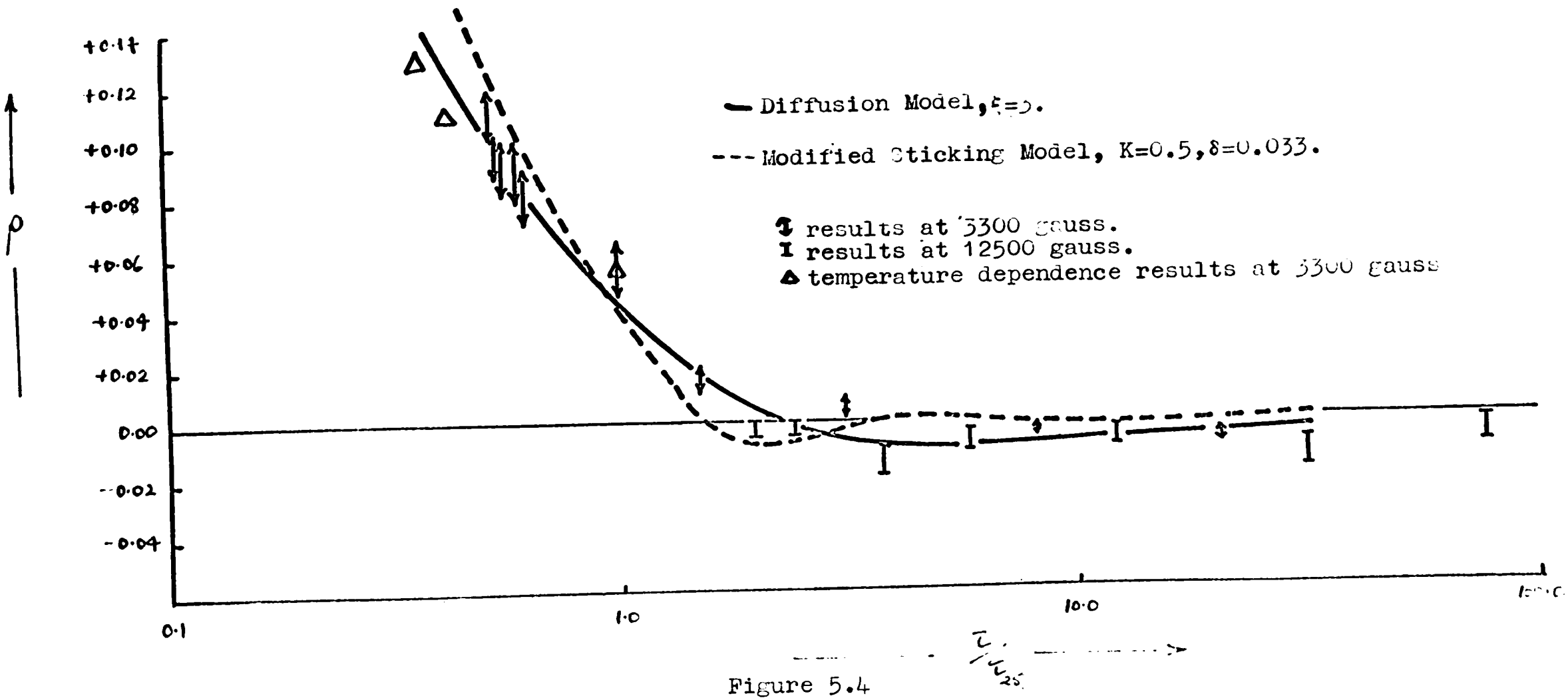

Figure 5.4

Plot of ρ vs. τ/τ_{25} for CF_3CCl_3.

C_6F_6. Comparison of temperature and carbon disulphide dilution studies.

× temperature results with ΔE 3.5 k.cals/mole.

△ temperature results with ΔE= 1.5 k.cals/mole.

○ carbon disulphide dilution results.

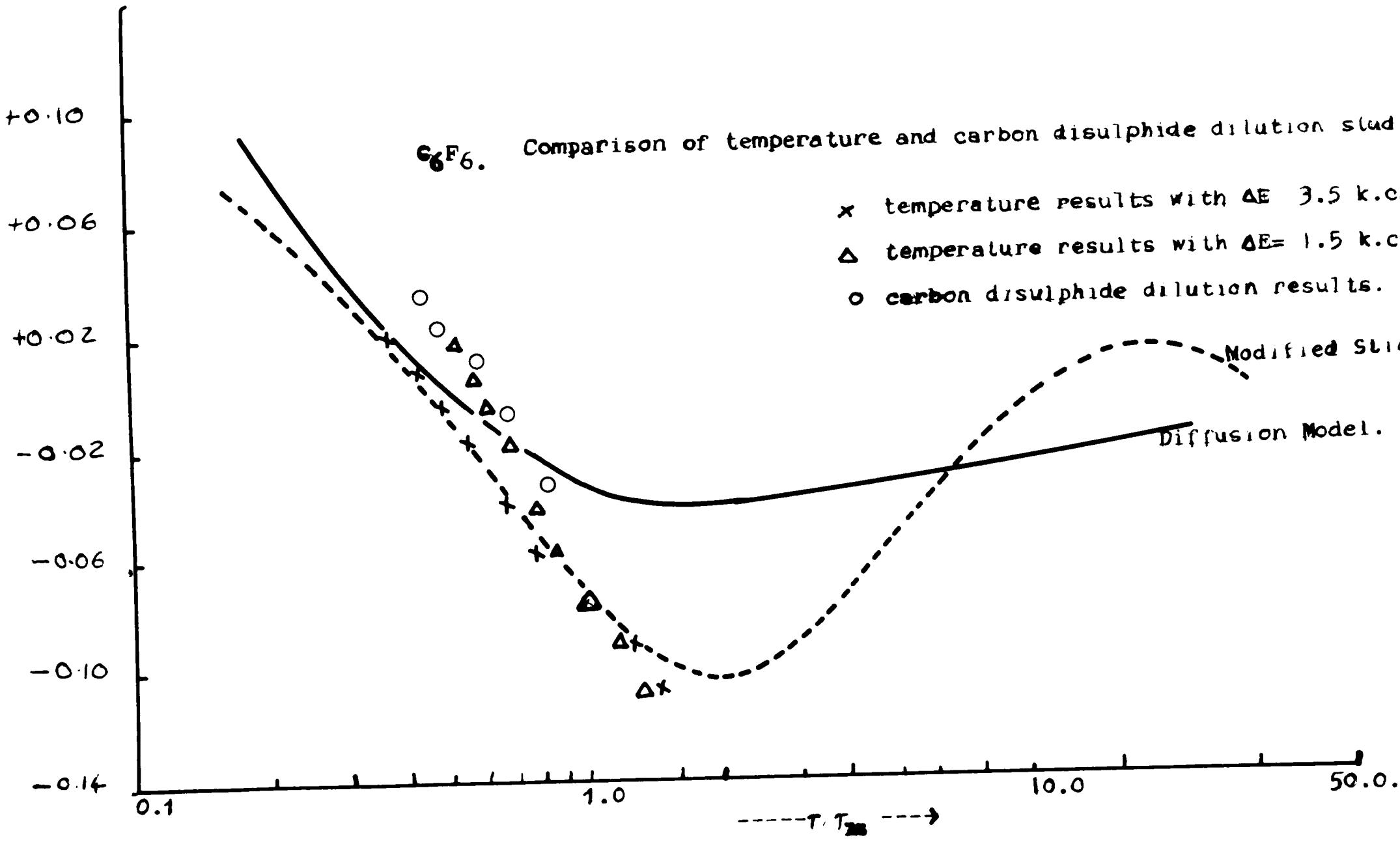

Figure 5.3

calculated for both models are given in chapter III). The K = 0.5 and δ = 0.03 curve crosses the ρ = 0 axis on three occasions. The enhancements seen at 12,500 gauss with solutions of the arcton made less viscous by addition of carbon disulphide were too small to extrapolate accurately but were all positive. Thus the corresponding ρ values were all negative and the ρ = 0 axis is an upper limit for all measurements at 12,500 gauss plotted between τ_c/τ_{25} = 2.0 and 3.8. For the Arcton/Cereclor S45 mixture of viscosity 2.5 cp (τ_c/τ_{25} = 3.2) a small negative enhancement ρ = +0.005 was seen at 3,300 gauss. At first sight this seems to confirm that the curve crosses the axis at least three times. However, if one of the crossing points lies between τ_c/τ_{25} = 3.8 and 3.2, increasing the temperature of a sample with τ_c/τ_{25} = 3.8 will result in a decrease in ρ , and the enhancement should change from positive to negative. No variable temperature probe is available for the 12,500 gauss spectrometer but when a sample of T.T.B.P. radical in the pure arcton was examined for a prolonged period with no cooling air, the enhancement remained positive even though the microwave power eventually heated the sample to its boiling point.

Since one point is plotted with a positive ρ in this region it must mean that either ρ is not a function of the product $\omega_s\tau_c$ and it is not permissible to compare values at

TABLE 5.3

CF_3CCl_3	% CS_2 (VOL)	η cp.	ρ (3300 gauss)	ρ (12500 gauss)
	0	0.79	+ 0.054	
	34	0.49	+ 0.081	Very small enhancements. always - ve.
	37.5	0.475	+ 0.090	
	50.0	0.44	+ 0.090	
	62.5	0.425	+ 0.095	
	80.0	0.415	+ 0.108	
	% Cereclor 345			
	0	0.79	+ 0.054	
	16	1.20	+ 0.015	- 0.007
	33.3	2.50	+ 0.005	- 0.006
	50.0	5.60	- 0.004	- 0.013
	66.7	16.30	- 0.007	- 0.004

TABLE 5.4

Arctor/CS_2 Solutions.

% CS_2	T°C	ρ (3,300 gauss)
50	49.5°C	.14
50	69.5°C	.14
0	73.0°C	.13

two different fields, as has been done in the figures, or there are large errors in τ_t/τ_{25}. This latter possibility would arise if the linear relationship between correlation time and viscosity did not hold for the viscous solutions. It might be expected that the correlation time for the small fluorinated molecule is much shorter than that predicted from the macroscopic viscosity of such solutions. If this is the case, the values obtained for the Cereclor 345 mixtures need to be shifted to lower values of τ_t/τ_{25} and the inconsistency in the ρ versus τ_t/τ_{25} curve would then be removed. Since most of the ρ values for these solutions lie on the horizontal portion of the curves, the correction will make little difference to the shapes of the experimental plots. It would appear then that the curve crosses the $\rho = 0$ axis once only in this region favouring the theoretical $\xi = 3$ curve of the Diffusion Model.

On the Diffusion Model the arcton results at high fields alone can be fitted equally well to any of the curves $\xi = 4$ to $\xi = 9$. The results in Table 5.4, show that heating a sample of arcton and 50% carbon disulphide from 49.5°C to 89.5°C produces no change in the ρ value. Further this same 'limiting' value was within experimental error the same as that obtained with the pure arcton at 73°C. Measurements at higher temperatures could not be carried out, since the radical decomposes. These results suggest that the limiting

low field value of $\rho = 0.14$, should fit on $\bar{\delta} = 9$. This is in contrast to the low field value of $\rho = 0.4$ (37). Thus, it may well be, as suggested in the previous chapter, that the low field results should not be interpreted using the same relaxation theory as at high fields.

Conclusion.

It would appear that neither model is completely satisfactory in interpreting the experimental results although qualitatively, the Diffusion Model is better. However, for the Modified Sticking Model, the assumption has been made that δ remains constant as the viscosity varies. This may not be the case, but the introduction of a functional dependence of τ_c in τ_d will result in an unwieldly and complicated model. An alternative function for the time dependence of the scalar interaction seems to be necessary. This could be obtained using the experimental results and working backwards, but this would be tedious and the function might then, although mathematically a correct description of the results, physically be not very meaningful.

Again, there is some evidence that the low field and high field results should perhaps not be interpreted using the same relaxation theory.

C H A P T E R VI

The Effect of Varying λd in the Scalar Spectral Density Function of the Diffusion Model.

Introduction.

From the results of the last chapter it appears that a satisfactory function for the time dependence of the scalar interaction has yet to be postulated. In deriving the expression for the scalar spectral density function $Je(\omega)$, for the Diffusion Model, Hubbard (5) made the assumption that $\lambda d \gg 1$. Accordingly, a simple and obvious alteration to this function is to investigate the dependence of $Je(\omega)$ on λd and calculate the corresponding ρ versus $(\omega_s \tau_c)^{1/2}$ curves.

Theory.

The equation for the scalar spectral density $Je(\omega)$ is given by Hubbard (5).

$$Je(\omega) = \frac{2\pi A^2 d^5}{Du} \left\{ \frac{u^2 - 2\lambda d u + 2(\lambda d)^2}{[4(\lambda d)^4 + u^4]} \right.$$

$$\left. + e^{-u} \frac{[2\lambda d(\lambda d + u)(\sin u - \cos u) + u(u + 2\lambda d)(\sin u + \cos u)]}{[2(\lambda d)^2 + 2\lambda d u + u^2]^2} \right\}$$

.....(6.1)

where $u = (\omega_s \tau_c)^{\frac{1}{2}}$

To find Je(o) Hubbard assumes that $\lambda d \gg u$ with the result that

$$Je(\omega) = \frac{\pi A^2 d^3}{\lambda^2 D u} \left[1 + e^{-u} (\sin u - \cos u)\right] \quad ..(6.2)$$

from which it follows that

$$Je(o) = \lim_{u \to o} Je(\omega) = \frac{2 A^2 d^3 \pi}{D\lambda^2} \quad ..(6.3)$$

The reduced spectral density is defined by

$$\dot{j}e(\omega) = \frac{Je(\omega)}{Je(o)}$$

Thus if $\lambda d \gg u$

$$\dot{j}e(\omega) = \frac{1}{2u} \left[1 + e^{-u} (\sin u - \cos u)\right] \quad ..(6.4)$$

However no such approximations were made in this work and $\dot{j}e(\omega)$ was calculated for various values of λd. Further since the expression for ρ on this model is given by

$$\rho = \frac{40\ j_d(\omega_s \tau_c) - 3\zeta\ je(\omega_s \tau_c)}{56\ j_d(\omega_s \tau_c) + 24 + 3\zeta\ je(\omega_s \tau_c)} \quad ...(6.5)$$

then values of ρ can be evaluated as a function of $(\omega_s \tau_c)^{\frac{1}{2}}$ for different values of ζ if $je(\omega_s \tau_c)$ is known.

Variation of $J_e(\omega)$ with λd

$J_e(o) = J_e(\omega)$ when $(\omega_s \tau_c)^{\frac{1}{2}} = 1 \times 10^{-8}$

$(\omega_s \tau_c)^{\frac{1}{2}}$	$\lambda d = 1$	$\lambda d = 5$	$\lambda d = 10$	$\lambda d = 50$	$\lambda d = 100$	$\lambda d = 1000$
1×10^{-8}	1.0000	1.0000	1.0000	1.0000	1.0000	1.0000
0.005	0.9932	0.9967	0.9972	0.9972	0.9972	0.9975
0.01	0.9865	0.9935	0.9943	0.9946	0.9947	0.9950
0.02	0.9732	0.9869	0.9885	0.9895	0.9896	0.9900
0.04	0.9466	0.9739	0.9770	0.9792	0.9795	0.9800
0.06	0.9202	0.9608	0.9655	0.9689	0.9693	0.9700
0.08	0.8940	0.9477	0.9450	0.9586	0.9592	0.9600
0.10	0.8681	0.9347	0.9426	0.9483	0.9491	0.9500
0.20	0.7441	0.8703	0.8857	0.8974	0.8989	0.9005
0.30	0.6321	0.8076	0.8300	0.8474	0.8496	0.8518
0.50	0.4486	0.6893	0.7238	0.7514	0.7548	0.7582
0.70	0.3152	0.5827	0.6264	0.6668	0.6711	0.6627
1.00	0.1858	0.4473	0.4993	0.5437	0.5495	0.5548
1.50	0.0606	0.2841	0.3394	0.3886	0.3954	0.4016
2.00	0.0337	0.1829	0.2320	0.2810	0.2878	0.2941
3.00	0.0129	0.0879	0.1232	0.1637	0.1698	0.1754
4.00	0.0063	0.0528	0.0796	0.1138	0.1191	0.1242
5.00	0.0036	0.0360	0.0581	0.0888	0.0938	0.0986
7.00	0.0015	0.0192	0.0350	0.0615	0.0663	0.0709
0.00	0.0005	0.0091	0.0190	0.0406	0.0450	0.0495

Table 6.1.

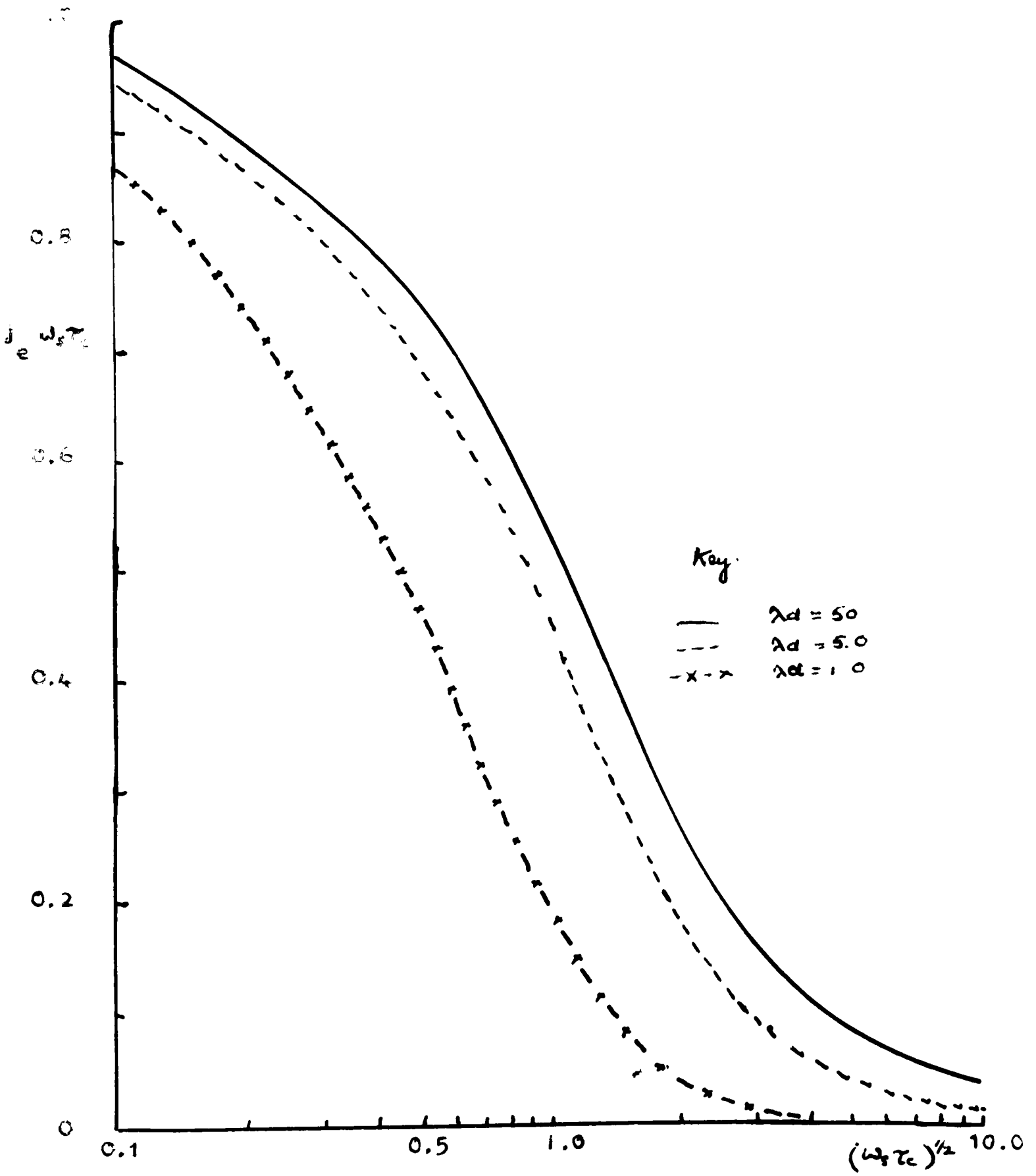

Figure 6.1 Variation of $J_e(\omega_s \tau)$ with λd

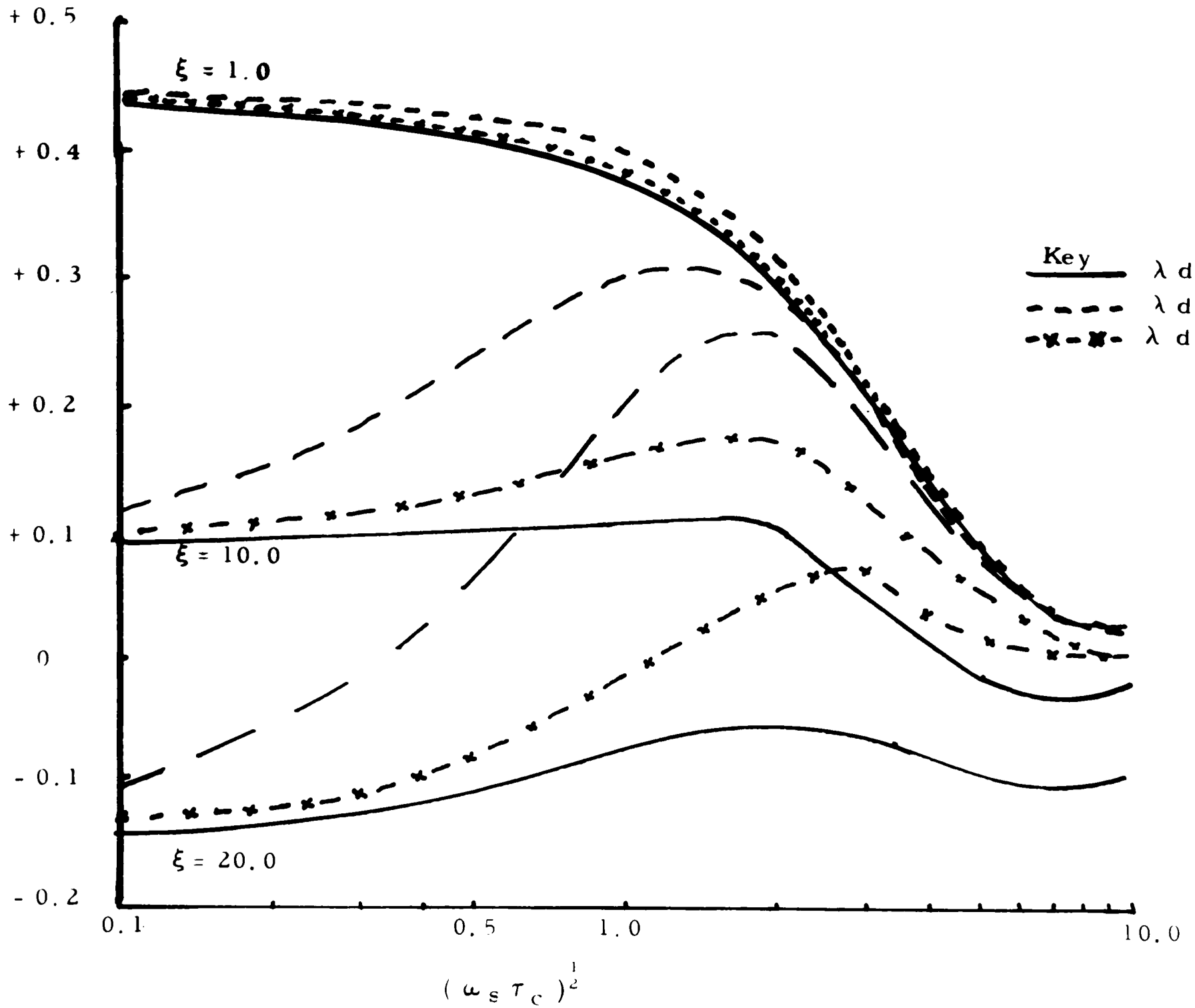

Figure 6.2. Dependence on λ d for ξ = 1.0, 10.0, 20.0.

Results and Discussion

Table 6.1 shows the values of $j_e(\omega)$ calculated using the various values of λd. It is interesting to note that $\lambda d = 1{,}000$, before the values of $j_e(\omega)$ agree with those calculated by Hubbard (5) by putting $\lambda d \gg u$ in equation (6.4). Fig. 6.1 shows $j_e(\omega)$ plotted as a function of $(\omega_s \tau_c)^{1/2}$ for various values of λd. Figure 6.2 shows several typical ρ versus $(\omega_s \tau_c)^{1/2}$ curves (with $\lambda d = 1$, 10, 20) calculated using these different values of $j_e(\omega)$.

The results of this variation of λd in the scalar interaction function are somewhat disappointing, for the agreement with experiment is worse than previously. However, in the calculation of scalar shifts in chapter 4, it was necessary to assume a value for λd. This work does show that a minimum value of $\lambda d = 1{,}000$ is required, if the approximations made by Hubbard are to be valid.

CHAPTER VII

Positive Enhancement with Proton Resonances. (47)

Introduction

Measurements of the proton electron Overhauser effect in solutions of free radicals in organic solvents can usually be interpreted in terms of dipolar interactions between the proton and the electrons. The proton polarization is inverted and may be increased by two orders of magnitude; quantitative agreement with results calculated from a model of randomly diffusing spheres is usually obtained as has been shown in chapters III and V.

On the other hand, fluorine nuclear resonances of the solvent molecules in solutions of free radicals are often positively enhanced, particularly at 12,500 gauss. One case of a positive enhancement has however been observed with protons. If a solution of the T.T.B.P. radical is prepared from an excess of the tri-tert-butyl phenol, then the proton resonances of the excess phenol may be observed. With the resolution obtained, three peaks are obtained, if these are not masked by a solvent resonance. The peak from the aromatic protons occurs at $\tau = 3.3$, that from the hydroxyl proton at $\tau = 5.5$, and that from the tertiary butyl groups at $\tau = 9.3$. The different tertiary butyl groups are not resolved, but

under conditions of very high resolution it is possible to distinguish them, the separation being o.1τ, the para being to higher field.

In every solvent so far investigated the tert-butyl resonance is positively enhanced at 3,300 and 12,500 gauss. Where the other two lines can be observed the resonances are inverted in the normal way. A search has been made for similar behaviour using different radicals and a variety of compounds containing tert-butyl and methyl groups, so that this unusual behaviour could be investigated in more detail.

Experimental

The double resonance experiments were carried out at 3,300 gauss. Solutions of the various radicals were prepared as described in chapter II. The concentrations of the radical solutions were estimated from the intensity of the electron resonance at 350 Mc/s as previously.

The e.s.r. spectra for the systems galvinoxyl/tri-tert-butyl phenol and for D.P.P.H./tri-tert-butyl phenol were measured on a Varian V 4500 e.s.r. spectrometer.

Scale 1 cm.= 1.33 gauss.

Figure 7.1(a).

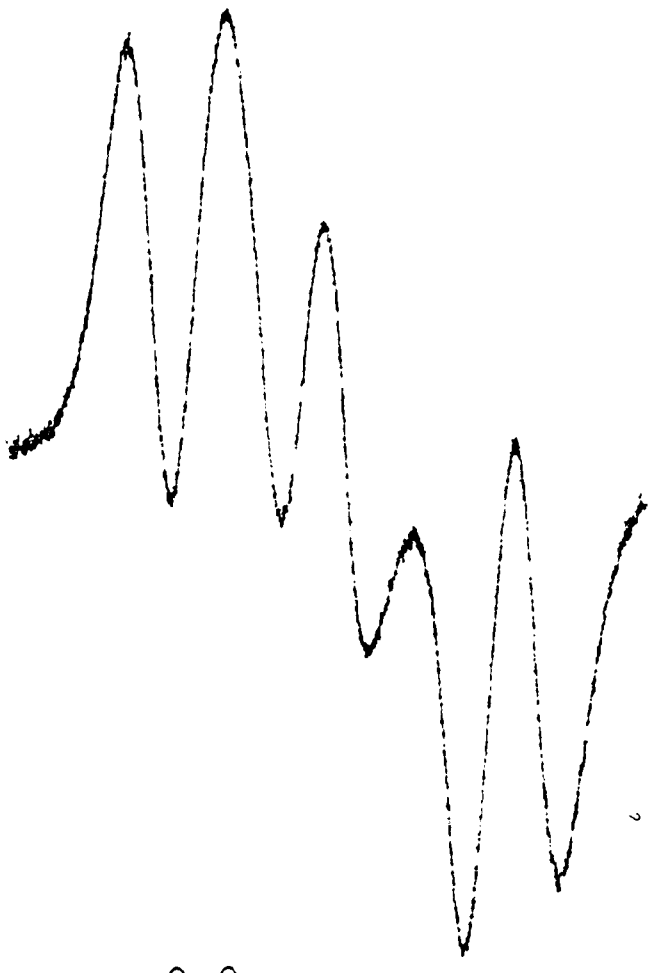

Scale 1 cm.= 8.8 gauss.

Figure 7.1(b).

Results.

A. The Overhauser Effect.

The sign of the Overhauser effect was observed for a series of samples containing T.T.B.P. radical and a variety of compounds containing methyl and tert-butyl groups. If necessary, carbon tetrachloride was added as solvent. The results are summarized in Table 7.1. It will be seen that all the enhancements are negative except for that of the tert-butyl protons of the tri-tert-butyl phenol which is positive. The signs of the enhancements of the resonances of tri-tert-butyl phenol in solution in carbon tetrachloride with several other radicals are shown in Table 7.2. The positive enhancement of the tert-butyl protons was again seen with galvinoxyl and with D.P.P.H.

B. E.S.R. Spectra.

Solutions of the tri-tert-butyl phenol in carbon tetrachloride to which small amounts of D.P.P.H. had been added gave e.s.r. spectra which were unsymmetrical (Fig. 7.1b). By using high concentrations (> 4M) of the phenol and low concentrations ($< 10^{-4}$M) of D.P.P.H., the e.s.r. spectra were partially resolved triplets, with a hyperfine splitting constant of approximately 1.7 gauss. This is the same value as the splitting constant, arising from the coupling of the

TABLE 7.1

Compound	Sign of enhancement at 3,300 g.		
	CH_3	Aromatic	Others
Mono-tert-butyl benzene	-	-	
1,3,5 tri methyl benzene	-	-	
Hexamethyl benzene	-		
1-methoxy 2-4-6 trimethyl benzene	-	-	-(OMe)
1-methoxy 4-tert-butyl benzene	-	-	-(OMe)
1-methoxy 2-6 tert butyl benzene	-	-	-(OMe)
1-methoxy 3,5 tert butyl benzene	-	-	-(OMe)
Di tert butyl benzene	-	-	
1,3,5 triphenyl benzene		-	
tri 2-butoxylethyl phosphate	-		$-(CH_2)$
tri-p-tert-butyl phosphate	-	-	
1-methoxy 2-4-6 tri-tert butyl benzene	-	-	-(OMe)
tri-tert butyl phenol	+	-	

TABLE 7.2

Sign of enhancement at 3,300 g. of tri-tert butyl phenol resonances.

Radical	CH_3	Aromatic
Phenoxide	+	-
P.D.M.	-	-
Galvinoxyl	+	-
D.P.P.H.	+	-
B.D.I.P.A.	-	-

meta protons to the electron on the T.T.B.P. radical. This is illustrated in Fig. 7.1(a) This simultaneous presence of the T.T.B.P. radical is in agreement with the work of Ayscough and Russell (38) who have studied the equilibrium:-

D.P.P.H. +  ⇌ D.P.P.H. - H + 

Similarly solutions of the tri-tert-butyl phenol in carbon tetrachloride to which small amounts of galvinoxyl had been added gave e.s.r. spectra which again were unsymmetrical and consistent with the presence of a second radical. This is shown in Fig. 7.4(a). By analogy with the above behaviour of D.P.P.H., it was postulated that an oxidation of the phenol by the galvinoxyl radical had occurred forming the T.T.B.P. radical. This was investigated by taking solutions in carbon tetrachloride of the T.T.B.P. and galvinoxyl radicals. The two samples were placed side by side in the probe and the spectrum recorded. Equal amounts of each sample were then mixed and the spectrum again recorded. This is illustrated in Fig. 7.2 (a)-(d). Since the latter two spectra were quite similar it appeared that the two radicals could co-exist in the same solution without reaction between them taking place. A further point was that these spectra had the same general shape as those produced by the tri-tert-butyl phenol + galvinoxyl. This is illustrated in Fig. 7.4 (a) and a

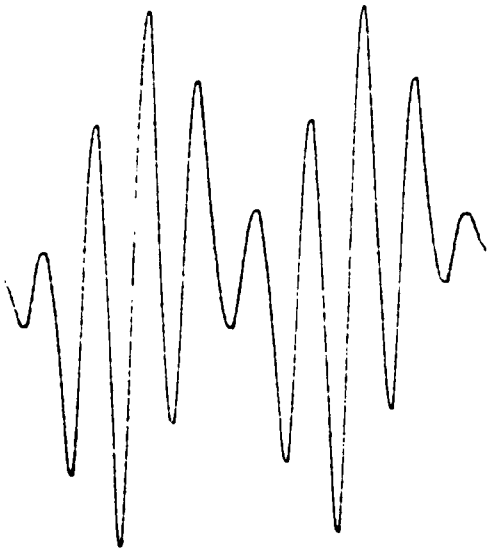

(a).Galvinoxyl.

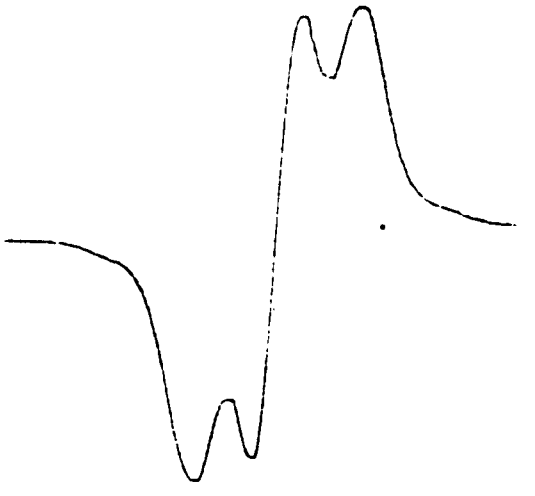

(b).T.T.B.P.

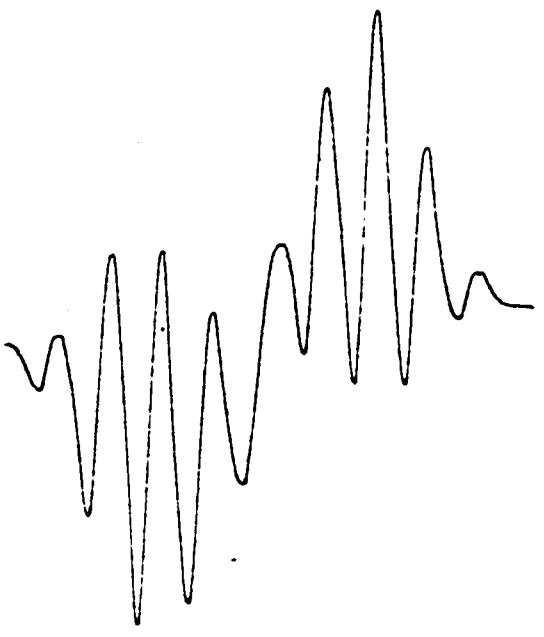

(c).

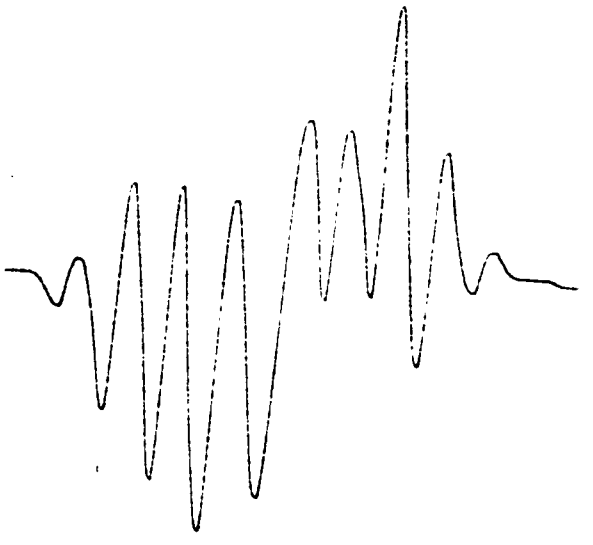

(d).

Galvinoxyl and T.T.B.P. (c) placed side by side in probe.
(d) mixed in same tube.

Figure 7.2

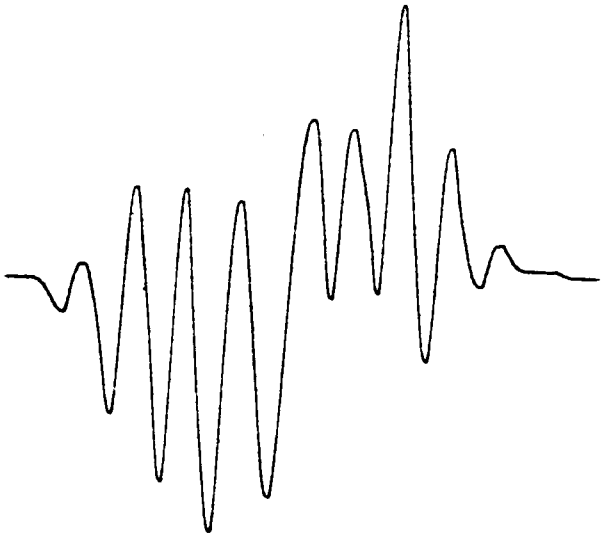

Figure 7.3. 50/50 mixture of Galvinoxyl and T.T.B.P.

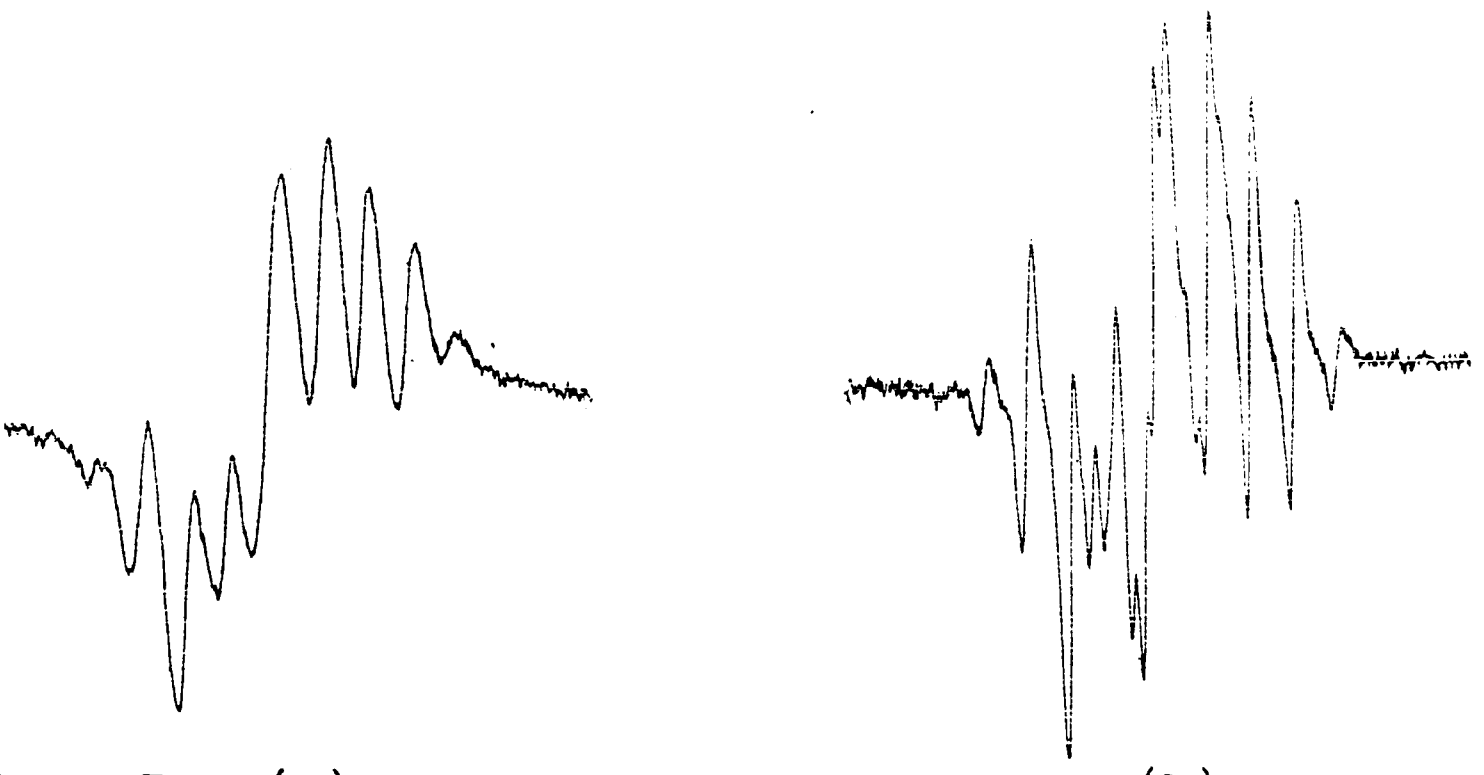

Figure 7.4 (a). (b).

Galvinoxyl and tri-tert-butyl phenol (a) freshly prepared (b) after several days.

spectrum of a 50/50 mixture (by volume) is shown for comparison purpose in Fig. 7.3. Fig. 7.4 (b) shows the spectrum obtained from the same solution as used in Fig. 7.4 (a) after several days; the extra fine structure probably arising from the coupling of the tertiary butyl groups of the galvinoxyl to the electron.

A study of the mechanism leading to collapse of the hyperfine structure in T.T.B.P. in concentrated solutions was also made. The concentrations at which the hyperfine splitting arising from the two meta protons was first resolved at room temperature are shown in Table 7.3 for a variety of solvents. The error for the results is ± 15%.

The collapse of the hyperfine structure might arise from:-

(I) electron-electron exchange.

(II) electron-phenoxide exchange.

(III) electron-phenol exchange (involving proton transfer).

Since the collapse is more or less independent of the concentration of unchanged tri-tert butyl phenol present, the third mechanism can be ruled out. This is in accord with the results of Krielick & Wiesmann (39) who quote a rate constant, $k_1 = 300\ m^{-1}\ l\ s^{-1}$ for the electron-phenol exchange in carbon tetrachloride. This would be too slow to account for the collapse of the hyperfine structure.

TABLE 7.3

Concentration at which hyperfine splitting appears.	Solvent	Viscosity (Centipoises)
4.0×10^{-3}M	Ethanol	1.20
3.0×10^{-3}M	Carbon tetra-chloride	0.97
3.0×10^{-3}M	* Arcton 113	0.79
1.0×10^{-3}M	Benzene	0.65
1.0×10^{-3}M	Methanol	0.60
6×10^{-3}M	Ethanol + EtO^-	2.0

* 1,1,1-tri chloro. 2-2-2 trifluoro-ethane.

The effect of adding a considerable excess of the parent phenol to any of these solutions resulted in a slight increase in the concentration at which hyperfine splitting appeared. This small effect was attributed to a small increase in the viscosity of the solution.

The second mechanism could be tested by addition of ethoxide ions to a solution of radical and the parent phenol in a suitable solvent. The ethoxide ions might be expected to favour the formation of the phenoxide anion, resulting in an increase in the rate for the exchange, with the consequence that the concentration at which hyperfine splitting appears would be lower than that observed in the absence of the phenol. This is not found to be the case.

Thus the mechanism is presumably radical - radical electron exchange, and using the concentration given in Table 7.3, the rate constant for this process is $k_{ex} = 10^{10}$ m $^{-1}$ l s $^{-1}$ in carbon tetrachloride.

Discussion.

When tri-tert-butyl methoxy benzene was examined in solution in carbon tetrachloride with T.T.B.P. radical, all the proton resonances were inverted in the normal manner. It would appear therefore that the positive enhancement is associated particularly with the tri-tert-butyl phenol.

When the radicals P.D.M. and B.P.I.D.A. were used with tri-tert-butyl phenol, all proton resonances were inverted, but with D.P.P.H. and galvinoxyl the tert-butyl proton resonances were once again positively enhanced. However, the e.s.r. spectra of these last two solutions indicated that some of the tri-tert-butyl phenol had been oxidised to

T.T.B.P. radical, so that all the solutions which showed positive proton polarisation probably contained this radical. The positive enhancement therefore seems to be particularly associated with solutions which contain <u>both</u> the tri-tert-butyl phenol <u>and</u> corresponding tri-tert-butyl phenoxide radical.

In such solutions, there is a proton exchange reaction

$$ROH + RO^{\cdot} \rightleftharpoons R\dot{O} + HOH$$

for which Weissmann and Kreilick (39) have found a rate constant $k_2 = 300\ m^{-1}l\ s^{-1}$. In the radical, the protons are subjected to a strong scalar coupling to the electron, but the rate constant for this exchange is far too low to modulate the scalar coupling fast enough to stimulate the relaxation transitions required to produce a positive enhancement of the nuclear resonance.

However, if there was some mechanism by which the scalar coupling could be suitably modulated at the tert-butyl protons of the radical, but not of the aromatic protons, then there could be built up a positive nuclear polarisation at the tert-butyl groups during the life of the radical and a negative polarisation (through simple modulated dipolar coupling) at the aromatic protons.

Since the rate constant for the build up of Overhauser nuclear polarisation, is the nuclear spin lattice relaxation time, the positive polarisation will only occur if the life-time of the radical τ_R is longer than the relaxation of the tert-butyl protons on the radical molecule, T_R . i.e.

$$\tau_R > T_R \qquad (1)$$

When the molecule accepts a proton and becomes a diamagnetic tri-tert-butyl phenol molecule, the positive polarisation will be transferred, but will start to decay to the negative value expected for dipolar coupling, with the relaxation time of the protons in the diamagnetic molecule, T_p. If, however, the molecule becomes a radical again before the negative polarisation is established, the average polarisation of the tert-butyl protons of the phenol will remain positive. If the lifetime of the phenol is τ_p , then the above condition is

$$T_p \gg \tau_p \qquad (2)$$

We do not have enough information to know if conditions (1) and (2) are fulfilled in a typical solution. We do know that from the relative concentrations in solutions

$$\tau_p \gg \tau_R \qquad (3)$$

and thus from (1) and (2) using (3),

$$T_P > T_R \qquad (4)$$

i.e.the relaxation time of protons radical molecules would have to be much shorter than that of protons in the diamagnetic phenol molecule. This is almost certainly the case.

The question now remains of how scalar coupling between the unpaired electrons and the tert-butyl protons of the radical could be suitably modulated. There is evidence (40, 41, 42, 43) that part of the scalar coupling of electrons to protons in radicals is transmitted by hyperconjugation. The overlap of the π-orbital on positions 2, 4 and 6 of the ring with the methyl group would have an angular dependence, and would be modulated by rotation of the tert-butyl group. The potential barrier hindering rotation of these groups about the C - C axis is probably low enough for the group to undergo randomly hindered rotation at frequencies of the order of $10^{10} s^{-1}$. This would be a high enough frequency to allow the scalar interactions to contribute significantly to the proton relaxation.

R E F E R E N C E S

1. based on Solomon, I. 1955 Phys. Rev. 99 559

2. Block, F. 1946 Phys.Rev. 70 446
   1956 Phys.Rev. 102 104

3. Abragam, A. Principles of Nuclear Magnetism O.U.P. (1961) p. 39.

4. Overhauser, A.W. 1953 Phys.Rev. 92 411.

5. Hubbard, P.S. 1966 Proc.Roy.Soc. A 291 537

6. Abragam, A., Combrisson, J., Solomon, I., 1957 Comptes Rend. 245 157.

7. Richards, R.E., White, J.W., 1954 Proc.Roy.Soc. A 279 481.

8. Kramer, K.D., Muller-Warmuth, W., Schindler, J., 1965 J.Chem.Phys. 43 31.

9. Kramer, K.D., Muller-Warmuth, W., 1964 S. Naturf. 19a 375.

10. Hubbard, P.S., 1963 Phys.Rev. 131 275.

11. Hubbard, P.S., 1965 J.Chem.Phys. 42 3346.

12. Abragam, A., Principles of Nuclear Magnetism O.U.P. 1961, p.300.

13. Pfeifer, H., 1961, Ann.Physik. 8, 1.

14. Abragam, A., Principles of Nuclear Magnetism O.U.P. 1961 p.300.

15. Bloembergen, N., 1957 J.Chem.Phys. 27, 572.

17. Solomon, I., Bloembergen, N., 1956 J.Chem.Phys. 25, 261.

18. Abragam, A., Principles of Nuclear Magnetism, O.U.P. 1961, p. 333.

19. Muller-Warmuth, W., 1966. Z. Naturforsch. 21a, 153.

20. Natusch, D.F.S., 1966, D.Phil. Thesis, Oxford.

21. Richards, R.E., White, J.W., 1962 Proc.Roy.Soc. A 269 287.

22. Kenworthy, J.G., Richards, R.E., 1965, J.Sci.Instrum. 42, 675

23. Kenworthy, J.G., Longster, G.F., Richards, R.E., 1965, Trans. Far.Soc. 62, 519.

24. Muller, E., Ley, K., Kridaisch, W., 1954, Chem.Ber. 87, 1605.

25. Muller, E., Ley, K. 1953, Z.Naturforsch 86, 694.

26. Kenworthy, J.G., 1964, D.Phil Thesis, Oxford.

27. Poindexter, E. private communication.

28. Abragam, A., Principles of Nuclear Magnetism, O.U.P. 1961, p. 312.

29. Bloembergen, N., 1957, J.Chem.Phys. 27, 595.

30. Symmons, M.C.R., 1963, Advances in Phys.Org.Chem. 1, 183.

31. Imbaud, J.P., Berthet, G. 1965, Compt.Rend. 261, 953.

32. Gutowsky, H.S., Jones, J., Fu-ming Chen, Meinzer, R., 1965, J.Chem.Phys. 42, 2625.

33. Ng, S., Tung, J., Sederholm, C.H., 1965, J.Chem.Phys. 42,79.

34. Jones, G.T. Powles, J.G., 1964, Mol.Phys. 8 607.

35. Bloembergen, N., Purcell, E.M., Pound, R.V. 1948, Phys. Rev., 73, 679.

36. McCall, D.W., Douglas, D.C., Anderson, E., 1959
J.Chem.Phys. 31, 1555.

37. Poindexter, E., Private Communication.

38. Ayscough, P.B., Russell, K.E., 1965 Canad.J.Chem. 43, 3039.

39. Kreilick, R.W., Weissman, S.I., 1962, J.Am.Chem.Soc. 84, 306.

40. Symmons, M.C.R., 1962 Tetrahedron 18, 333.

41. Colpa, J.P., de Boer, E., 1963-4, Mol.Phys. 7, 333.

42. Bersohn, J., 1956. J.Chem.Phys. 24, 1066.

43. Stock, L.M., Suzuki, J., 1965. J.Am. Chem.Soc. 87, 3909.

The chapters to which the following references are given are based upon published work.

44. Dwek, R.A., Kenworthy, J.G., Natusch, D.F.S., Shields, D.J. (Chap.III)
Richards, R.E. 1966, Proc.Roy.Soc. A291
487.

45. Dwek, R.A., Kenworthy, J.G., Ladd, J.A., Richards, R.E. (Chap. V)
1966, Mol. Phys. in press.

46. Dwek, R.A., Kenworthy, J.G., Richards, R.E., 1966, (Chap. V)
Chem. Comm. No. 3, 74.

47. Dwek, R.A., Kenworthy, J.G., Richards, R.E., 1966, (Chap.VII)
Mol. Phys. in press.

A P P E N D I X

1. THE SPECTROMETERS.

2. COMPUTER PROGRAMMES.

Reprinted from the *Journal of Scientific Instruments*, VOL. 42, pp. 675–676, SEPTEMBER 1965

Apparatus for nuclear–electron double resonance at 3300 gauss with moderately high resolution

J. G. KENWORTHY and R. E. RICHARDS
Physical Chemistry Laboratory, South Parks Road, Oxford
MS. received 28*th May* 1965

Abstract. The essential features of the construction of a nuclear–electron double resonance spectrometer are described. Both a helix and a resonant cavity have been used as the microwave resonators and the performances of both probe systems are compared. An example of the performance is given.

1. Introduction

The requirements of a nuclear–electron double resonance spectrometer operating at 3300 gauss with low resolution have been described (Richards and White 1962). A new spectrometer operating at this field has now been constructed with much improved resolution and convenience of operation. It is similar in design to the high resolution spectrometer operating at 12500 gauss (Richards and White 1963), and is designed to study solutions of free radicals at room temperature.

2. The magnet

A small permanent magnet manufactured by Mullard Ltd. has been used. The gap is 2 in. wide and the pole faces are 5 in. in diameter. Small adjustments to the field of up to 3% can be made by laying steel shunts across the yoke. This facilitates the adaption of the spectrometer to new microwave oscillators, the frequencies of which may vary slightly. Small corrections to the field required during normal operation are made by adjusting the current through a set of bias coils.

The inherent homogeneity of the magnet is poor, being about 1 part in 10^4 over a 5 mm sphere, because of the large gap to pole face diameter ratio. It has, however, been improved by using shim coils to correct for z gradient and curvature (Anderson 1961), and if a full set of 13 Golay (1958) current shims is then used to make small corrections a homogeneity of 3 parts in 10^7 can be achieved without spinning the sample. This corresponds to a proton line width of 5 c/s which is adequate for most double resonance work, since the nuclear resonance lines are broadened by the presence of the free radicals.

It is significant that such good resolving power can be obtained with a magnet having a ratio of pole face diameter to gap of as little as $2\frac{1}{2}$. Long term stability is achieved by enclosing the magnet in an insulated temperature-regulated box.

3. The nuclear resonance spectrometer

The nuclear resonance spectrometer is almost identical with that already described (Richards and White 1963) for the spectrometer at 12500 gauss. A tunable oscillator is used as the local oscillator for the superheterodyne r.f. receiver, so that the band width of the i.f. amplifiers may be kept to a minimum, whilst still permitting the receiver to be tuned exactly to the nuclear resonance frequency, which may have to be changed slightly when a new microwave oscillator is fitted.

4. The electron resonance spectrometer

The electron resonance spectrometer is also similar in principle to the system used at 12500 gauss. The frequency of the microwave radiation must be sufficiently stable to allow the centre of the electron resonance line to be continuously irradiated. This requires a frequency stability of better than 1 in 10^4. It is also necessary that the intensity of the radiation should not vary during a measurement. In practice a change in intensity of less than 1% would probably not produce a measurable change in enhancement.

English Electric K350 and K336 klystrons fed from well-stabilized power supplies have been found to be satisfactory microwave sources. The intensity of the power applied to the sample may be varied by means of an attenuator fitted with a vane of silicon carbide. We do not know how much of the applied power actually reaches the sample. The output of the K336 is approximately 10 w and with non-polar samples, all this power may be applied without heating the sample unduly. The output of the K350 is rather less than 10 w and the maximum achievable enhancements are lower.

Neither valve is easily tunable, and this is a disadvantage when a replacement becomes necessary.

Power measurement is achieved by sampling the applied power with a directional coupler and feeding it to a crystal via a calibrated glass vane attenuator. The attenuator is adjusted until the meter on the crystal output shows a standard deflection, and the relative power is then read off from the calibration chart for the attenuator. An absolute calibration was obtained by comparison with a Hewlett–Packard X-band bolometer and power meter.

5. The probe

Two types of probe system have been tried. In the first one a helix serves both as the microwave resonator and as the coil for the detection of the nuclear resonance. In the second one a separate coil is placed inside a microwave cavity.

5.1. *The helix*

A sketch of the helix with its screening can removed is shown in figure 1. The sample, in a 1 mm diameter glass tube, is placed inside the inner helix which has 10 turns and forms the microwave resonator. The large outer helix acts merely as an extension of the coaxial earth shield as far as the microwaves are concerned, but if it is removed there is a considerable decrease in nuclear resonance sensitivity. The outer helix is in series with the inner one and wound in the same sense, and so it obviously increases the inductance

of the nuclear magnetic resonance coil, but reduces the sample filling factor. With a higher inductance the resistive losses in the leads to the probe become less important and the nuclear magnetic resonance sensitivity improves. This improvement must more than offset the loss resulting from the reduced filling factor.

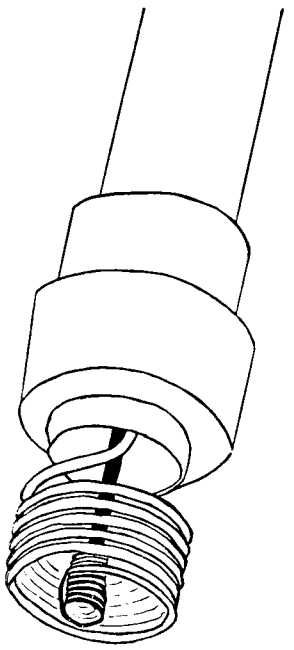

Figure 1. The helix.

The method of matching the helix to the waveguide is identical with that described previously (Richards and White 1962).

When the microwave power is applied considerable sample heating occurs, and cooling is achieved by immersing the whole probe in a bath of carbon tetrachloride. Polar samples may be used and enhancements can be achieved even with aqueous samples. The helix is, however, fragile and changing samples is inconvenient and involves difficult readjustment of the matching controls.

5.2. *The cavity*

An H_{011} cylindrical cavity is used. In order to reduce the size sufficiently for it to fit the magnet gap, it is filled with a polystyrene dielectric. Tuning is achieved by screwing the bottom of the cavity up and down on a fine thread. The small air gap between the bottom of the dielectric and the bottom of the cavity does not seem to be important. The nuclear magnetic resonance coil is wound on a thin quartz former which fits into a hole through the middle of the polystyrene. The microwaves are fed in via a coaxial lead and coupling loop. The sample is cooled by blowing air over it from beneath. A sketch of the cavity is shown in figure 2.

With non-polar solvents, sample tubes of 5 mm diameter may be used, but polar samples must be in 1 mm diameter tubes. The cavity does not function very well with very polar solvents, such as water, but with suitable samples it is very much more convenient to use than the helix.

6. Performance

Figure 3 shows an enhancement of the proton resonance of a sample of dimethyl formamide, containing 2,5 di-tertiary butyl semiquinone radical, obtained with the helix. In this sample, which is a concentrated solution of radical, the line width is dominated by the paramagnetism of the sample, and not by the magnet, but even with pure dimethyl formamide the resolution is not good enough to resolve the two methyl resonances. The maximum enhancement observed with this solvent is -130. With the same sample in the cavity, the maximum enhancement was -100, but an enhancement of -180 has been observed with the cavity and a sample of tri-butyl phenoxyl radical in chloroform. Since the cavity is more convenient we prefer to use it if possible.

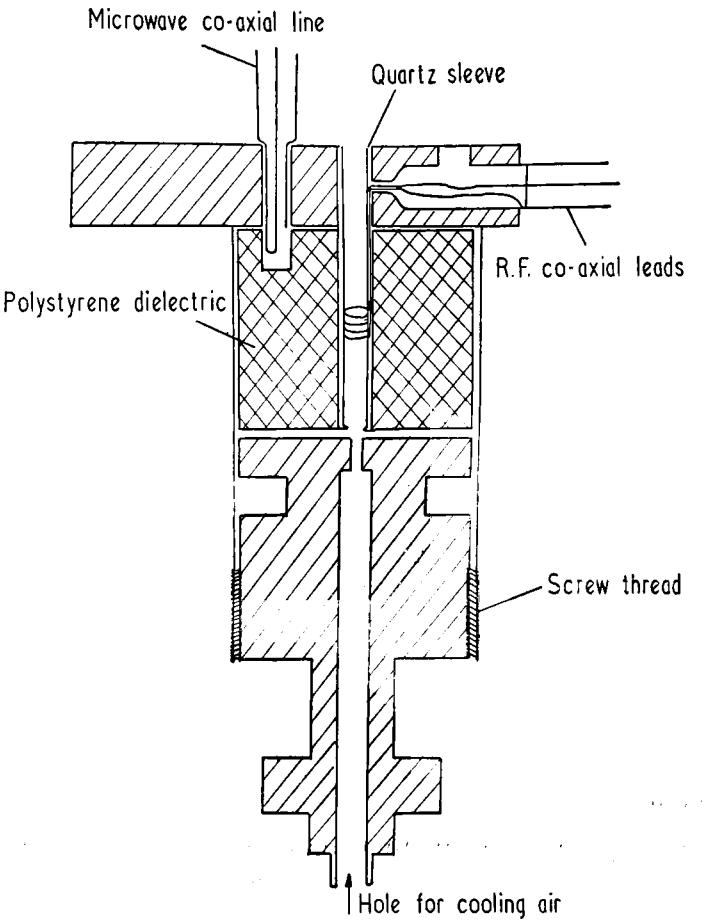

Figure 2. The double resonance cavity.

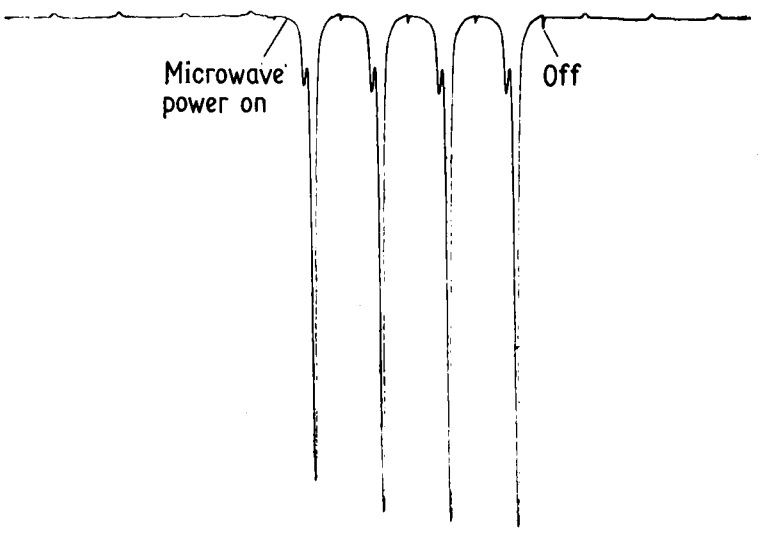

Figure 3. Overhauser enhancement of the proton resonance of dimethyl formamide containing 2,5 di-tertiary butyl semiquinone radical. The spectrum is being repeatedly scanned from low field to high field (left to right in the figure).

Acknowledgments

The instrument was constructed with the aid of a grant from the Paul Instrument Fund of the Royal Society. Dr. John Alcock and Mr. D. F. S. Natusch gave valuable help in the design and manufacture of the microwave cavity.

References

ANDERSON, W. A., 1961, *Rev. Sci. Instrum.*, **32**, 241–50.
GOLAY, M. J. E., 1958, *Rev. Sci. Instrum.*, **29**, 313–5.
RICHARDS, R. E., and WHITE, J. W., 1962, *Proc. Roy. Soc.* A, **269**, 287–300.
—— 1963, *Proc. Roy. Soc.* A, **279**, 474–80.

UNWIN BROTHERS LIMITED, WOKING AND LONDON (B4582)

Reprinted without change of pagination from the
Proceedings of the Royal Society, A, *volume* 279, *pp.* 474–480, 1964

Apparatus for nuclear electron double resonance at 12500 gauss

By R. E. Richards, F.R.S., and J. W. White
Physical Chemistry Laboratory, University of Oxford

(*Received* 18 *October* 1963)

Apparatus is described for measuring nuclear electron double resonances at magnetic fields of 12500 G, in the microwave radiation of about 35000 Mc/s and at nuclear resonance frequencies from 3 to 60 Mc/s. The microwave circuit permits saturation of solutions of certain organic free radicals in solution in non-polar solvents when placed in a microwave cavity with a radio-frequency coil mounted inside. The resolving power of the nuclear resonance spectrometer is better than 1 in 10^8. Recordings are presented to illustrate the performance of the apparatus.

1. Introduction

When the electron resonance in a solution of a paramagnetic solute is partially or completely saturated, striking changes in the nuclear resonance spectrum are often brought about (Overhauser 1953; Anderson 1960; Richards & White 1962*a*, *b*, 1963); the nuclear resonance may be enhanced or reversed or even shifted. The nature of the effect can give detailed insight into the mechanisms of the interactions in the solution, and in some cases the signal/noise of the nuclear resonance

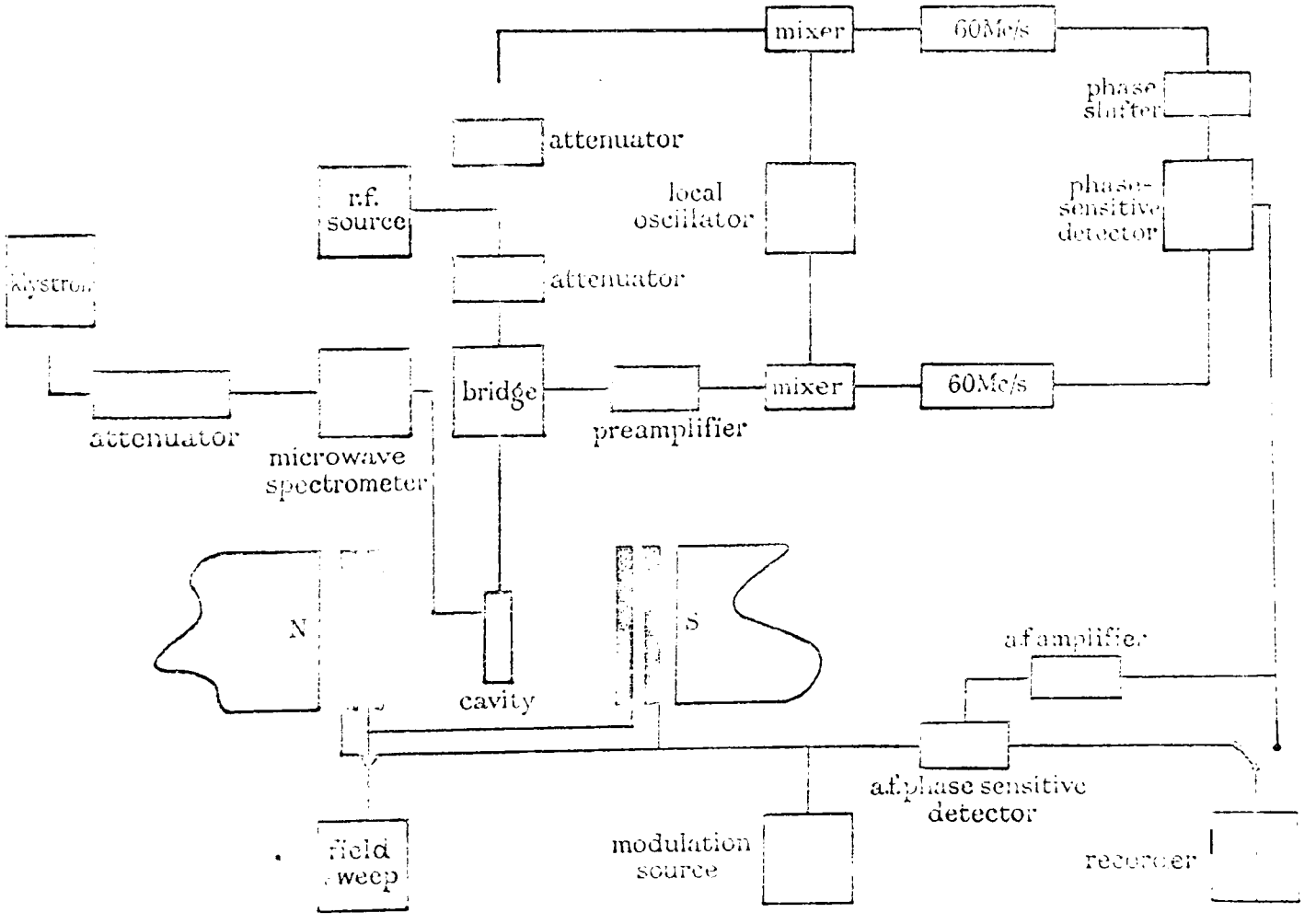

Figure 1. Block diagram of apparatus.

can be so greatly increased as to make it possible to observe resonances too weak to be seen under normal conditions.

Experiments on these effects have so far been conducted at low magnetic fields (3000 G) and with low resolving power. The instrument described here has been constructed to explore the effects obtained at magnetic fields of 12500 G with the homogeneity normally used for high resolution n.m.r. The layout of the whole instrument is shown in the block diagram (figure 1).

2. The magnet

A large permanent magnet has been generously provided by Mullard Ltd. The field strength is 12500 G in a gap 6·5 in. by 1·585 in. The pole pieces are optically polished and can be tilted slightly to optimize the field homogeneity, using a design similar to that of the smaller magnet described by Evans & Richards (1960). The yoke is provided with four mechanically coupled shunts which give a total field shift of $\pm 1\,\%$ from 12500 G. Additional removable shunts can be used to reduce reversibly the field by a further 1 % if required. The homogeneity of the magnetic field is about 1 in 10^6 over a 5 mm sphere. A set of nine Golay current shims (Golay 1958) is fitted in the gap which permit a homogeneity of about 2 in 10^8 to be achieved over a 5 mm diameter sample without spinning.

The magnet rests on a layer of expanded polystyrene on a supporting frame, and is surrounded by an aluminium box which can be held accurately at a fixed temperature. The air inside the box can be circulated to improve the uniformity of the magnet temperature. This system of temperature control easily maintains a magnetic field stability good enough for high-resolution work.

3. The microwave spectrometer

The microwave source is an Elliott-Litton 8FK1 klystron. To obtain the necessary frequency stability, a very stable power supply has been built, and the cooling water for the value is circulated from a constant-temperature bath.

The power supply was designed and constructed by Mr D. Cook in this laboratory. It provides electronically regulated supplies for the filament, the focus electrode and the cathode of the klystron. The cathode supply can be set between 1 and 4 kV at a maximum current of 250 mA; at 4 kV the nipple is only a few millivolts and the voltage stabilization ratio is 40000 to 1.

The frequency stability of the klystron was measured by setting the spectrometer on the side of a very narrow electron resonance line. No fluctuations could be observed, which means that there were none of as much as 5 p.p.m. The temperature coefficient of the frequency was found by allowing the cooling water of the klystron to cool off very slowly while the nuclear resonance in a radical solution was constantly retraced. As the frequency of the klystron drifted into the electron resonance line of the radical, the nuclear resonance became weaker, was inverted more and more strongly until the centre of the electron resonance was reached. Some sections of this recording are shown in figure 2. The temperature coefficient turned out to be 7 Mc s^{-1} $deg C^{-1}$.

The power output of the klystron is not always stable; one valve showed a very-low-frequency periodic variation of power of as much as 10%, while another has less coherent fluctuations of higher frequencies. By adjustment of the operating conditions of the valve and perhaps sacrificing some power, noise can often be minimized; unless this can be achieved it is hard to observe electron resonances in solutions of radicals with concentrations less than 0·01 M.

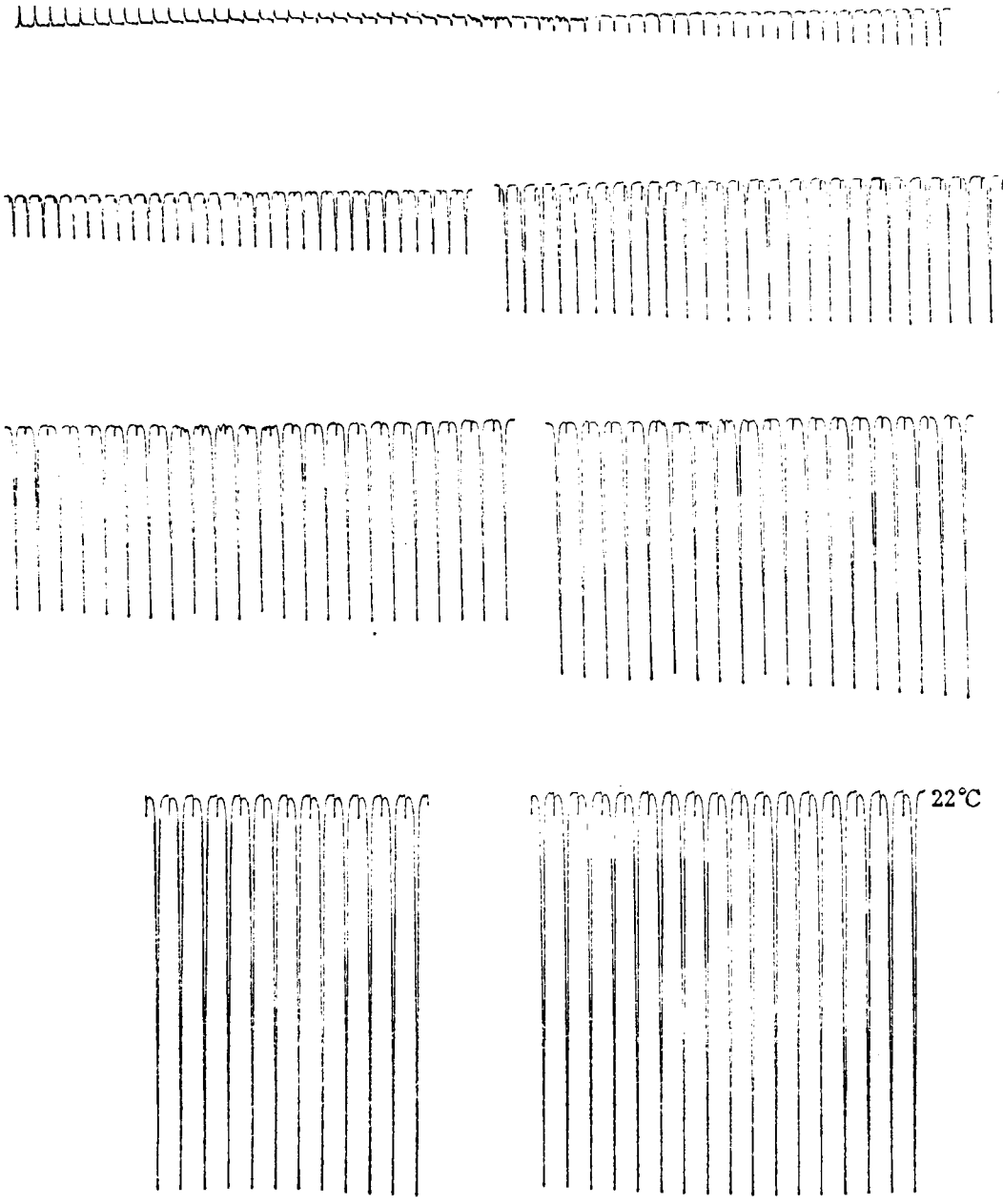

FIGURE 2. Temperature coefficient of klystron frequency.

The microwave circuit is shown in figure 3. The radiation passes through an isolator, I, to a wave-guide switch, S, and thence to a load, L_1, or to the spectrometer. After the switch there is a microwave bridge which serves as an attenuator; by varying the phase-shifter, P, in one arm, the power can be shared between the cavity and the load, L_2, by means of the magic tees, T. A fraction of the microwave power is taken via directional couplers to a wavemeter, W, and to a bolometer, B. The power is monitored at B with a Hewlett-Packard model 430C power meter. The main power passes through the matching unit, M, to the cavity.

Reflected power can be monitored by the crystals, X. Electron resonance signals can be displayed on an oscillograph or recorded by using magnetic field modulation and a phase-sensitive detector in the usual way.

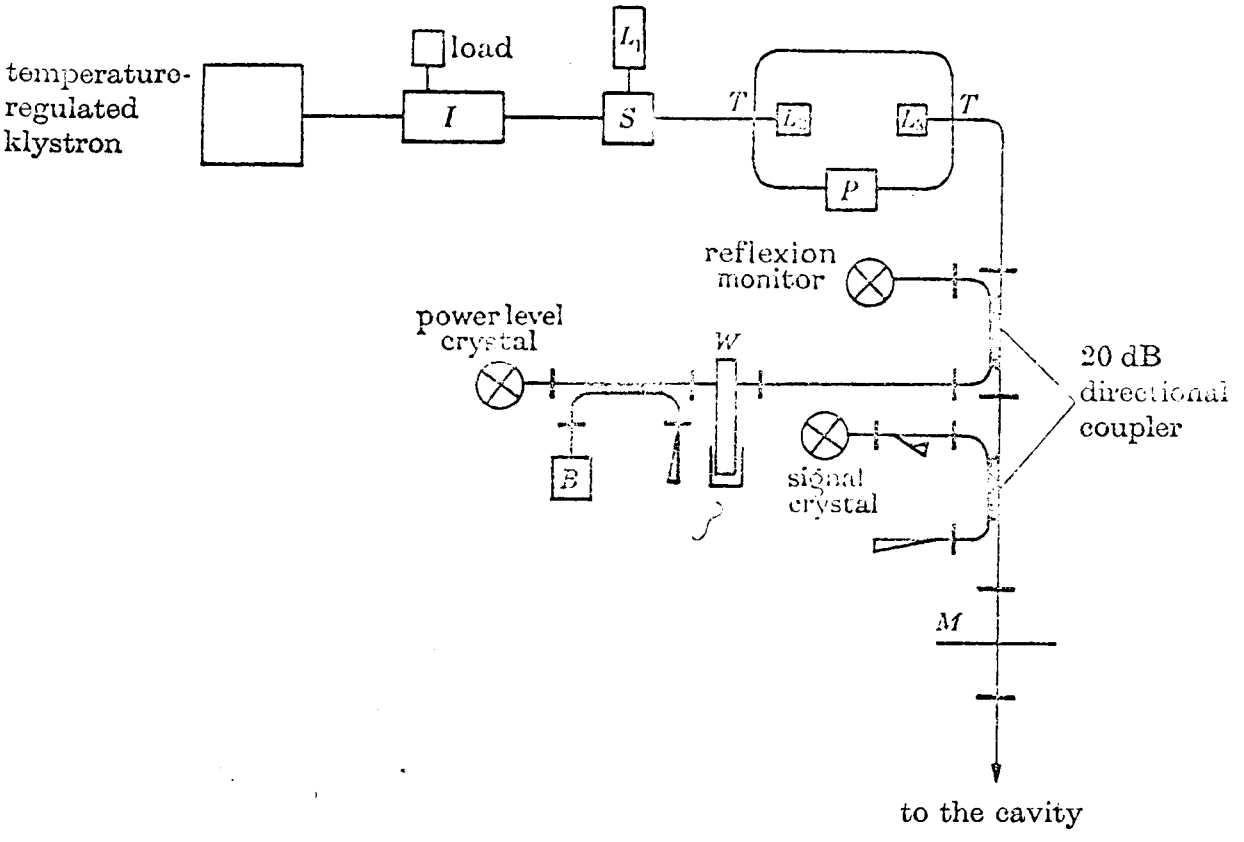

FIGURE 3. Microwave circuit.

4. THE NUCLEAR RESONANCE SPECTROMETER

The radio-frequency source is a Schomandl frequency syntheziser ND 5 and NDF 1 with the NB 7 harmonic amplifier. The frequency synthesizer is locked to a 100 kc/s g.t. crystal oscillator in the laboratory. A variable speed synchronous drive has been added to the NDF 1 to enable the output of the frequency source to be swept in frequency at various speeds.

The source drives a twin-T r.f. bridge with the nuclear resonance coil inside the microwave cavity. The radio-frequency amplifier was built by Decca Radar Ltd, and consists of wide band preamplifiers and two 60 Mc/s i.f. amplifiers. Plug-in crystal-controlled local oscillators (113·2 Mc/s for the proton resonance at 53·2 Mc/s) are used for different frequencies. There is a phase-shifter in one of the i.f. amplifiers and a 60 Mc/s phase detector. The output from the detector can be displayed directly on an oscillograph or a recorder.

When microwave power is applied to it, the sample is heated, and a small drift in the bridge balance occurs which can cause serious zero instability in recordings. In normal use, therefore, the magnetic field is modulated at a suitable frequency between 20 c/s and 5 kc/s (usually 1 kc/s) and the nuclear resonance is detected on the first audio sidebands. The audio component of the signal is amplified, detected with a phase detector and displayed. The zero is then independent of bridge balance.

The nuclear resonance may be scanned either by sweeping the frequency source or the field. Frequency scan is limited to a few kilocycles per second by the band width of the r.f. bridge. If the n.m.r. spectrum lies well inside the electron resonance line it is usually more convenient to sweep the field.

5. The probe

The probe consists of an aluminium TE_{01n} microwave cavity with an r.f. coil inside (figure 4). The walls of the cavity are very thin, to assist optimum magnetic field homogeneity for the nuclear resonance measurements. Tuning is achieved

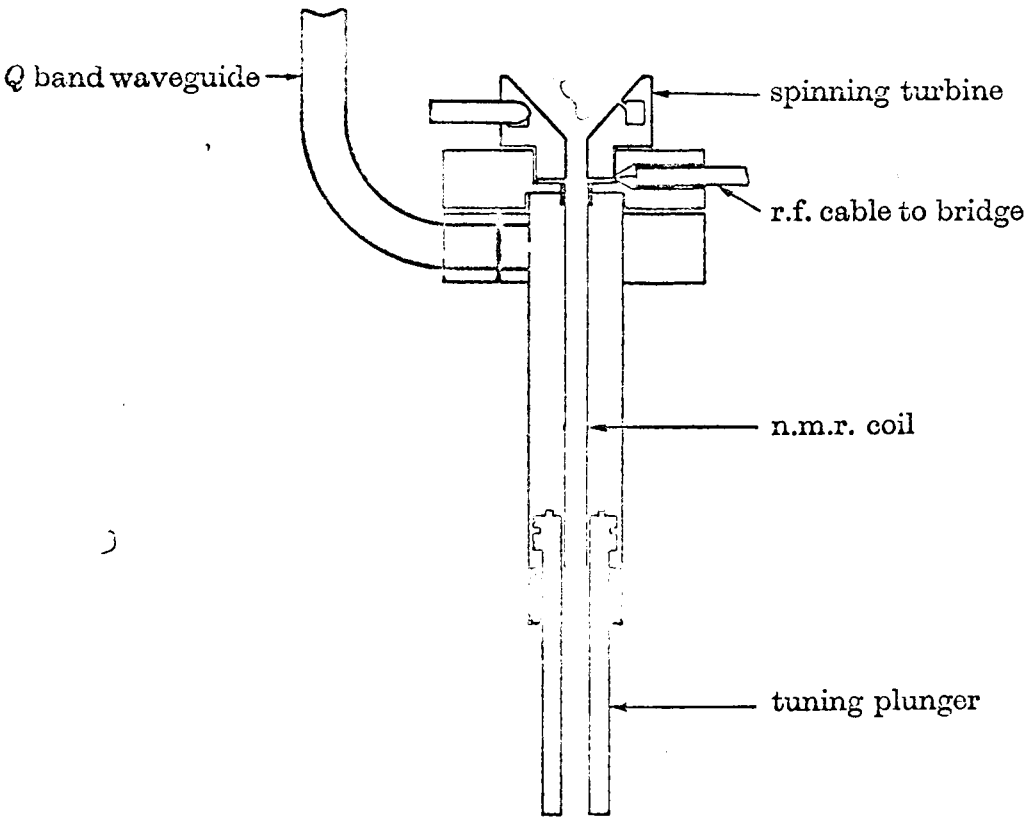

Figure 4. The probe.

by a plunger which has been shaped to give maximum Q when there is a thin-walled quartz sleeve (5 mm o.d.) along the axis, and has a quarter-wave choke to reduce leakage. The power is coupled into the side of the cavity well away from the nuclear resonance coil. The cavity is matched by the coupling iris, the plunger and the transformer, M, shown in figure 3. The quartz sleeve passes through an annular disk of Teflon in the roof of the cavity and slides through the axial hole in the plunger.

The r.f. coil is mounted on the quartz sleeve 4·8 cm from the top of the cavity and for work at 53·2 Mc/s is four turns of 42 s.w.g. copper wire. The sample is contained in a thin-walled glass tube which hangs freely in the quartz sleeve from the spinner mounted above the cavity. Cooling air can be forced into the cavity through the axial hole in the plunger.

6. Performance

The nuclear resonance spectrometer has the performance expected from a high resolution apparatus at this field strength. The field homogeneity is shown by the recordings of the quartet proton resonance of acetaldehyde in figure 5, (*a*) without spinning the sample and (*b*) with spinning. This resolving power is adequate for most double resonance work.

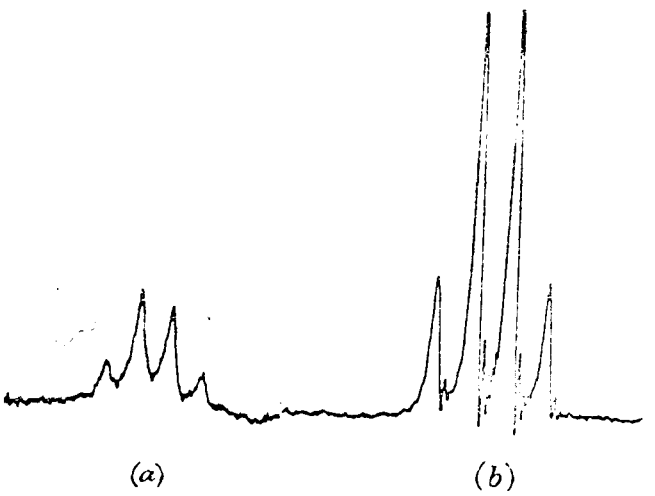

(*a*) (*b*)

Figure 5. CHO resonance of acetaldehyde at 53·2 Mc/s; (*a*) without sample spinning, (*b*) with sample spinning.

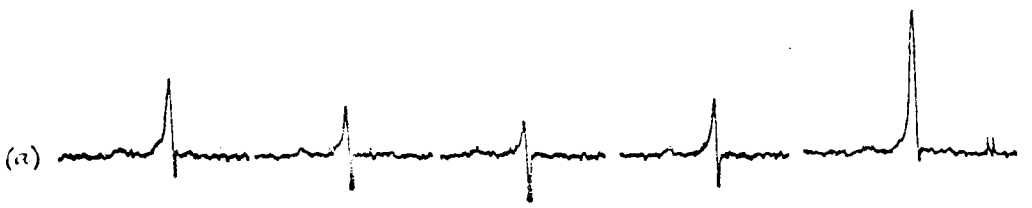

(*a*)

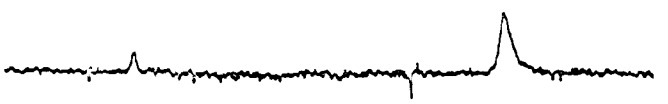

(*b*)

Figure 6. (*a*) Shape of nuclear resonance near zero nuclear polarization for different matching between cavity and waveguide. (*b*) Nuclear resonance with correct matching.

The electron resonance spectrometer is extremely simple and has rather low signal to noise because the Q of the cavity with r.f. coil inside is only about 500. Nevertheless, with a microwave power of about 1 W at the cavity, the electron resonance H_1 field, $H_{1,e}$, is great enough partially to saturate the electron resonance of free radicals such as semiquinones and phenoxy radicals. With powers of 1 W, we have found it possible to use only non-lossy samples; with lossy solvents such as water or alcohols, the heating effect of the microwaves is often great enough to destroy the sample.

With H_0 fields as homogeneous as obtained in this instrument, special care must be taken to ensure adequate homogeneity of the $H_{1,e}$ field. If this field is inhomogeneous over the sample, some parts of the sample become more strongly saturated than others so that distorted nuclear resonance signals are obtained. This is

illustrated in figure 6 where it is shown that the dynamic dipolar coupling between electrons and nuclei in a solution of 2·5 di-*tert.*-butyl phenoxy in benzene causes the nuclear resonance to be inverted when microwave power is applied. The repeated proton resonances in figure 6(*a*) correspond to microwave powers sufficient nearly to equalize the nuclear populations. At some power settings part of the sample has its nuclear resonance inverted while the other part still has a positive polarization. By careful adjustment of the matching transformer, M, the shape of the $H_{1,c}$ field in the cavity can be slightly changed until it is uniform enough over the sample to give the recordings shown in figure 6(*b*).

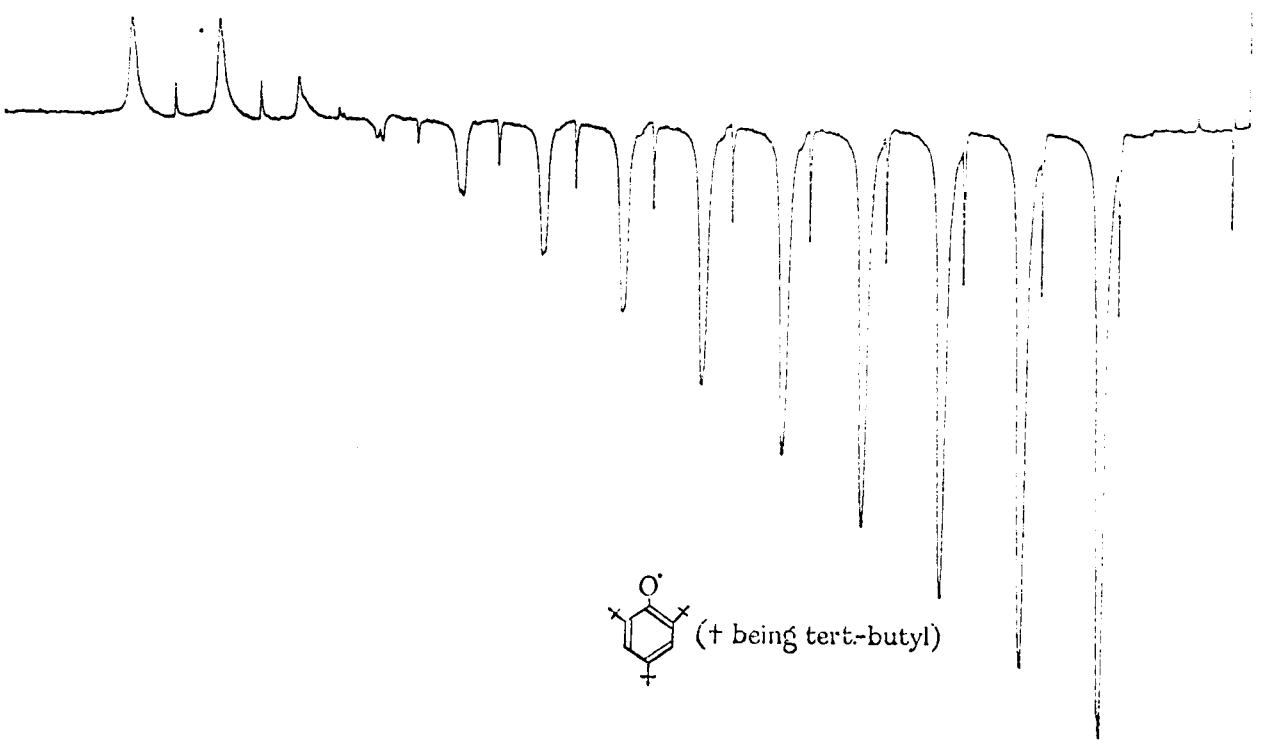

FIGURE 7. Power dependence of the dynamic nuclear polarization of the protons in a benzene solution of the radical indicated.

Figure 7 reproduces a typical set of recordings showing the power dependence of one nuclear resonance line in a particular sample. It is more convenient to make a rapid set of recordings at different powers for each chemically shifted line in turn, than to scan the whole spectrum each time, to avoid unnecessary heating of the sample.

This instrument has been developed and constructed with a grant from the Paul Instrument Fund of the Royal Society for which we are most grateful. We also thank Mullard Ltd for most generously supplying the large permanent magnet.

REFERENCES

Anderson, W. E. 1960 *N.m.r. and e.p.r. spectroscopy, Varian Ass.* London: Pergamon.
Evans, B. A. & Richards, R. E. 1960 *J. Sci. Instrum.* **37**, 353.
Golay, M. J. E. 1958 *Rev. Sci. Instrum.* **29**, 313.
Overhauser, A. W. 1953 *Phys. Rev.* **92**, 411.
Richards, R. E. & White, J. W. 1962*a* *Proc. Roy. Soc.* A, **269**, 287.
Richards, R. E. & White, J. W. 1962*b* *Proc. Roy. Soc.* A, 269, 301.
Richards, R. E. & White, J. W. 1963 *Disc. Faraday Soc.* no. 34.

Offprinted from the *Transactions of The Faraday Society*,
No. 519, Vol. 62, Part 3, March, 1966

MEASUREMENT BY E.S.R. OF FREE RADICAL CONCENTRATIONS, AND ELECTRON EXCHANGE KINETICS IN SOLUTIONS OF POTASSIUM PENTACYANOTRIOSOCHROMATE

Measurement by E.S.R. of Free Radical Concentrations, and Electron Exchange Kinetics in Solutions of Potassium Pentacyanotriosochromate

By J. G. Kenworthy, G. F. Longster * and R. E. Richards

Physical Chemistry Laboratory, South Parks Road, Oxford

Received 7th October, 1965

The advantages and disadvantages of using low magnetic fields when measuring concentrations of free radicals by electron resonance spectroscopy are discussed and several ways of integrating the differentiated absorption line which is usually obtained are considered. A spectrometer operating at 130 gauss is described.

The determination of the rate constants for the electron exchange between anions of potassium pentacyanonitrosochromate, $K_3Cr(CN)_5NO \cdot H_2O$, in several solvents is described.

I. MEASUREMENTS OF CONCENTRATIONS OF FREE-RADICALS USING A LOW FIELD E.S.R. SPECTROMETER, AND A DOUBLE INTEGRATING SYSTEM

The area under the absorption mode of an electron resonance signal is proportional to the number of unpaired spins in the sample. Thus the concentrations of different solutions of free-radicals may be compared by observing the electron resonance absorption curves, and comparing the areas under them. If a standard of known concentration is available then absolute spin concentrations may be determined.

Most electron resonance spectrometers work at frequencies in the micro-wave region of the spectrum, when a resonant cavity is used. The signal amplitude obtained for a given applied power, depends upon the Q of the cavity and this is often seriously affected by dielectric loss in the sample. This is particularly important with polar samples, and serious errors can occur when comparing samples with different dielectric constants. These considerations are not so important when operating in the radio-frequency region of the spectrum, and a spectrometer has been used which operates at 350 Mc/sec. The corresponding magnetic field is about 130 gauss.

For a given sample volume, a low field spectrometer suffers from a decrease in sensitivity compared with an instrument operating at 3500 gauss, the corresponding field for a 3 cm electron spin resonance spectrometer. However, it is often convenient to use larger samples at low field, and by so doing some of the lost sensitivity may be regained. With aqueous samples, for example, particularly small sample sizes must be used at 3500 gauss, but at 130 gauss the sample size is limited only by the dimensions of the coil.

INTEGRATION OF THE LINE

It is convenient when observing broad resonance lines such as electron resonance spectra to modulate the magnetic field at an audio-frequency and then to use a

* present address: Imperial Chemical Industries Limited, Petrochemical and Polymer Laboratory, The Heath, Runcorn, Cheshire.

phase-sensitive detector. When the field modulation amplitude is very much less than the line width a differential of the true absorption line is obtained. Several methods are available for obtaining the area under the absorption line. (i) The differential line may be recorded and then integrated twice graphically. Satisfactory results can be achieved but the calculations are tedious. (ii) The area under the absorption line is proportional to the first moment of the differentiated line. Verdier, Wipple and Schomaker,[1] have shown that this is true, even if the line is modulation broadened. However, the calculations are again tedious. This method may be suitable for use with a multi-channel spectrum accumulator (C.A.T.) which will automatically give the first moment of a line. Such instruments are commercially available but are expensive. (iii) The differential line may be integrated electronically. To do this the base line of the differential signal must be very stable, and the output of the phase-sensitive detector must be balanced exactly to zero when there is no signal. Incorrect adjustment causes drift in the baseline of the integrated signal. Any inherent drift in the integrator will have a similar result. In practice it is difficult to obtain a drift-free integral especially if the signal to noise ratio is poor. The second integration may be performed by drawing an approximation to the drifting baseline, and using a planimeter to measure the area under the curve.

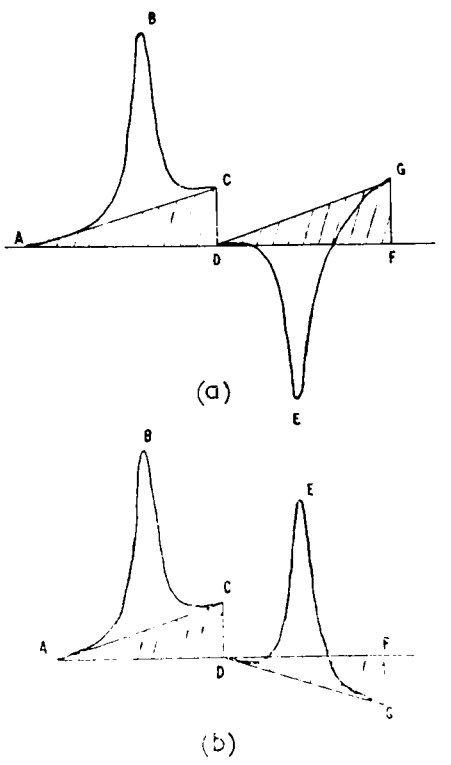

FIG. 1.—(*a*) and (*b*) Compensating for a drifting baseline.

Alternatively, a second electronic integrator may be used, and drift compensated for as follows. If the line is swept from low field to high field, the output of the first integrator will follow the line A, B, C in fig. 1(*a*). The line AC represents the drifting base-line. The reading on the second integrator will represent the whole area ABCD. That is the area under the line plus the drift. If the first integrator is now reset, and the line swept in the other direction, the signal will be inverted but the drift will stay in the same direction, and the output of the first integrator will follow the line DEG in fig. 1(*a*). If, however, at point C the connections to the second integrator are reversed, the signal which this integrator received will be represented by fig. 1 (*b*), and the integral recorded will be twice the area under the line, the drift having been eliminated. This will only be so if the drift is constant and linear. Also any inherent drift in the second integrator will cause an error, but this may be eliminated by repeating the experiment with the connections to the second integrator always reversed relative to the first experiment, and averaging the two results. This is by far the most convenient method of doing the double integration.

SPECTROMETER

MAGNET.—The magnetic field of about 130 gauss is produced with a pair of Helmholtz coils of about 14 in. diam., each having 10,000 turns and a resistance of 600 ohms. A stabilized magnet power supply is used. It was designed by Mr. D. Cook, and the output may be swept linearly from 250 mA to 400 mA by

Measurement by E.S.R. of Free Radical Concentrations, and Electron Exchange Kinetics in Solutions of Potassium Pentacyanotriosochromate

By J. G. Kenworthy, G. F. Longster * and R. E. Richards

Physical Chemistry Laboratory, South Parks Road, Oxford

Received 7th October, 1965

The advantages and disadvantages of using low magnetic fields when measuring concentrations of free radicals by electron resonance spectroscopy are discussed and several ways of integrating the differentiated absorption line which is usually obtained are considered. A spectrometer operating at 130 gauss is described.

The determination of the rate constants for the electron exchange between anions of potassium pentacyanonitrosochromate, $K_3Cr(CN)_5NO \cdot H_2O$, in several solvents is described.

I. MEASUREMENTS OF CONCENTRATIONS OF FREE-RADICALS USING A LOW FIELD E.S.R. SPECTROMETER, AND A DOUBLE INTEGRATING SYSTEM

The area under the absorption mode of an electron resonance signal is proportional to the number of unpaired spins in the sample. Thus the concentrations of different solutions of free-radicals may be compared by observing the electron resonance absorption curves, and comparing the areas under them. If a standard of known concentration is available then absolute spin concentrations may be determined.

Most electron resonance spectrometers work at frequencies in the micro-wave region of the spectrum, when a resonant cavity is used. The signal amplitude obtained for a given applied power, depends upon the Q of the cavity and this is often seriously affected by dielectric loss in the sample. This is particularly important with polar samples, and serious errors can occur when comparing samples with different dielectric constants. These considerations are not so important when operating in the radio-frequency region of the spectrum, and a spectrometer has been used which operates at 350 Mc/sec. The corresponding magnetic field is about 130 gauss.

For a given sample volume, a low field spectrometer suffers from a decrease in sensitivity compared with an instrument operating at 3500 gauss, the corresponding field for a 3 cm electron spin resonance spectrometer. However, it is often convenient to use larger samples at low field, and by so doing some of the lost sensitivity may be regained. With aqueous samples, for example, particularly small sample sizes must be used at 3500 gauss, but at 130 gauss the sample size is limited only by the dimensions of the coil.

INTEGRATION OF THE LINE

It is convenient when observing broad resonance lines such as electron resonance spectra to modulate the magnetic field at an audio-frequency and then to use a

* present address: Imperial Chemical Industries Limited, Petrochemical and Polymer Laboratory, The Heath, Runcorn, Cheshire.

phase-sensitive detector. When the field modulation amplitude is very much less than the line width a differential of the true absorption line is obtained. Several methods are available for obtaining the area under the absorption line. (i) The differential line may be recorded and then integrated twice graphically. Satisfactory results can be achieved but the calculations are tedious. (ii) The area under the absorption line is proportional to the first moment of the differentiated line. Verdier, Wipple and Schomaker,[1] have shown that this is true, even if the line is modulation broadened. However, the calculations are again tedious. This method may be suitable for use with a multi-channel spectrum accumulator (C.A.T.) which will automatically give the first moment of a line. Such instruments are commercially available but are expensive. (iii) The differential line may be integrated electronically. To do this the base line of the differential signal must be very stable, and the output of the phase-sensitive detector must be balanced exactly to zero when there is no signal. Incorrect adjustment causes drift in the baseline of the integrated signal. Any inherent drift in the integrator will have a similar result. In practice it is difficult to obtain a drift-free integral especially if the signal to noise ratio is poor. The second integration may be performed by drawing an approximation to the drifting baseline, and using a planimeter to measure the area under the curve.

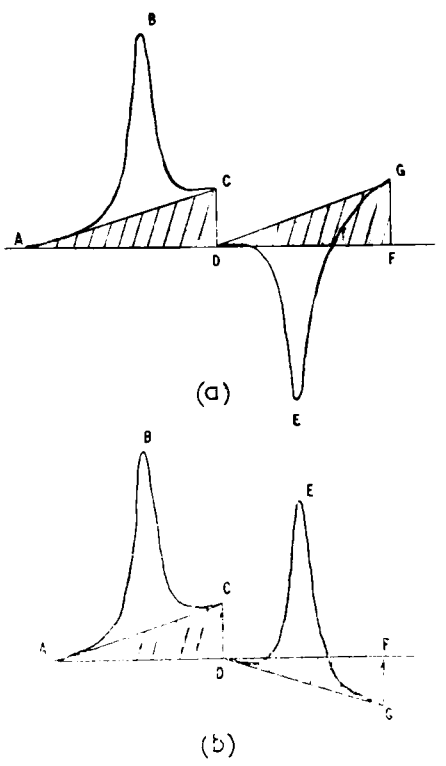

FIG. 1.—(*a*) and (*b*) Compensating for a drifting baseline.

Alternatively, a second electronic integrator may be used, and drift compensated for as follows. If the line is swept from low field to high field, the output of the first integrator will follow the line A, B, C in fig. 1(*a*). The line AC represents the drifting base-line. The reading on the second integrator will represent the whole area ABCD. That is the area under the line plus the drift. If the first integrator is now reset, and the line swept in the other direction, the signal will be inverted but the drift will stay in the same direction, and the output of the first integrator will follow the line DEG in fig. 1(*a*). If, however, at point C the connections to the second integrator are reversed, the signal which this integrator received will be represented by fig. 1 (*b*), and the integral recorded will be twice the area under the line, the drift having been eliminated. This will only be so if the drift is constant and linear. Also any inherent drift in the second integrator will cause an error, but this may be eliminated by repeating the experiment with the connections to the second integrator always reversed relative to the first experiment, and averaging the two results. This is by far the most convenient method of doing the double integration.

SPECTROMETER

MAGNET.—The magnetic field of about 130 gauss is produced with a pair of Helmholtz coils of about 14 in. diam., each having 10,000 turns and a resistance of 600 ohms. A stabilized magnet power supply is used. It was designed by Mr. D. Cook, and the output may be swept linearly from 250 mA to 400 mA by

means of a motor driven helipot. A ten-speed gearbox gives a variety of sweep rates. The supply is stabilized to better than 1 in 10^4 which corresponds to a field stability of better than 13 milligauss. The field inhomogeneity over a 7 mm diam. sample is considerably less than this.

DETECTION SYSTEM.—The radio-frequency detection system is a marginal oscillator operating at 350 Mc/sec, which was purchased from Alpha Scientific Laboratories Inc., California. The oscillator was modified so as to permit the level of oscillation to be monitored. Small adjustments could then be made to the feedback control in order to maintain a constant level of oscillation with each sample. One kc/sec field modulation is used, and the audio-output of the Alpha unit is amplified, and fed via a calibrated attenuator to an audio-phase sensitive detector.[2] The output from this detector may be either displayed on a pen recorder, or integrated as described above.

INTEGRATORS.—The integrators are of the Miller type. This design requires a high-stability d.c. amplifier, and both Solartron type AA 1023 and Fenlow A 10 amplifiers have been used.

PERFORMANCE

With radical concentrations greater than approximately 10^{-4} M, relative concentrations may be measured to an accuracy of better than 5 %. With more dilute solutions, which give reduced signal to noise the accuracy is less. Fig. 2 shows a plot of the areas measured under the absorption curves against relative concentrations for a series of samples prepared by quantitative dilution of a solution of 2,5-di-tertiary butyl semiquinone radical in dimethyl formamide.

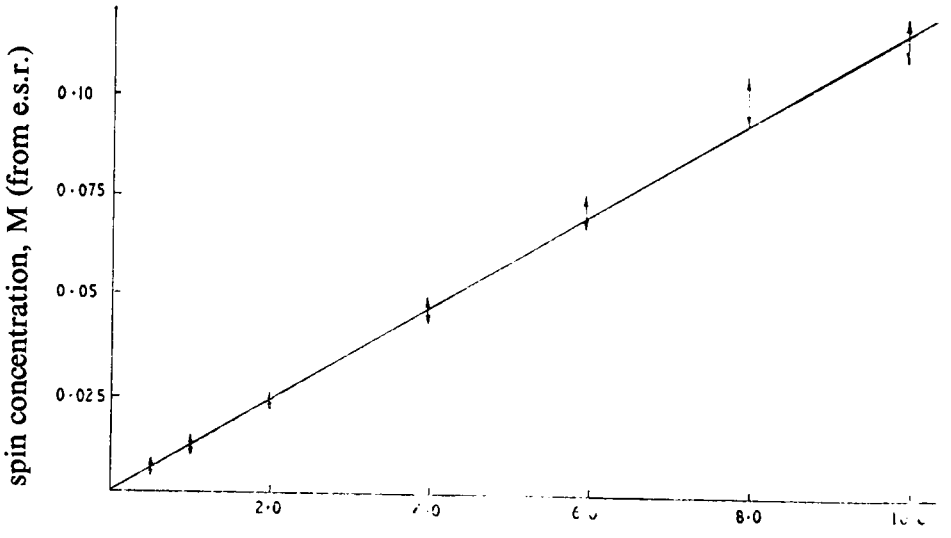

FIG. 2.—Measured spin concentration against known relative concentration for samples of 2,5-di-t-butyl semiquinone in dimethyl formamide.

The accuracy of absolute concentration measurements depends upon the accuracy to which the concentration of the standard is known. Some difficulty was experienced in finding a suitable stable standard. An obvious choice would seem to be a solution of a paramagnetic inorganic salt, but such resonances do not occur within the range of scan of the spectrometer.

Experiment suggested that the purest solid radical available was a sample of potassium nitrosyl disulphonate $K_2(SO_3)_2NO$ prepared according to Palmer.[3] Solutions of this salt are most stable if strongly alkaline but even then decompose

slowly with time. A freshly prepared solution was used to calibrate the signal from a sample of natural calcite, which was then used as a stable secondary standard. Care was taken always to place the calcite crystal at the same orientation to the field.

II. ELECTRON EXCHANGE IN POTASSIUM PENTACYANONITROSOCHROMATE SOLUTIONS

In dilute solution the electron resonance spectrum of the pentacyanonitrosochromate anion $[Cr(CN)_5(NO)]^{3-}$ is a triplet as a result of coupling of the electron to the nitrogen atom. In concentrated solutions the spectrum collapses to a single line because of the averaging effect of electron exchange between anions. Rate constants for the exchange can be determined by investigation of the line widths of solutions of sufficiently low concentration for the fine structure to be visible.

When the exchange rate is below that required to cause the collapse of the fine structure the exchange frequency is given by [4]

$$W_e = 1/\tau = 0{\cdot}75\sqrt{3}\gamma(\Delta H - \Delta H_0), \tag{1}$$

where W_e is the exchange frequency, τ the average time which a particular electron spends between exchanges, γ the gyromagnetic ratio of the electron, and ΔH and ΔH_0 are the peak-to-peak line-widths of the differential line in gauss, with and without exchange respectively. If the exchange between radical anions is a bimolecular process the average time between exchanges is given by

$$\tau = 1/kc, \tag{2}$$

where k is the second order rate constant and c is the radical concentration. From eqn. (1) and (2),

$$kc = 0{\cdot}75\sqrt{3}\gamma(\Delta H - \Delta H_0). \tag{3}$$

Fig. 3 shows plots of line width against concentration for solutions of potassium pentacyanonitrosochromate in various solvents. The widths were measured on differentiated signals, each being the average value of the peak-to-peak separation of the three lines in the spectrum. The concentrations were measured by double integration, as described above.

The solutions in water, curve (1), show a marked deviation from linearity at low concentrations, and this behaviour is also seen to a lesser degree in the solutions in the 50/50 acetone+water mixture, and very slightly in formamide. The slope of the linear portions of the curves correspond to bimolecular rate constants between $1{\cdot}7 \times 10^8$ l. mole^{-1} sec^{-1} (water) and $5{\cdot}4 \times 10^8$ l. mole^{-1} sec^{-1} (acetone+water, 80/20). The other solvents give values, in units of 10^8 l. mole^{-1} sec^{-1}, as follows: 1·8 (glycine in water), 1·9 (formamide) 2·0 (acetone+water, 50-50), and 2·2 (dimethyl sulphoxide).

There appears to be a very approximate inverse relationship between the rate constant and the dielectric constant of the solvent. It may be that this indicates that two ions of opposite sign are involved in the exchange, and hence it is possible that cation participation is important in the rate-determining step.

The curvature shown by the aqueous solutions implies some extra broadening mechanism, as the value of ΔH_0 obtained by extrapolation to zero radical concentration is greater in this case. A possible explanation of curvature may be that in dilute aqueous solutions the exchange is retarded by the " ice-like " structure resulting from hydrogen bonding and only when the salt concentration becomes sufficient to break down the structure does the exchange become a second-order

effect. The linearity of the solutions in aqueous glycine may possibly be accounted for similarly, as a result of the breakdown of the hydrogen bonding of the water by the added glycine. In the formamide solutions, where some hydrogen bonding is possible, some curvature of the line may be expected, and is observed; but anhydrous dimethyl sulphoxide, in which hydrogen bonding is absent behaves as an ideal solvent, and shows no curvature.

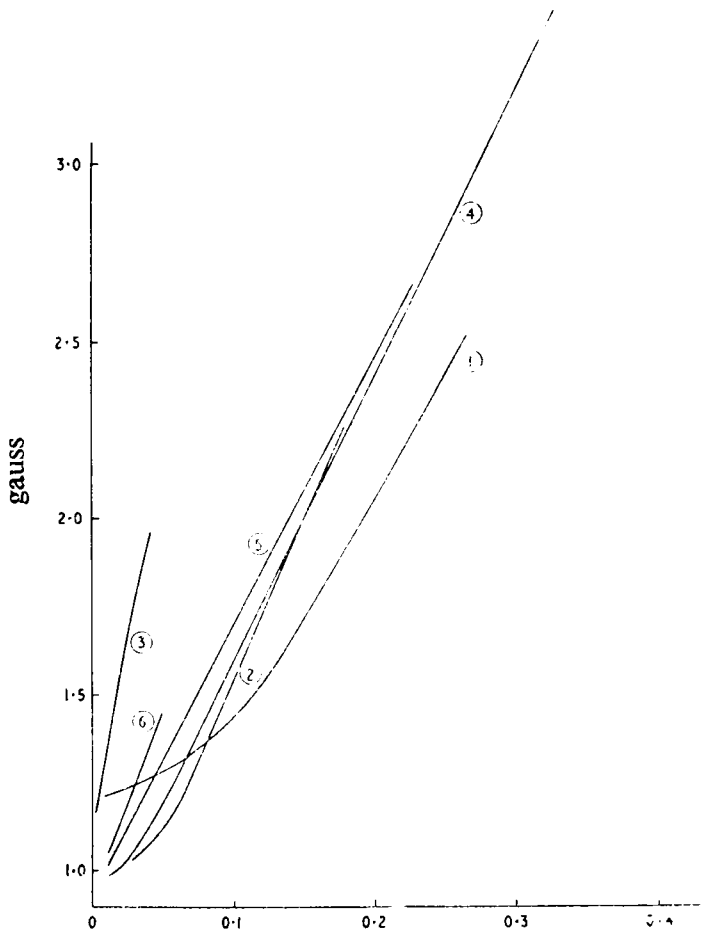

FIG. 3.—Variation of line width with concentration for solutions of potassium nitrosyl chromicyanide in different solvents.

Solvent: 1, water; 2, acetone+water 50/50 v/v; 3, acetone+water 80/20 v/v; 4, formamide; 5, glycine in water (20 % wt/wt); 6, dimethyl sulphoxide.

One of us (J. G. K.) acknowledges a research studentship from the Science Research Council. We thank the Hydrocarbon Research Group of the Institute of Petroleum and the Science Research Council for grants in aid of apparatus. G. F. L. is grateful for the hospitality of the Physical Chemistry Laboratory during the work, and thanks Imperial Chemical Industries Ltd., Petrochemical and Polymer Laboratory, for leave of absence.

[1] Verdier, Wipple and Schomaker, *J. Chem. Physics*, 1961, **34**, 118.
[2] Johnson, *N.M.R. and E.P.R. Spectroscopy* (Varian Workshop) (Pergamon Press, 1960).
[3] Palmer, *Experimental Inorganic Chemistry* (Cambridge University Press, 1954).
[4] Jones, *J. Chem. Physics*, 1963, **38**, 2929.

PRINTED IN GREAT BRITAIN AT
THE UNIVERSITY PRESS
ABERDEEN

COMPUTER PROGRAMMES.

FORMULA 1, is for calculating values of $j_d(\omega\tau)$ as a function of $(\omega\tau)^{\frac{1}{2}}$ for different λd.

$Je(\omega)$ is given by equation (6.1),

and

$$j_e(\omega) = \frac{Je(\omega)}{Je(0)} = \frac{Je(\omega)}{\lim_{\omega \to 0} Je(\omega)}$$

FORMULA 2, is for calculating ρ as a function of $(\omega\tau)^{\frac{1}{2}}$, using the values of $j_e(\omega)$ from FORMULA 1, for different ξ.
ρ is given by equation (6.5).

FORMULA 3, is for calculating ρ as a function of $(\omega\tau)$ for the Modified Sticking Model, for different K and δ.

```
      TITLE

FAPAG  FORMULA  1

CHAPTER  0
A→20
B→20
A0=0.00000001
A1=0.005
A2=0.01
.
.                    ..... (ωτ)^½
.
.
.
A19=10.0

B0=1.0
.
.                 . . .    Aα.
.
B19=1000

L=0(1)19
NEWLINE
NEWLINE
PRINT  (BL) 3,3
V=BLBL
W=VV
T=0(1)19

A=XSIN(AT)
B=XCOS(AT)
C=XEXP(-AT)
D=V/AT
Z=ATAT
E=Z+ 2V-2BLAT
F=4W+ZZ
G=2V+2BLAT+Z
G=GG
H=A-B
X=2V+2BLAT
X=HX
Y=A+B

H=2BLAT+Z
H=HY+X
A=DE/F+DCH/G
JUMP1,T≠0
U=AX          . . . . . Je(0)
1)A=A/U       . . . . . je(ω)
NEWLINE
PRINT(AT)3,3
PRINT(A)2,4
REPEAT
REPEAT
END
CLOSE
→
??
```

```
    TITLE
FAPAG  FORMULA2
CHAPTER0
A→30
B→30
C→30
E→30
C1=
.      .... 3
.
C30=
B1=
.      .... jα(ω)
.
B30=
1)READ(E0)  ... λα
I=1(1)30
NEWLINE
NEWLINE
PRINT(CI)
NEWLINE
PRINT(E0)
C=3CI
J=1(1)30
JUMP2,I≠1
READ(EJ)  ... (ωτ)^n
READ(AJ)   .... j_c(ω)
2)X=40BJ-CAJ
Y=56BJ+CAJ+24
Z=X/Y
W=XLOG(.166666666667)
NEWLINE
PRINT(EJ)3,3
PRINT(Z)3,3
PRINT(W)3,3
REPEAT
REPEAT
JUMP1
END
CLOSE
→
!??
**********
```

DATA TAPE AS PER OUTPUT OF PREVIOUS PROGRAMME.

```
TITLE
PAPAG  FORMULA 3
CHAPTERo
A→20
B→20
C→20
D→20
Ao=
•          .....      Jα (W5)
•
A20=

Bo=
•                  ..    (W5τ)
•
B20=
Co=
•                  ...   K'
•
C20=

Do=
•
•                  .....  σ
•
D20=

U=1/36
K=o(1)10
L=o(1)20
 NEWLINE
 NEWLINE
 CAPTION
 K=
 PRINT(CK)3,1
 CAPTION
 DELTA=
 PRINT(DL)3,1
 F=5CKDL
 I=o(1)20
 V=5AI
 W=7AI+3
 X=1+UDLDLBIBI
 X=F/X
 Y=V-X
 Z=W+X
 A=Y/Z
 NEWLINE
 PRINT(BI)3,2
 PRINT(A)1,3
 REPEAT
 REPEAT
 REPEAT
 END
 CLOSE
.→
??
.**********
```